Materials Science and Engineering, R23 (1998) 41–100

R Reports: *A Review Journal*

Theory of sintering: from discrete to continuum

Eugene A. Olevsky *

Institute for Mechanics and Materials, University of California, San Diego, 9500 Gilman Drive, La Jolla, CA 92093-0404, USA

Received 15 July 1997; accepted 17 November 1997

Abstract

Theoretical concepts of sintering were originally based upon ideas of the discrete nature of particulate media. However, the actual sintering kinetics of particulate bodies are determined not only by the properties of the particles themselves and the nature of their local interaction with each other, but also by macroscopic factors. Among them are externally applied forces, kinematic constraints (e.g. adhesion of the sample's end face and furnace surface), and inhomogeneity of properties in the volume under investigation (e.g. inhomogeneity of initial density distribution created during preliminary forming operations). Insufficient treatment of the questions enumerated above was one of the basic reasons hindering the use of sintering theory. A promising approach is connected with the use of continuum mechanics, which has been successfully applied to the analysis of compaction of porous bodies. This approach is based upon the theories of plastic and nonlinear-viscous deformation of porous bodies. Similar ideas have recently been embodied in a continuum theory of sintering. The main results of the application of this theory for the solution of certain technological problems of sintering are introduced including their thermo–mechanical aspects.

Keywords: Sintering; Porous material; Continuum theory; Constitutive modeling

1. Introduction

Sintering is one of the most important technological processes in the powder metallurgy and ceramic industries. A rational theory of sintering should predict the routes of production of the required structure of a sintered body in order to provide its physico–chemical and physico–mechanical properties which are determined by this structure.

Theoretical concepts of sintering were originally based upon ideas of a discrete organization of porous media. Sintering was considered as the collective result of thermally activated adhesion processes which produce the growth of contacts between particles and their coalescence. An orientation toward study of the mechanisms of interparticle interaction was characteristic for many of the elaborated approaches in the theory of sintering. Thus, these approaches were directed toward investigation of the local kinetics of the process. Data obtained on the basis of these conceptions were usually generalized as the behavior of a macroscopic porous body. At this juncture, important regularities of sintering kinetics, contact formation and driving force nature have been clarified to a large degree [1–17]. The results obtained have been embodied in a number of kinetic relationships describing densification under free sintering. These relationships include characteristics of structure morphology, physical and mechanical properties of porous material.

However, the sintering kinetics of real porous bodies are determined not only by the properties of the powder particles and the nature of their interaction, but also by macroscopic factors. Among

* Corresponding author.

0927-796X/98/$19.00
PII S0927-796X(98)00009-6

them are kinematic constraints (for example, adhesion of porous sample's end face and furnace surface), externally applied forces and, also, inhomogeneity of properties in the volume under investigation (for example, inhomogeneity of initial density distribution caused by preliminary pressing of the porous sample).

Insufficient treatment of the questions enumerated above was one of the basic reasons hindering the use of sintering theory. It is obvious that the indicated problems can be solved only in terms of a macroscopic description, which should be based upon concepts which differ in principle from those of local analysis.

These problems with implementation of theoretical ideas into sintering practice can be a reason for the limited number of monographs dedicated exclusively to sintering [18–27]. (Apparently, a recent publication of German [27] is the only example of an extended monograph comprising both theoretical concepts and practical aspects of sintering.)

A promising approach is connected with the use of continuum mechanics, which has been successfully applied to the description of compaction of porous bodies and which is based upon the theories of plastic deformation of porous bodies [28–39].

This approach formed a scientific direction which can be designated as a continuum theory of sintering [40–145] (related references include both continuum models and close rheological concepts). This approach is also based upon theories of nonlinear-viscous deformation of porous bodies [146–165] which are extensively used in continuum models of sintering under pressure.

Among the earlier models, the rheological theory of sintering [19] was the closest to this direction. One of the most characteristic phenomena inherent in sintering is a change of dimensions of a porous body. This enables analysis of sintering as a macroscopic process of volume and shape deformation caused by substance flow of the porous body skeleton. In this sense, sintering can be treated as a subject of *rheological* investigation [19].

In essence, Frenkel [1] was the first to implement the rheological approach for sintering. The relationship determining sintering kinetics, was derived by Frenkel on the basis of the analysis of two model problems: joint sintering of two equal spherical particles and shrinkage of a spherical pore in an infinite viscous medium.

These ideas were amplified and further developed by Mackenzie and Shuttleworth [6]. They elaborated a method of macroscopic description of sintering as a uniform overall compression of a porous medium characterized by two moduli of viscosity. Mackenzie derived the relationships of the porosity dependence for these moduli.

A complete thermodynamically grounded rheological theory of sintering was built by Skorohod [19]. The Skorohod's book *Rheological Basis of the Theory of Sintering* [19] was published in 1972 in Russian and is, unfortunately, almost unknown to the English-reading audience. In the book, the theory of sintering of powder materials is sequentially formulated. The theory is based upon the phenomenological concept of the generalized-viscous flow of porous bodies. Here, one can find the derivation (based upon the stochastic approach) of the relationships for the dependencies of rheological parameters (such as bulk, shear viscosities and effective sintering stress) of porosity and the solution of the problem of the deformation of a viscous porous body under sintering simultaneous to a uniaxial loading. The book also contains an analysis of the main molecular mechanisms of the viscous flow of real amorphous and crystalline bodies, the kinetics of interparticle contact growth and models of non-isothermal sintering and sintering accompanied by heterodiffusion.

Independently this direction was developed by Scherer [40] who introduced a model of viscous sintering of amorphous (glass) materials based upon the idea of cylindrical shaped powder particles. Scherer derived the kinetic equations for the rate at which a cubic array of cylinders densifies by viscous flow driven by surface energy reduction. For sintering under pressure, the constitutive equations

are based upon the analogy with thermoelasticity. Herewith, the strain rate of sintered material is represented as a sum of free sintering and viscous material response items. A linear-viscous character of this model should be noted. A development of the rheological concepts further led to the creation of the above-mentioned continuum theory of sintering.

The present review is dedicated to the description of the basic ideas and results obtained in the framework of this scientific direction which has been intensively developed since the mid-1980s.

Statistical data on the number of publications related to sintering in general and related to the continuum modeling of sintering are represented in Fig. 1.

While the constitutive relationships and the calculation results, represented in the review, assume viscous or plastic mechanisms of material flow under sintering, the thermodynamical basis of the represented continuum theory of sintering is the same for other possible mechanisms (see, for example, Ref. [125]).

This review is organized as follows.

Section 2 includes the description of the phenomenological model of sintering based upon the ideas of thermodynamics of irreversible processes. Here three cases are considered: linear-viscous incompressible material with voids, incompressible non-linear-viscous material, and nonlinear-viscous porous material. Dependence of the constitutive parameters of porosity (bulk and shear viscosity moduli and effective Laplace (sintering) stress) are analyzed in Section 3. In Section 4, the solution to the problem of sintering combined with uniaxial loading (sinter-forging and sinter-tension) is represented. In Section 5, the effect of the strain rate sensitivity on the kinetics of sintering is analyzed. Effect of porous structure topology is considered in Section 6. Here, two factors are studied: pore size distribution and pore shape. In Section 7, the evolution of inhomogeneous density (porosity) distribution during sintering is analyzed for certain simple and complex-shaped porous bodies. The directions of further development are represented in Section 9.

2. Phenomenological model of sintering

The following is a formulation of the continuum theory of sintering of porous viscous materials.

A porous medium is considered as a two-phase material including the phase of substance ('porous body skeleton') and the phase of voids (pores). The skeleton, in turn, can be a multiphase material. The skeleton is assumed to be made of individual particles having in general nonlinear-viscous incompressible isotropic behavior. The voids (pores) are isotropically distributed. The overall response is therefore isotropic.

The free energy F per unit mass of porous medium is, by hypothesis, a function of the absolute temperature T and of the specific volume ϑ

$$F = F(T,\vartheta) \tag{1}$$

with

$$\vartheta = \frac{1}{\hat{\rho}} \tag{2}$$

where $\hat{\rho}$ is the volumetric mass of porous material.

The second law of thermodynamics can be expressed in terms of the Clausius–Duhem inequality:

$$\sigma_{ij} : \dot{\varepsilon}_{ij} - \hat{\rho}\dot{F} - \hat{\rho}S\dot{T} \geq 0 \tag{3}$$

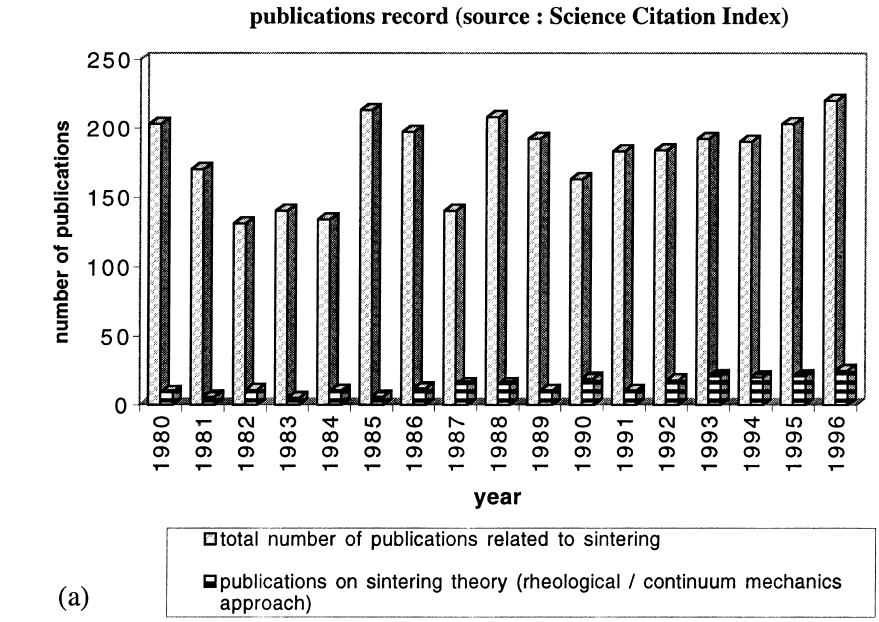

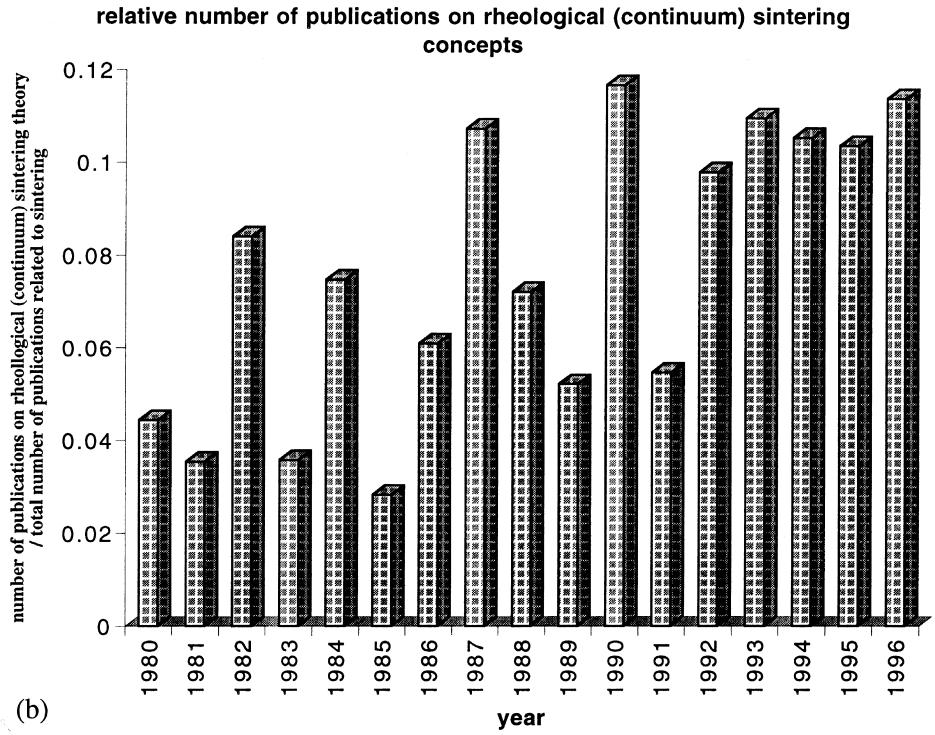

Fig. 1. Publications related to sintering (source: *World Science Citation Index*). (a) Absolute number of publications. (b) Normalized number of publications on continuum modeling of sintering (with respect to the total number of publications related to sintering).

σ_{ij} and $\dot{\varepsilon}_{ij}$ are the Cauchy stress tensor and the strain rate tensor, respectively; S is the entropy per

Introducing Eq. (1) into Eq. (3), we obtain

$$\sigma_{ij}-\frac{\partial F}{\partial \vartheta}\delta_{ij}\ \ \dot{\varepsilon}_{ij}-\hat{\rho}\ \ \frac{\partial F}{\partial T}+S\ \ \dot{T}\geq 0 \tag{4}$$

where δ_{ij} is the Kronecker symbol.

In deriving the latter equation, we have used the following result:

$$\frac{\dot{\vartheta}}{\vartheta}=-\frac{\dot{\hat{\rho}}}{\hat{\rho}}=\dot{\varepsilon}_{ii} \tag{5}$$

The second part of Eq. (5) comes from mass conservation.

Note that, for a viscous material, σ_{ij} and S depend on the strain rate $\dot{\varepsilon}_{ij}$ but not on $\dot{T}$. Therefore, since Eq. (4) holds for any $\dot{T}$, we have:

$$S=-\frac{\partial F}{\partial T} \tag{6}$$

and Eq. (4) reduces to the following dissipation inequality:

$$(\sigma_{ij}-P_{\mathrm{L}}\delta_{ij})\,\dot{\varepsilon}_{ij}\geq 0 \tag{7}$$

where we have defined the effective Laplace pressure (sintering stress) by:

$$P_{\mathrm{L}}=\left.\frac{\partial F}{\partial \vartheta}\right|_{T} \tag{8}$$

The condition (Eq. (7)) is in particular satisfied if there exists a dissipative potential D defined as a homogeneous function of order $m+1$ of the strain rate $\dot{\varepsilon}_{ij}$ (see below), such that:

$$\sigma_{ij}-P_{\mathrm{L}}\delta_{ij}=\frac{\partial D}{\partial \dot{\varepsilon}_{ij}} \tag{9}$$

Note that the dissipation inequality is satisfied as a consequence of the Euler identity:

$$\dot{\varepsilon}_{ij}\frac{\partial D}{\partial \dot{\varepsilon}_{ij}}=(m+1)D\geq 0$$

In general, D is also a function of the specific volume ϑ or, equivalently, a function of the porosity θ defined as a ratio of the volume of pores and the total volume:

$$\theta=\frac{V_{\mathrm{pores}}}{V_{\mathrm{total}}} \tag{10}$$

To have some understanding of the effect of the porosity on the overall response, we consider different model materials.

2.1. Linear-viscous incompressible material with voids

We consider first the case of a linear-viscous incompressible fluid containing isotropically distributed voids. The overall behavior is isotropic.

The dissipation potential in this case is:

$$D=\eta\gamma^2+\frac{1}{2}\zeta e^2 \tag{11}$$

where η and ζ are the effective shear and bulk moduli. The following notations are used:

$$\gamma=\sqrt{\dot{\varepsilon}_{ij}'\dot{\varepsilon}_{ij}'} \tag{12}$$

$$e=\mathrm{tr}\dot{\varepsilon}=\dot{\varepsilon}_{ii}$$

where $\dot{\varepsilon}_{ij}'$ is the deviator of the strain rate tensor, and e is the shrinkage rate defined by Eq. (5).

In Section 3, it is shown that:

$$\eta=\varphi\eta_0 \tag{13}$$

$$\zeta=2\psi\eta_0$$

with

$$\varphi=(1-\theta)^2 \tag{14}$$

$$\psi=\frac{2}{3}\frac{(1-\theta)^3}{\theta}$$

Note that η and ζ are only dependent on the shear modulus η_o of the porous body skeleton (incompressible fluid).

Using Eq. (13), the potential D can be expressed as:

$$D=(1-\theta)\eta_o W^2 \tag{15}$$

with

$$W=\sqrt{\frac{\varphi\gamma^2+\psi e^2}{1-\theta}} \tag{16}$$

defining an equivalent strain rate.

From Hill's identity we have:

$$D=\langle d\rangle$$

where d is the microscopic dissipative potential and $\langle\rangle$ designates the volume average over the porous material.

Since $d=0$ in the pores, we have:

$$D=(1-\theta)\langle d\rangle_{\text{skeleton}}=(1-\theta)\eta_o\langle\gamma^2\rangle_{\text{skeleton}}$$

From Eq. (15) it follows that:

$$W=\sqrt{\langle\gamma^2\rangle_{\text{skeleton}}} \tag{17}$$

The constitutive law is given by Eqs. (9) and (15):

$$\sigma_{ij}=2\eta_o(\varphi\dot{\varepsilon}_{ij}'+\psi e\delta_{ij})+P_L\delta_{ij} \tag{18}$$

providing that:

$$\frac{\partial W}{\partial \dot{\varepsilon}_{ij}} = \frac{1}{(1-\theta)W}(\varphi \dot{\varepsilon}_{ij}' + \psi e \delta_{ij}) \tag{19}$$

From Eq. (18) we have:

$$p = \frac{1}{3}\mathrm{tr}\sigma = 2\eta_o \psi e + P_L \tag{20}$$

and

$$\tau = \sqrt{\sigma_{ij}'\sigma_{ij}'} = 2\eta_o \varphi \gamma \tag{21}$$

where σ_{ij}' is the deviatoric stress tensor.

Substituting into Eq. (16) e and γ from Eq. (20), Eq. (21), we have:

$$W = \frac{1}{2\eta_o}\frac{1}{\sqrt{1-\theta}}\sqrt{\frac{\tau^2}{\varphi} + \frac{(P-P_L)^2}{\psi}} \tag{22}$$

Defining an equivalent stress σ as:

$$\sigma = \frac{1}{\sqrt{1-\theta}}\sqrt{\frac{\tau^2}{\varphi} + \frac{(P-P_L)^2}{\psi}} \tag{23}$$

Eq. (22) can be written as:

$$\sigma = 2\eta_o W \tag{24}$$

2.2. Incompressible nonlinear-viscous material

The second example considered is an incompressible material ($\theta = 0$).

From Eq. (14) we have $\varphi \to 1$ and $\psi \to \infty$ when $\theta = 0$.

Because of the matrix incompressibility, we have $e \to 0$. It can be demonstrated in general that $\psi e^2 \to 0$. Therefore, $W \to \gamma$ and the dissipative potential of a linear-viscous fluid is derived from Eq. (15):

$$D = \eta_o \gamma^2 \tag{25}$$

An extension into nonlinear-viscous behavior is obtained by considering the following dissipation potential:

$$D = \frac{A}{m+1}\gamma^{m+1} \tag{26}$$

where m is the strain rate sensitivity and A is a material parameter depending in general on the temperature.

The deviatoric stress is obtained from Eq. (9):

$$\sigma_{ij}' = \frac{\partial D}{\partial \dot{\varepsilon}_{ij}} = A\gamma^{m+1}\dot{\varepsilon}_{ij}, \ (\dot{\varepsilon}_{ij} = \dot{\varepsilon}_{ij}') \tag{27}$$

and we have with the definition (Eq. (21)) of τ:

$$\tau = A\gamma^m \tag{28}$$

When m varies from $m=1$ to $m=0$, the material response is transferred from that of a linear-viscous incompressible fluid to that of a rigid perfectly plastic incompressible material. With $m=1$, we have the dissipation of a linear-viscous fluid:

$$D=\frac{A}{2}\gamma^2 \tag{29}$$

with viscosity $\eta_o=A/2$. When $m\to 0$, it can be seen from Eq. (28) that at the limit, the behavior of a perfectly plastic material is obtained with shear yield stress $A/\sqrt{2}$.

2.3. Nonlinear-viscous porous material

From the foregoing consideration, a general framework can be proposed that provides the constitutive law for a nonlinear-viscous porous material.

Using a power-law dependence, the dissipation potential of a porous material can be represented:

$$D=\frac{A}{m+1}(1-\theta)W^{m+1} \tag{30}$$

Assuming that the material in the matrix is incompressible and nonlinear-viscous with potential:

$$D_{\text{matrix}}=\frac{A}{m+1}\gamma^{m+1},$$

for $\theta=0$ we have $W=\gamma$, and the potential (Eq. (26)) of an incompressible nonlinear-viscous material is obtained. For $m=1$, we have the potential of a linear-viscous porous material ($A=2\eta_o$).

Using Eqs. (9) and (30), we obtain the following constitutive law:

$$\sigma_{ij}=AW^{m-1}(\varphi\dot{\varepsilon}_{ii}'+\psi e\delta_{ij})+P_L\delta_{ij} \tag{31}$$

from which we have:

$$\tau=A\varphi W^{m-1}\gamma \tag{32}$$

$$p=A\psi W^{m-1}e+P_L$$

Extracting γ and e and substituting into Eq. (16) leads to the following relationship between the equivalent stress σ and the equivalent strain rate W:

$$\sigma=AW^m \tag{33}$$

Note that the form of expression (Eq. (33)) coincides with the form of relationship (Eq. (28)) obtained for the incompressible matrix material.

The next step is a generalization of the relationship (Eq. (33)) between equivalent stress and equivalent strain rate:

$$\sigma=\sigma(W) \tag{34}$$

where $\sigma(W)$ is an arbitrary function of W.

In this general case, the constitutive relationship for a nonlinear-viscous porous material can be represented in the form:

$$\sigma_{ij}=\frac{\sigma(W)}{W}(\varphi\dot{\varepsilon}_{ii}'+\psi e\delta_{ij})+P_L\delta_{ij} \tag{35}$$

The relationship (Eq. (35)) is the basic constitutive expression for the continuum theory of sintering. It can be demonstrated that this relationship can be used for the description of a wide range of possible processes of powder treatment. The left-hand part of this equation (σ_{ij}) corresponds to externally applied stresses. The first term of the right-hand part [$\sigma(W)/W(\varphi\dot{\varepsilon}_{ii}'+\psi e\delta_{ij})$] is the material resistance, and the second term of the left-hand part ($P_L\delta_{ij}$) corresponds to the influence of capillary stresses (sintering factor). In cases when (i) externally applied (σ_{ij}) or (ii) capillary stresses (P_L) are equal to zero, Eq. (35) describes (i) free sintering or (ii) treatment by pressure without sintering, respectively. If all the terms are represented, ($\sigma_{ij}\neq 0$, $P_L\neq 0$) Eq. (35) describes sintering under pressure.

From Eq. (35) we have:

$$\tau=\frac{\sigma(W)}{W}\varphi\gamma \tag{36}$$

$$p=\frac{\sigma(W)}{W}\psi e+P_L$$

From Eq. (36) one can obtain an important relationship between the invariants of stress–strain rate state:

$$(p-P_L)\varphi\gamma=\tau\psi e \tag{37}$$

3. Dependence of the constitutive parameters on porosity

This problem is a particular case of the determination of effective properties for a heterophase body. For porous materials, a considerable amount of work has been carried out by many authors (see, for example, for linear-viscous materials Refs. [19,66,67,71,86,103,104] and, for materials with power-law creep properties, Refs. [101,157,159,160]). As an example, the expression for the normalized bulk modulus ψ derived by some authors both for linear-viscous and for power-law constitutive properties of the porous body skeleton are represented in Fig. 2.

Below, an approach for the determination of the bulk and shear viscosity moduli, suggested by Skorohod [19], is described.

3.1. Derivation of the expressions for the normalized shear and bulk viscosity moduli for porous material (determination of the functions $\varphi(\theta)$ and $\psi(\theta)$)

From this point on a hydrodynamic analogy of the theory of elasticity is employed. The latter means that due to a similarity between the constitutive equations describing the behavior of linear-viscous and linear-elastic materials, a corresponding problem can be solved assuming elastic properties of the material and the results obtained can be interpreted in the framework of linear-viscous formulation.

3.1.1. Determination of the normalized shear modulus ($\varphi(\theta)$)

Consider the porous medium as a two-phase material of the matrix type. The incompressible *elastic* matrix corresponds to a substance, and the second phase (inclusions) corresponds to voids.

For a small concentration of spherical inclusions ($\theta\ll 1$), one can use a formula known from mechanics of composite materials: [1]

[1] See, for example, R.M. Christensen, Mechanics of Composite Materials, John Wiley and Sons, 1979.

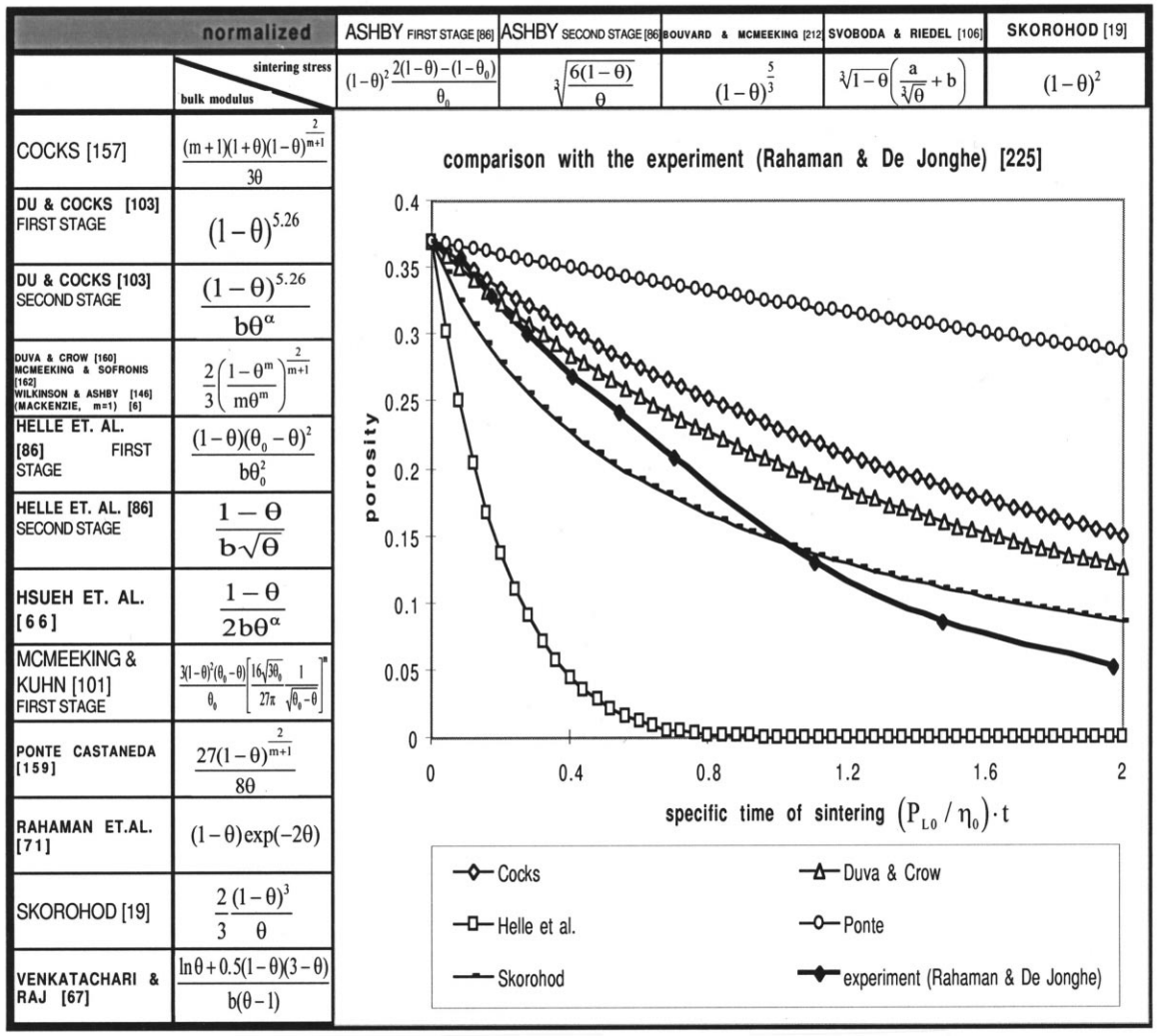

$$\frac{\dot{\theta}}{1-\theta} = -\frac{P_L}{2\eta_0\psi}$$

Fig. 2. Expressions for the bulk viscosity and the effective Laplace pressure as functions of porosity (b and θ_0 are material parameters related to the grain size and porosity of a loose powder, respectively) and the comparison of sintering kinetics for different models and the experiment of Rahaman and De Jonghe [166]. For all the models, Ashby expression for the effective Laplace pressure was used, for Skorohod's model—the expression derived by Skorohod [19].

$$\mu = \mu_o\left(1-\frac{5}{3}\theta\right) \tag{38}$$

where μ_o is the shear elastic modulus of the matrix, and μ is the effective shear elastic modulus for a porous material.

For shear viscosity of a porous material, by hydrodynamic analogy, one can write:

$$\eta = \eta_o\ \ 1-\frac{5}{3}\theta \tag{39}$$

To expand the above-mentioned result for the range of larger porosities, following Skorohod [19], one can use a method of differential scheme.

Let us represent the dependence (Eq. (39)) in a differential form:

$$d\eta = -\frac{5}{3}\eta_o d\theta \tag{40}$$

In accordance with the method of differential scheme, the shear viscosity of the fully-dense material has to be substituted by the effective viscosity of the porous material and differential of porosity is given by the substituting expression: $d\theta/(1-\theta)$. Then we obtain:

$$d\eta = -\frac{5}{3}\eta\frac{d\theta}{1-\theta} \tag{41}$$

Integrating, we derive:

$$\eta = \eta_o(1-\theta)^{5/3} \tag{42}$$

Solving the same problem for cylindrical pores and comparing the results, Skorohod [19] determined the following approximation for the shear modulus:

$$\eta = \eta_o(1-\theta)^2 \tag{43}$$

Comparing Eqs. (13) and (43), we obtain the first expression in Eq. (14).

3.1.2. Determination of the normalized bulk modulus ($\psi(\theta)$)

First, let us consider the case of small porosity ($\theta \ll 1$). Assume that distances between pores are much larger than their size. We can consider a representative element—a spherical pore which is surrounded by a layer of an incompressible *elastic* substance (see Fig. 3).

If R_1 is the pore radius, and R_2 is the radius of the whole element, than the following condition is valid:

$$\frac{R_1^3}{R_2^3} = \theta \tag{44}$$

Assume that an external pressure P is applied at the surface of the representative element. Then, solving the corresponding elastic problem, one can find the displacement u_2 of the external boundary of the representative element:

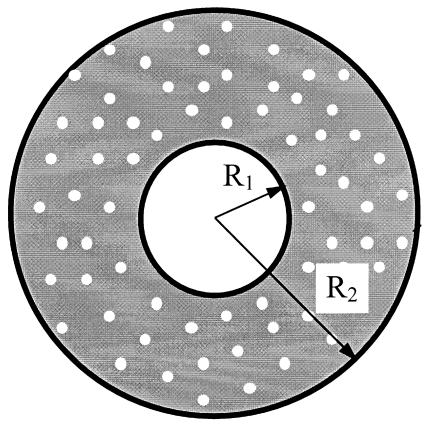

Fig. 3. Representative element for the determination of the bulk modulus.

$$u_2 = -\frac{PR_1^3 R_2}{(R_2^3 - R_1^3)4\mu_o} = -\frac{PR_2}{4\mu_o}\frac{(\theta)}{1-\theta} \tag{45}$$

A mean radial deformation $\bar{\varepsilon}_r$ of the representative element can be written:

$$\bar{\varepsilon}_r = \frac{u_2}{R_2} = -\frac{P}{4\mu_o}\frac{\theta}{1-\theta} \tag{46}$$

Considering the representative element as a compressible body with the bulk modulus K, one can write:

$$\bar{\varepsilon}_r = -\frac{P}{3K} \tag{47}$$

From Eqs. (46) and (47) we obtain:

$$K = \frac{4}{3}\mu_o\frac{1-\theta}{\theta} \tag{48}$$

For a linear-viscous body, the corresponding relationship can be represented:

$$\zeta = \frac{4}{3}\eta_o\frac{1-\theta}{\theta} \tag{49}$$

where ζ is the bulk viscosity for the porous material.

The expression (Eq. (49)) was obtained by Mackenzie and Shuttleworth [6].

Let us consider a body with arbitrary porosity. Using the self-consistent approach, we can consider each pore as a spherical cavity in a compressible substance with elastic moduli K and μ.

If a pressure P is applied at infinity, then the displacement u_1 at the pore boundary is [19]:

$$u_1 = PR_1\left(\frac{1}{3K} + \frac{1}{4\mu}\right) \tag{50}$$

The mean volume deformation of the pore can be written:

$$3\bar{\varepsilon}_r = 3\frac{u_1}{R_1} = -P\left(\frac{1}{K} + \frac{3}{4\mu}\right) \tag{51}$$

As the substance is considered to be incompressible, the mean volume deformation of the porous body should be equal to a sum of the volume deformations of all the pores, i.e.:

$$\frac{\Delta V}{V} = -\frac{P}{K} = -P\left(\frac{1}{K} + \frac{3}{4\mu}\right)\theta \tag{52}$$

From the latter expression we obtain:

$$K = \frac{4}{3}\mu\frac{1-\theta}{\theta} \tag{53}$$

And for a linear-viscous material:

$$\zeta = \frac{4}{3}\eta\frac{1-\theta}{\theta} \tag{54}$$

which is an evident generalization of Eq. (49).

Substituting the expression (Eq. (43)), obtained for the shear modulus η, into Eq. (54), we have:

$$\zeta = \frac{4}{3}\eta_o \frac{(1-\theta)^3}{\theta} \tag{55}$$

Introduce the following designations:

$$\zeta = 2\eta_o \psi \tag{56}$$

$$\psi = \frac{2}{3}\frac{(1-\theta)^3}{\theta}$$

3.2. Derivation of the expression for the effective Laplace pressure (sintering stress)

At the microscopic level, the determination of local capillary stresses is important (acting at the surface of one pore or particle). A substantial number of publications is dedicated to this topic, see Refs. [167–204].

In the framework of the continuum theory of sintering, the effective Laplace pressure (sintering stress) defined by Eq. (8) corresponds to the result of the collective action of local capillary stresses in a porous material. The relationship between the effective and local Laplace pressure depends on the procedure of averaging of the above mentioned local stresses over a macroscopic porous volume.

A question of the determination of the effective Laplace pressure ('sintering stress,' 'sintering potential,' 'sintering (driving) force') has been studied by many authors [10,19,43,44,49,51,57,59, 64,66,69,74,81,86,101,105,107,116,117,125,127,131–133,143,205–213]. The expressions for the normalized effective Laplace pressure obtained by different authors are represented in Fig. 2.

Coble [10] constructed a model for sintering of a porous material comprising cylindrical voids. The sintering rate was taken to be proportional to the pore surface area and to the driving force for sintering which was derived entirely from the cylindrical pore curvature. At the same time, experimentally the driving force for sintering was analyzed by Lenel et al. [205].

Skorohod [19] suggested a stochastic approach for determination of the effective Laplace pressure (see below).

Gregg and Rhines [206] introduced the term 'sintering force' which refers to the force necessary to just stop the sintering contraction along one axis of the sintered body. The experiments on sintering of copper powders showed the increase of sintering force with density up to 95% of the relative density and the decrease of the sintering force for densities higher than 95%.

Beere [207] determined the 'driving force for sintering' as the difference in vacancy concentrations at the pore surface and the grain boundary. The sintering force in this model can be expressed as a function of porosity through the dependence between pore volume fraction and dihedral angle between grain surfaces. The expressions for the sintering force were obtained for the volume and grain boundary diffusion mechanisms. Here the sintering force is inversely proportional to the grain size.

Bordia and Scherer [81] demonstrated that, for linear-viscous models, the effective Laplace pressure can be expressed as a product of the volume shrinkage rate and the effective bulk viscosity. Thus, the effective Laplace pressure can be derived for the models which provide explicit relationships for these two values.

Rahaman et al. [59] obtained an expression for the sintering stress using the Zener relation. The sintering stress is represented as the ratio between surface tension and the product of the grain size and porosity. Thus, in the framework of this model, the sintering stress increases with density for a fixed grain size. However, the experiments on sintering of CdO powder indicated the decrease of the sintering

stress with increasing density when grain growth occurs (which is in agreement with the results of Beere [207]).

Hsueh et al. [66], using a visco-elastic analysis and based upon experimental data for hot pressing experiments of Al_2O_3 powder, came to the conclusion of the constancy of the sintering stress. It should be noted that hot pressing involves additional factors in comparison with free sintering (such as friction forces, for example), which can be a reason for the deviation of these results from those obtained by Beere [207] and Rahaman et al. [59].

De Jonghe and Rahaman [74] determined the thermodynamic meaning of the sintering stress for two-dimensional porous bodies. They postulated that the sintering stress for a densifying powder compact can be considered as an equivalent applied stress that would produce the same densification rate for the system, at identical geometry but with surface tension effects absent. Basically, this definition is limited by the case of homogeneous porous material.

Ashby [86] introduced two expressions for the effective Laplace pressure considering two stages of sintering (see Fig. 1). At the first stage (when the relative density is not higher than 92%), an open character of porosity prevails. Here, for the derivation of the effective Laplace pressure, the expression for the average contact area as a function of the relative density is used. At the second stage, pores are separated. Here, the effective Laplace pressure is defined as a ratio of the double surface tension and the pore radius. The expression for the dependence of the pore radius on the relative density (obtained by Swinkels and Ashby [16]) is substituted into the relationship for the effective Laplace pressure which, thus, becomes a function of the relative density as well. For both stages, the effective Laplace pressure increases with the increase of the relative density. These results have been modified by Cocks [125] who introduced an additional item responsible for the increase in grain boundary area.

Later, the expression for the effective sintering stress (sintering potential) was derived for the different controlling mechanisms of material flow under sintering.

McMeeking and Kuhn [101] and Bouvard and McMeeking [213] developed a relationship for the effective Laplace pressure for diffusion controlled creep at the earlier (first) stage of sintering. Here the effective Laplace pressure increases with the increase of the relative density. This result is also modified by Cocks [125] by introduction of an additional term responsible for the increase in grain boundary area.

Besson and Abouaf [105] noted that the dependence of the effective Laplace pressure on the relative density seems to be related to the material, processing (cold compaction) and testing conditions.

Cocks and Aparicio [133] defined the effective 'sintering force' as the applied force which provides the stress field which is in equilibrium with this force and surface tension and satisfies the boundary condition for the capillary stresses at the pore surface while stress gradients are absent at the pore surface.

Riedel et al and Svoboda et al. [127,131,132,143] in a series of works elaborated models of sintering with diffusional creep (grain boundary) as a controlling mechanism of material flow. The expressions for effective sintering stress include the specific grain boundary energy [127], the inter-particle neck geometrical parameters [131], and the contribution of the solid–liquid interface energy (in the case of liquid-phase sintering) [143]. Here the effective sintering stress increases with increasing relative density for large values of the dihedral angle between grain surfaces and decreases with increasing relative density for small values of the dihedral angle.

Below we represent the derivation of the expression for the effective Laplace pressure based upon the stochastic approach [19] employed by Skorohod.

As it is shown in Section 2, the effective Laplace pressure is equal to the derivative of the free energy per unit mass with respect to the volumetric mass of the porous material (Eq. (8)). For the

consideration of sintering, the free energy can be reduced to the free surface energy and, therefore, one can write:

$$P_{\mathrm{L}}=\frac{\mathrm{d}F_{\mathrm{s}}}{\mathrm{d}V} \tag{57}$$

Here, F_{s} is the free surface energy, and V is a porous volume.

Introduce the value ξ which is a specific surface area of a porous body:

$$\xi=\frac{\Omega}{V_{\mathrm{m}}} \tag{58}$$

where Ω is a full free surface area (surface of pores); V_{m} is the volume of substance (matrix) in the porous material.

The derivative $\mathrm{d}\xi/\mathrm{d}\theta$ determines the moving force for sintering:

$$\frac{\mathrm{d}F_{\mathrm{s}}}{\mathrm{d}V}=\alpha\frac{\mathrm{d}\xi}{\mathrm{d}\theta}(1-\theta)^2 \tag{59}$$

where α is a surface tension.

For the derivation of Eq. (59), the following relationships are taken into consideration:

$$\frac{V-V_{\mathrm{m}}}{V}=\theta;\qquad \frac{\mathrm{d}F_{\mathrm{s}}}{\mathrm{d}V}=\frac{\mathrm{d}F_{\mathrm{s}}}{\mathrm{d}\xi}\cdot\frac{\mathrm{d}\xi}{\mathrm{d}\theta}\cdot\frac{\mathrm{d}\theta}{\mathrm{d}V};\qquad \frac{\mathrm{d}F_{\mathrm{s}}}{\mathrm{d}\Omega}=\alpha;\qquad \frac{\mathrm{d}\theta}{\mathrm{d}V}=\frac{(1-\theta)^2}{V_{\mathrm{m}}} \tag{60}$$

The value ξ is a function of the porosity and the mean curvature of the pore surface, which can be estimated for porous powder systems as being inversely proportional to the mean radius of powder particles r_{o}:

$$\xi=\frac{B}{r_{\mathrm{o}}}g(\theta) \tag{61}$$

where B is a constant which is equal to 3 for spherical particles. The function $g(\theta)$ should satisfy certain requirements: it should be monotonously increasing with respect to θ, it should be equal to zero when $\theta=0$ and it should be finite when $\theta\to 1$. The latter requirement is connected with the fact that the surface of a porous body cannot be larger than the full summarized surface of particles, which is equal to B/r_{o}.

For an ideal statistical composition of isomeric quasi-spherical pores and particles, on the basis of an elementary probabilistic analysis, it follows [19]:

$$g(\theta)=\theta$$

Finally, we obtain:

$$P_{\mathrm{L}}=\frac{3\alpha}{r_{\mathrm{o}}}(1-\theta)^2 \tag{62}$$

3.3. Kinetics of free sintering of linear-viscous porous material

For linear-viscous properties of the porous body skeleton, Eq. (20) is valid. Hence:

$$e=\frac{p-P_{\mathrm{L}}}{2\eta_0\psi}$$

In the case of free sintering, the external stresses are absent, and $p=0$. Thus:

$$e=\frac{P_L}{2\eta_0\psi}$$

The continuity condition gives:

$$e=\frac{\dot{\theta}}{1-\theta}$$

Then:

$$\frac{\dot{\theta}}{1-\theta}=-\frac{P_L}{2\eta_0\psi}$$

Substituting expressions derived by different authors for the sintering stress P_L and the normalized bulk viscosity modulus ψ, one can obtain various models of free sintering kinetics (Fig. 2). A comparison of models for sintering kinetics based upon different expressions for ψ and the same expression (Ashby [86]) for P_L is represented in Fig. 2. Here ψ from Skorohod's model is coupled with P_L derived by Skorohod [19]. The calculation results are compared with experiment of Rahaman and De Jonghe [166] on free sintering of spherical glass powder.

The fit of most of models to experimental data in Fig. 2 is rather poor. A deviation of many sintering models from the experimental data on shrinkage kinetics led Bordia and Scherer [81] to the idea of the definition of the effective sintering stress (P_L) as a ratio between the determined volume shrinkage rate and the bulk viscosity modulus. At the same time, the data in Fig. 2 can support the choice of the above-mentioned ψ and P_L (Eqs. (56) and (62)) which provide the best agreement with the experimental data.

4. Sintering combined with uniaxial loading

An evident application of the continuum (rheological) approach is the problem of sintering of a porous body subjected to a uniaxial load (sinter forging or tension). For most materials, the Laplace pressure produced by the surface tension does not exceed the value of several MPa. Therefore, only for processes of relatively low external loading, a competitive influence of sintering shrinkage and creep deformation due to externally applied stresses can be observed. Also, one should take into consideration the time factor. Being a relatively slow process, sintering can be essential for the uniaxial deformation which acts during a comparable time interval. This means that sintering should have enough time to provide deformation of the same order of magnitude that caused by forging. Thus, in many cases, sinter forging is a relatively slow process (continued during a time comparable to the time of a free sintering) occurring under a relatively low level of applied uniaxial stresses (comparable to the Laplace pressure).

Sintering under applied stresses has been studied in a number of works, see Refs. [19,44,45, 59,60,67,68,71,73–75,81,85,93,105,110,112,128,130,166,206,214–228].

One of the first experimental works on sintering under uniaxial load has been performed by Fedorchenko and Andrievski [214]. A static uniaxial load was applied to copper and nickel porous samples during sintering. Based upon the idea of the superposition of the Laplace pressure and applied stress, the determination of the sintering stress has been carried out by means of the extrapolation of the dependence 'load-dilatation.'

Skorohod [19], using the rheological theory of sintering, obtained the constitutive relationship for sintering under uniaxial applied load. The model is based upon the idea of linear-viscous properties of the matrix material.

Gregg and Rhines [206] (see also Section 3.2) carried out the experiments on sinter tension with an uncompressed copper powder. Here no dependence of the sintering force of the relative density was envisaged.

Savitskii [25] De Jonghe and Rahaman [217] and Rahaman et al. [59,60] used a loading dilatometer for examination of how creep and densification affect one another when they occur simultaneously. In the mentioned work, as an object under investigation CdO powder compacts were considered during sintering under low uniaxial stresses between 0 and 0.25 MPa. The results of the experiment were used for the determination of the functional dependence of the effective stress in creep, and the sintering stress in densification, on relative density and grain size. The sintering stress was found to decrease with increasing relative density when the grain size is not fixed. For a given grain size, sintering stress increased with the relative density.

Venkatachari and Raj [67] reported on experiments in sintering of magnesia-doped alumina powder samples under a superimposed uniaxial load. While Rahaman et al. [60] measured only the axial strain and derived the radial displacements from the measurement of the change in density in specimens obtained from a series of interrupted tests, in the experiments of Venkatachari and Raj [67] the two component strains were obtained from measurements of the axial and the radial displacements in specimens of a cylindrical shape. The experiments have provided a direct measure of the intrinsic sintering pressure which was found to lie in the range of 0.4 to 0.8 MPa. It was found that the rate of densification followed a linear dependence of the total mean pressure and a cubic dependence of the average grain size. In opposite to Rahaman et al. [60], where externally applied stress was smaller than the triple Laplace pressure (see Eq. (75) below), Venkatachari and Raj [67] applied axial stresses which were larger than the triple Laplace pressure. This enabled the determination of the Laplace pressure (using results of Raj [46]) by the same extrapolation methodology which has been used by Fedorchenko and Andrievski [214]. Later, the experimental results of Venkatachari and Raj [67] were used by Kwon et al. [130] for confirmation of the constitutive relationships derived for the description of thermotreatment of alumina powder compacts. The creep strain rates in the model of Kwon et. al. [130] were obtained based upon the constitutive equations of Helle et al. for hydrostatic response and by Rahaman et al. [59,60] for deviatoric response.

Scherer [68] obtained numerical solutions, in the framework of the linear-viscous model, for the evolution of the radius, height and relative density of a porous cylindrical specimen sintered under a constant uniaxial load.

Rahaman et al. [71] investigated sinter forging of a soda-lime glass powder. It was found that, for a constant applied stress, the ratio of the creep rate to the densification rate is almost independent of both temperature and density. The same result was obtained by Rahaman and De Jonghe [218] for zinc oxide powder. These observations were consistent with Scherer's model [68]. However, both densification rate and viscosity, having an exponential dependence on viscosity, showed much stronger dependence on density compared with predictions of the Scherer's model. This discrepancy was related by the authors to the peculiarities of pore size distribution in the samples investigated as well as to the lenticular pore shape causing anisotropic shrinkage under pressureless sintering. In the later work, Rahaman and De Jonghe [166] considered sintering of a well-characterized, spherical glass powder with a relatively narrow particle size range. In this case, the experimental data showed good agreement with Scherer's theory of viscous sintering.

Later Chu et al. [223] analyzed the effect of temperature and green density [226] on densification and creep during sintering. The data [223] showed that the ratio of the densification rate to the creep

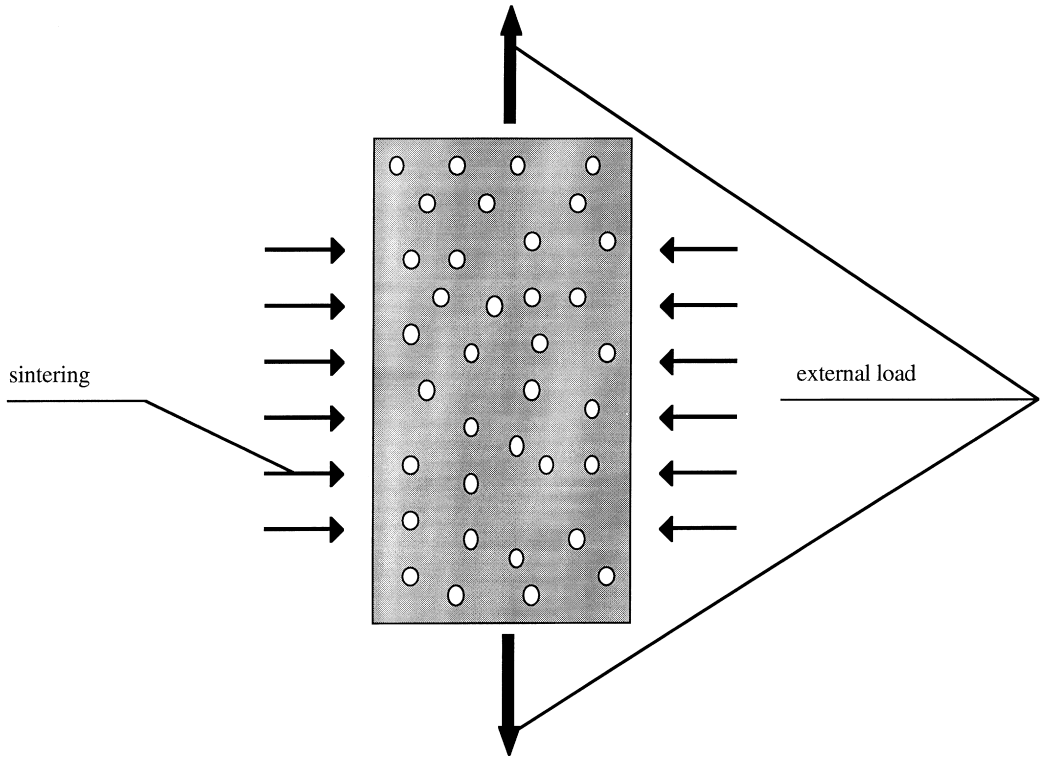

Fig. 4. Sintering under uniaxial loading.

rate (which is related in the framework of the continuum theory of sintering to the ratio between the applied stress and effective Laplace pressure) is nearly independent of temperature (which means a weak dependence of surface energy of temperature). The ratio of the densification rate to the creep rate increased almost linearly with increasing green density [226] (which means a corresponding linear dependence of the effective Laplace pressure of the relative density).

Geguzin et al. [220] studied sintering of copper porous specimens under uniaxial tensile load. It was established (see Eq. (75)) that densification is absent when the applied axial tensile stress is equal to the triple Laplace pressure.

Bordia and Raj [56] used sinter forging experiments for the determination of the sintering rate by means of measuring the contaminant shear and densification rate in TiO_2–Al_2O_3 composites.

Olevsky and Skorohod [73] and Skorohod et al. [85,93,110] applied the continuum concept of sintering for the analysis of both sinter forging and sinter tension processes. The results of modeling were in good agreement with the experimental data of Fedorchenko and Andrievski [214], Gegusin et al. [220] and Andrievski [222]. Here, the model was not limited by the framework of the linear viscosity. Sintering under uniaxial loading has been studied for both linear- and nonlinear-viscous (in particular, plastic) constitutive properties of the matrix (see below).

Panda and Lagraff [221] considered uniaxial deformation of nickel aluminide powders under elevated temperatures (above 1373°K). Here the effect of Laplace pressure was neglected. A model for densification by power-law creep was applied to the data. However, power-law relationships were used for the hydrostatic and the deviatoric invariants of the stress–strain rate state separately, which apparently led to the great overestimation of the measured densification rates.

Bordia and Scherer [81] have compiled a review of previous models describing bodies that sinter under constraint. A critical examination of the various models revealed that some of them implied a

negative Poisson's ratio, which is allowed on thermodynamic grounds but is inconsistent with experimental observation. Here also the differences in determination of the Poisson's ratio for uniaxial load under sintering should be noted (including and not including items corresponding to the densification due to sintering). Bordia and Scherer suggested sinter forging experiments under different stresses in order to determine the effective shear, bulk viscosity moduli and the effective Laplace pressure.

Ducamp and Raj [224] have carried out sinter forging experiments on powder compacts of borosilicate glass. The shear and densification strains were measured simultaneously during the forging process. This information was analyzed to obtain the shear viscosity of the glass and the Laplace pressure, both as a function of the relative density. The effective viscosity of the porous glass was empirically fitted to an exponential function of the relative density. The Laplace pressure was found to increase with density.

Besson and Abouaf [105] used sinter forging for the determination of the effective constitutive properties of porous alumina. Here the effective stress and strain rate were determined (similar to Olevsky and Skorohod [85] and Skorohod et al. [110]) and the dependence between these parameters was found to follow the Coble creep law.

Skorohod et al. [112] and Olevsky [128] formulated and solved (by the finite element method) a boundary-value problem of sinter forging. It was found that, depending on punch velocity, different situations of material flow might occur. A possibility of a barrel-like or 'waist' shape of the lateral surface of a cylindrical porous specimen was indicated (see below).

Let us consider a series of problems concerning sintering of a homogeneous body under uniaxial tension or compression (Fig. 4). In this case only one component of the stress tensor differs from zero: $\sigma_z = 3p$. Furthermore, the strain rate tensor $\dot{\varepsilon}_{ij}$ is diagonal, therefore:

$$\dot{\varepsilon}_r = \dot{\varepsilon}_\phi, \qquad e = \dot{\varepsilon}_z + 2\dot{\varepsilon}_r, \qquad \gamma = \sqrt{\frac{2}{3}}\,|\dot{\varepsilon}_z - \dot{\varepsilon}_r| \tag{63}$$

For invariants of the stress state:

$$p = \frac{1}{3}\sigma_z, \qquad \tau = \sqrt{\frac{2}{3}}\,|\sigma_z - \sigma_r| = \sqrt{\frac{2}{3}}\,|\sigma_z| \tag{64}$$

Let us designate the coefficient of transverse compression in uniaxial loading (analogy of the Poisson's ratio) as

$$\nu = -\frac{\dot{\varepsilon}_r}{\dot{\varepsilon}_z} \tag{65}$$

From Eqs. (63)–(65) and (20) it follows that the relationship between the coefficients of transverse compression and axial tension (taking into consideration the continuity condition $e = \dot{\theta}/1-\theta$) is:

$$\nu = \frac{2-3\theta+3(P_L/\sigma_z)\theta}{4-3\theta-3(P_L/\sigma_z)\theta} \tag{66}$$

In the absence of sintering, when $P_L = 0$, the following equation for the analogy of the Poisson's ratio of a body with the porosity θ is valid:

$$\nu = \frac{2-3\theta}{4-3\theta} \tag{67}$$

It follows from Eq. (63) and the definition of the coefficient of transverse compression that:

$$e=(1-2\nu)\,\dot{\varepsilon}_z \tag{68}$$

Accordingly:

$$\dot{\varepsilon}_z=\frac{\dot{h}}{h} \tag{69}$$

where h is the current height of a cylindrical sample subjected to uniaxial deformation; $\dot{h}$ is the rate of change of the current height.

Considering the porous body skeleton as linear-viscous, one obtains from Eqs. (66), (68) and (69):

$$\dot{\theta}=3(1-\theta)\,\frac{\eta_0\varphi(\dot{h}/h)-P_L}{\eta_0(6\psi+\varphi)} \tag{70}$$

The solution of Eq. (70) is written in the form:

$$t=t_i\int_{\theta_i}^{\theta(t)}\frac{\eta_o(6\psi+\varphi)}{3(1-\theta)[\eta_o\varphi(\dot{h}/h)-P_L]}\,d\theta \tag{71}$$

where θ_i and t_i are the initial values of porosity and time.

For the case of uniaxial tension, the effects of sintering and the external applied load are opposed. Taking into account the expression for the effective sintering stress (Eq. (67)), we arrive at the conclusion that for a suitable choice of $\dot{h}/h$, for which the equality

$$\frac{\dot{h}}{h}=\frac{3\alpha}{r_o\eta_o} \tag{72}$$

is satisfied, a condition of 'zero' densification is realized (the rate of change of porosity is zero).

Solution of the differential Eq. (72) gives:

$$h=h_i\exp(\tau_s) \tag{73}$$

where h_i is the initial height of the sample and τ_s is the specific time of sintering:

$$\tau_s=\int_t\frac{P_L}{\eta}\,dt \tag{74}$$

where t is real time.

Eq. (73) is the equation of the curve separating the regions of densification and expansion in the coordinates τ_s and h for the case of a cylindrical specimen sintered under uniaxial tension (Fig. 5a). Actually, when $3\alpha/r_o\eta_o\leqslant\dot{h}/h$ expansion occurs under tension, and when $3\alpha/r_o\eta_o>\dot{h}/h$ densification occurs, that is, in this case the Laplace pressure prevails over the viscous stresses caused by application of the external load.

It is interesting to consider this question from not only a kinematic point of view, but also in terms of the stress state. From Eq. (20) it follows:

$$\dot{\theta}=\frac{1}{6}(1-\theta)\,\frac{\sigma_z-3P_L}{\eta_o\psi} \tag{75}$$

The regions of expansion and densification in the coordinates σ_z, P_L for the case of sintering combined with tensile loading are separated by the line $\sigma_z=3P_L$ (Fig. 5b).

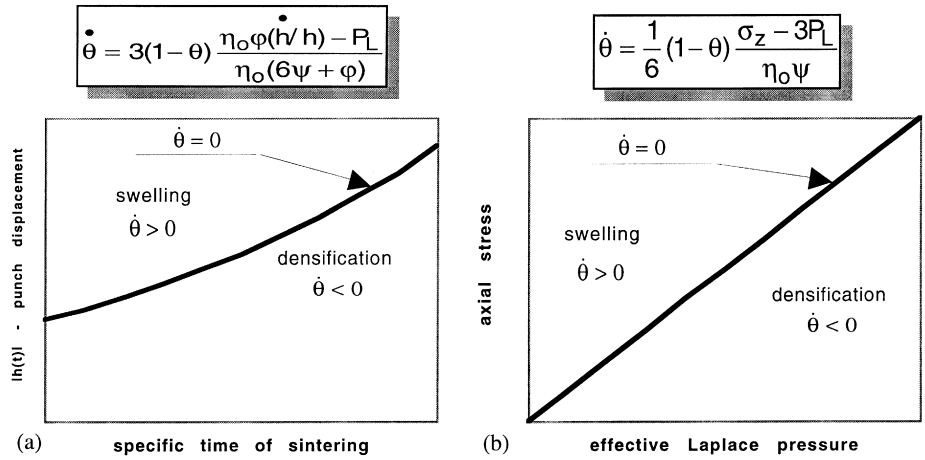

Fig. 5. Conditions of 'zero densification'. (a) Required punch movement law. (b) Required applied axial stress.

Taking account of the expressions for ψ and φ we obtain from Eq. (75):

$$\int_{\theta_i}^{\theta} \frac{d\theta}{\theta\ \frac{\lambda}{3(1-\theta)^2} - 1} = 3\tau_s \tag{76}$$

where θ_i is the initial porosity, $\lambda = \sigma_z/(3\alpha/r_o)$.

From Eq. (76) it follows that at $\lambda > 3(1-\theta)^2$ the porous body densifies, and at $\lambda < 3(1-\theta)^2$ it expands. This result is qualitatively supported by experimental data [222] confirming the phenomenon of densification during the sintering of silver briquettes under tension when the ratio of the applied axial stress to the Laplace pressure is small. If $3\alpha/r_o = 0.05$ MPa [214] and $\tau_s = 0.11$ [19,222] then the curve $\theta(\lambda)$ of Eq. (76) is in almost complete accord with the data of Ref. [222], which describe the effect of uniaxial tension on the kinetics of densification of silver briquettes at 900°C for 15 min (Fig. 6). Thus, the nonmonotonous character of the change of porosity with the ratio of the axial tension to the local value of the Laplace pressure during sintering with combined tension can be explained by the purely viscous flow model.

A tensile stress may occur in the sintered specimen not only when the externally applied load is tensile, but also (in the case of a very slow deformation) under uniaxial compression when the external surface and the punch surface are fully bonded. It is not difficult to show that for a linear-viscous solid:

$$\sigma_z = \frac{3\varphi}{6\psi+\varphi}\ 6\eta_o\psi\frac{\dot{h}}{h} + P_L \tag{77}$$

From this it follows that the above-mentioned effect appears when:

$$-\frac{P_L}{6\eta_o\psi} < \frac{\dot{h}}{h} < 0 \tag{78}$$

The physical explanation of this effect is that the deformation velocity at the surface of the body which is attached to the pressing equipment (a punch) is slower than the velocity of this surface during free sintering. If there is no bonding between the face of the specimen and the compressing punch, and

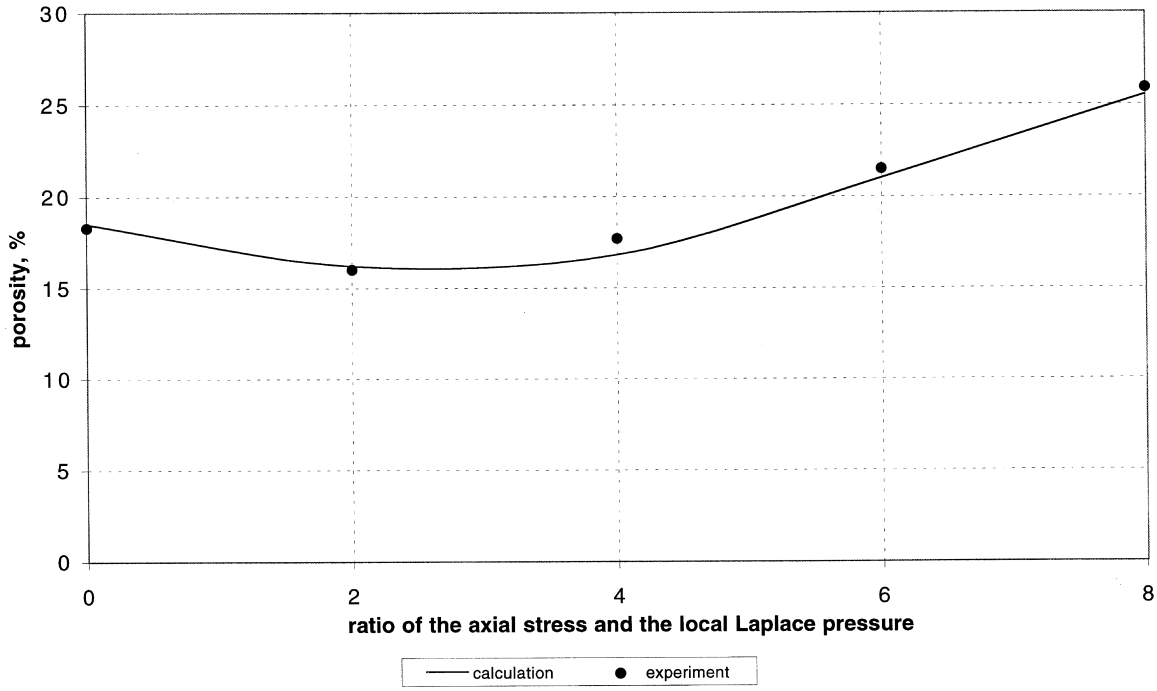

Fig. 6. Comparison of the calculation and experimental data [222] on sinter-tension of a silver powder specimen.

$$\frac{\dot{h}}{h}=\frac{P_{\mathrm{L}}}{6\eta_{\mathrm{o}}\psi} \tag{79}$$

then 'tearing' of the specimen from the equipment might occur (in this case $\sigma_{\mathrm{z}}=0$).

One more effect observable during free compression deserves attention. In the absence of sintering the radial flow rate is positive—the specimen material flows away from the central axis (and increases the specimen's diameter). During sintering it may be expected that radial flow will be retarded and in certain cases even changes direction (a phenomenon observed in many sinter forging experiments).

From Eqs. (63) and (65)Eqs. (68)–(70) it follows that:

$$e_{\mathrm{r}}=-\frac{P_{\mathrm{L}}}{2\eta_{\mathrm{o}}(2\psi+1/3\varphi)}-\frac{\psi-1/3\varphi}{2\psi+1/3\varphi}\frac{\dot{h}}{h} \tag{80}$$

Since $\dot{h}<0$, the lateral surface remains motionless during sintering if (considering Eq. (62))

$$\frac{\dot{h}}{h}=-\frac{3\alpha}{2\eta_{\mathrm{o}}r_{\mathrm{o}}}\frac{\theta}{2/3-\theta} \tag{81}$$

If, however

$$0>\frac{\dot{h}}{h}>-\frac{3\alpha}{2\eta_{\mathrm{o}}r_{\mathrm{o}}}\frac{\theta}{2/3-\theta} \tag{82}$$

the lateral surface area and the radius decrease. Thus, under slow deformation (or at low externally applied axial stress) the material might flow toward the central axis of the porous specimen.

5. Effect of the strain rate sensitivity (nonlinearity of the constitutive properties) on the kinetics of sintering

5.1. Free sintering

For crystalline powder materials, one of the dominant mechanisms of deformation under sintering is a power-law creep [28,86]. In this case, the relationship between the equivalent stress S and equivalent strain rate W is expressed by Eq. (33).

An expression for the rate of shrinkage for the case of free sintering can be obtained from the constitutive Eq. (36):

$$e=-\frac{P_{\mathrm{L}}}{\psi[\sigma(W)/W]} \tag{83}$$

It follows from Eq. (83) and the continuity condition (see above):

$$\dot{\theta}=-\frac{P_{\mathrm{L}}(1-\theta)}{\psi[\sigma(W)/W]} \tag{84}$$

Taking into consideration Eq. (33), we obtain:

$$\dot{\theta}=\frac{P_{\mathrm{L}}(1-\theta)}{A\psi}W^{1-m} \tag{85}$$

For free sintering with initially uniform conditions, there is no shape change. Therefore, the shape change rate γ in Eq. (16) is equal to zero. Hence, we have the following expression for the equivalent strain rate W:

$$W=\sqrt{\frac{\psi}{1-\theta}}|e|=\sqrt{\frac{2}{3}}\frac{|\dot{\theta}|}{\sqrt{\theta}} \tag{86}$$

Eliminating W from Eqs. (85) and (86), we have the differential equation describing sintering kinetics:

$$\dot{\theta}=-\left[\frac{1}{A}\frac{P_{\mathrm{L}}}{\psi}\right]^{\frac{1}{m}}\left[\frac{2}{3\theta}\right]^{\frac{1-m}{2m}} \tag{87}$$

Taking into consideration the expressions (Eqs. (62) and (56)) for P_{L} and ψ, we obtain after integration the following kinetic relationship:

$$\theta=\left[\frac{1-m}{2m}\sqrt{\frac{3}{2}}\sqrt[m]{\sqrt{\frac{3}{2}}\frac{3\alpha}{r_{\mathrm{o}}}\frac{1}{A}}(t-t_{\mathrm{i}})+\theta_{\mathrm{i}}^{(m-1)/2m}\right]^{\frac{2m}{m-1}},\ 0<m<1 \tag{88}$$

The limiting case of a linear-viscous material, when $m=1$, is expressed by the exponential law.

The kinetic equation for the free sintering of a porous material with rigid-plastic properties may be obtained by allowing the strain rate sensitivity m in Eq. (88) to approach zero. In this case $A=\tau_{\mathrm{o}}$,

where τ_o is the yield point of the matrix in the rigid-plastic material. Considering Eqs. (85)–(87), it may be concluded that when

$$\theta > \frac{2}{3}\left(\frac{\tau_o}{P_{Lo}}\right)^2 \tag{89}$$

the rate of densification approaches infinity, and when

$$\theta < \frac{2}{3}\left(\frac{\tau_o}{P_{Lo}}\right)^2 \tag{90}$$

it approaches zero.

If $P_{Lo} < \tau_o$ and the porosity is high enough to satisfy the inequality (Eq. (89)), then sintering occurs at an infinite rate (instantaneous densification) until porosity reaches the value $\theta = 2/3(\sqrt{\tau_o/P_{Lo}})^2$. After this the process stops. Consequently, the hyperbolas in Fig. 7a change to straight lines parallel to the coordinate axes.

5.2. Sinter forging (sintering under uniaxial pressure)

For sinter forging, the valid relationship for the invariants of the stress–strain rate state is:

$$\frac{\sigma_z}{3} - P_L = A\psi W^{m-1} e \tag{91}$$

where σ_z is the axial stress. The equivalent strain rate may be represented as follows:

$$W = \frac{\sqrt{\psi}}{\sqrt{1-\theta}}|e|\sqrt{\frac{6}{(1-3P_L/\sigma_z)^2}\frac{\psi}{\varphi}+1} \tag{92}$$

Substituting the expression for W from Eq. (92) into Eq. (91) and solving the equation obtained relative to $\dot{\theta}$, we obtain:

$$\frac{\dot{\theta}}{1-\theta} = \mathrm{sgn}(\sigma_z - 3P_L)\left\{P_L \frac{|\sigma_z - 3P_L|}{3\psi A\sqrt{\left[\frac{\psi}{1-\theta}\frac{6}{(1-3P_L/\sigma_z)^2}\frac{\psi}{\varphi}+1\right]^{m-1}}}\right\}^{\frac{1}{m}} \tag{93}$$

Plots $\dot{\theta}$ vs. σ_z/P_L for various values of n are given in Fig. 7b.

Methods of accelerating the densification process during sintering by the application of external *compressive* stress are well known. It is natural to assume that *tensile* stresses will retard densification during sintering. Instead (see Section 4), a range of tensile stresses exists under the action of which the porosity of a body undergoing sintering does not increase (assuming that the matrix has linear-viscous properties). Investigation of the process, assuming nonlinearity of the constitutive properties—exponential creep (Eq. (33)) indicates that a stronger assertion is justified: for nonlinear-viscous materials with a sufficiently high degree of nonlinearity a range of tensile stresses exists over which the rate of sintering is increased. In these cases, *the activation of sintering by the application of tensile stresses* occurs.

5.3. Plastic flow and sintering under the action of external forces

The constitutive behavior, in virtue of Eq. (35), is described by the following relationship:

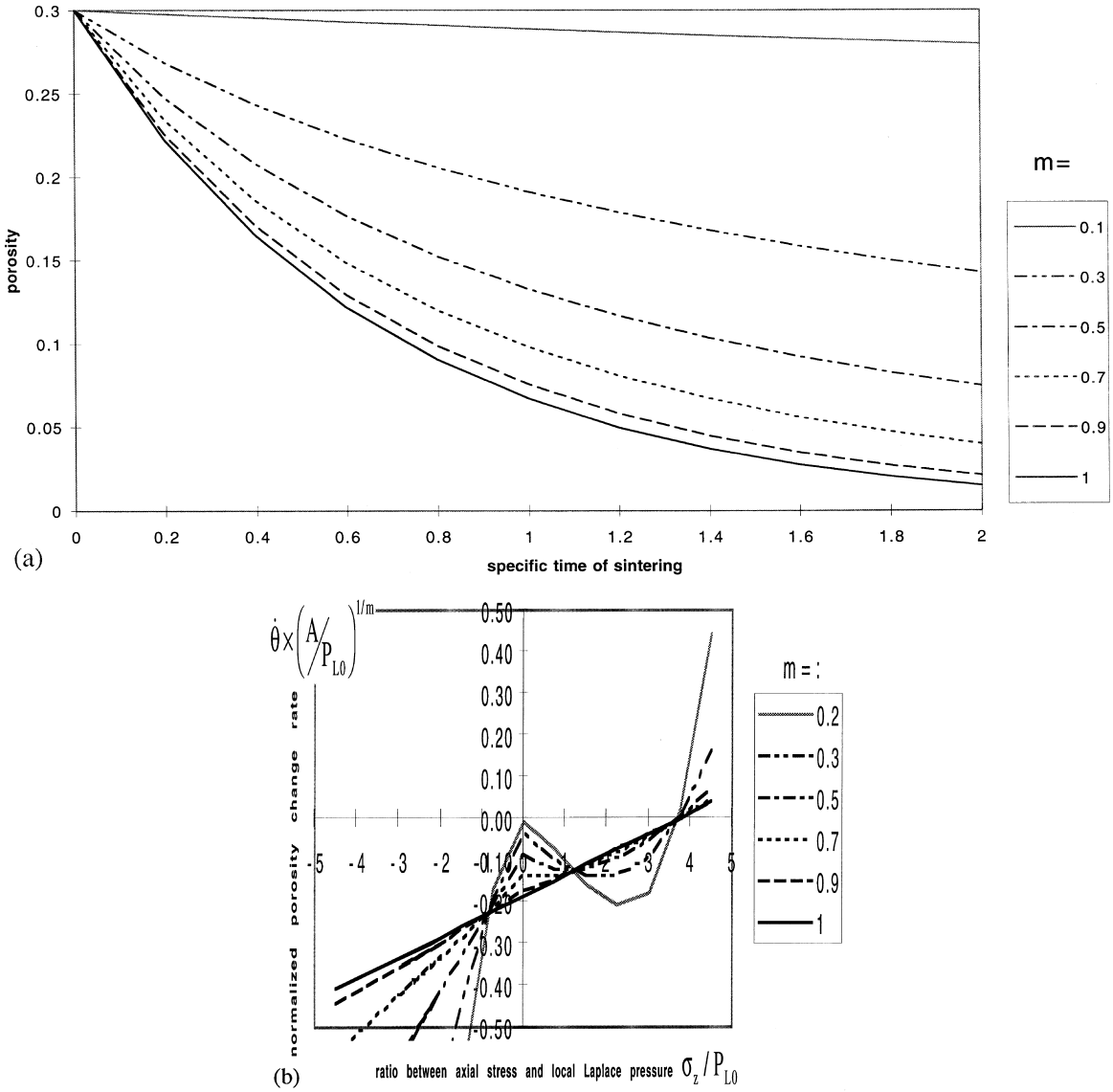

Fig. 7. Kinetics of sintering for nonlinear-viscous material. (a) Power law. (b) Sintering of a nonlinear-viscous material under uniaxial load.

$$\sigma_{ij}=\frac{\sqrt{1-\theta\tau_o}}{\sqrt{\psi e^2+\varphi\gamma^2}}[\varphi\dot{\varepsilon}_{ij}+(\psi-1/3\varphi)e\delta_{ij}]+P_L\delta_{ij} \tag{94}$$

Following Eq. (94), we obtain for the invariants:

$$p=\frac{\sqrt{1-\theta\tau_o}}{\sqrt{\psi e^2+\varphi\gamma^2}}\psi e+P_L \tag{95}$$

$$\tau=\frac{\sqrt{1-\theta\tau_o}}{\sqrt{\psi e^2+\varphi\gamma^2}}\varphi\gamma \tag{96}$$

It is not difficult to obtain an expression for the yield surface from the latter equations:

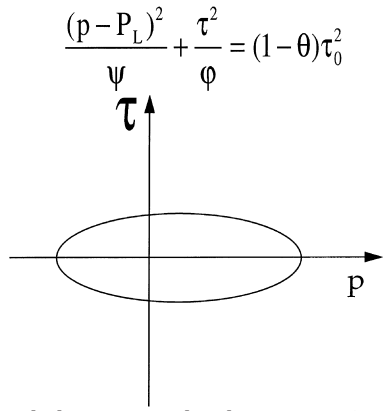

Fig. 8. Loading surface for rigid-plastic material under sintering (and externally applied stresses).

$$\frac{(p-P_L)^2}{\psi}+\frac{\tau^2}{\varphi}=(1-\theta)\tau_o^2 \tag{97}$$

5.3.1. Overall compression

Eq. (97) corresponds to an ellipse in the p–τ plane, which is nonsymmetrical relative to the τ axis (Fig. 8). This means that sintering (capillary forces) produces different resistance of the material to stretching and compression. Actually, under overall compression the flow conditions of a porous material ($\gamma=0$) may be given as:

$$p=-\sqrt{1-\theta}\sqrt{\psi}\tau_o+P_L \tag{98}$$

Hence, the presence of P_L aids the flow of the material under compression, and retards it (the yield limit increases) under tension.

5.3.2. Uniaxial loading (sinter forging)

An analogous effect: different initial yield limits in tension and compression are observed also under uniaxial loading.

Substituting Eq. (64) into Eq. (97), we have:

$$\frac{(\sigma_z/3-P_L)^2}{\psi}+\frac{2}{3}\frac{\sigma_z^2}{\varphi}=(1-\theta)\tau_o^2 \tag{99}$$

As a result of solving Eq. (99) with respect to σ_z we obtain: for compression ($(\dot{h}/h)<0$): when

$$0<\frac{P_L}{\tau_o}\le\sqrt{\frac{(\varphi+6\psi)(1-\theta)}{6}}:$$

$$\sigma_z=3\frac{P_L\varphi-\sqrt{\varphi\psi(\varphi+6\psi)(1-\theta)\tau_o^2-6P_L^2}}{\varphi+6\psi}$$

Along with that, if the Laplace pressure is larger than the yield limit of a porous body in overall compression and smaller than the yield limit of a porous body in uniaxial compression:

$$\sqrt{(1-\theta)\psi}<\frac{P_L}{\tau_o}<\sqrt{\frac{(\varphi+6\psi)(1-\theta)}{6}},$$

then the axial stress determined by Eq. (100) is tensile ($\sigma_z > 0$) under compression. The same effect was observed for a linear-viscous porous material (see Section 4). It is explained by a smaller value of the deformation velocity at the surface of the porous body under uniaxial compression than during free sintering. This situation may occur under slow punch movement.

When

$$\frac{P_L}{\tau_o} > \sqrt{\frac{(\varphi+6\psi)(1-\theta)}{6}}$$

the Laplace pressure is so high that the invariants of the stress state do not satisfy the equation of the yield surface (Eq. (97)), i.e., the material is not able to plastically deform. For tension ($\dot{h}/h > 0$):

$$\sigma_z = 3\frac{P_L\varphi + \sqrt{\varphi\psi(\varphi+6\psi)(1-\theta)\tau_o^2 - 6P_L^2}}{\varphi+6\psi} \tag{101}$$

when

$$0 < \frac{P_L}{\tau_o} \le \sqrt{\frac{\varphi(1-\theta)}{6}}$$

volume expansion (swelling) occurs; and for

$$\sqrt{\frac{\varphi(1-\theta)}{6}} < \frac{P_L}{\tau_o} < \sqrt{\frac{(\varphi+6\psi)(1-\theta)}{6}}$$

we have densification under tensile loading.

The case

$$\frac{P_L}{\tau_o} = \sqrt{\frac{\varphi(1-\theta)}{6}} \tag{102}$$

is analogous to the condition of 'zero densification' considered for linear-viscous constitutive behavior. Here the compressive capillary stresses are compensated by the external tensile ones. It should be noted that the condition of 'zero densification' has an instantaneous character for linear-viscous constitutive properties (when the punch movement law is *not* exponential vs. time—see Eq. (73)). On the contrary, for rigid-plastic properties this condition, when Eq. (102) is satisfied, has a permanent character for all the time of the sinter forging process. This means that densification is absent and the porous material deforms as an incompressible one.

5.3.3. Torsion

Analysis of Eq. (94) makes it possible to also evaluate the kinetics of sintering under torsion. In this case:

$$\tau = \sqrt{2}\tau_{r\varphi},\ p = 0,\ \gamma = |\dot{\beta}| \tag{103}$$

where $\dot{\beta}$ is the rate of twisting. Substituting Eq. (103) into Eq. (94), we obtain:

$$\tau_{r\varphi} = \sqrt{\frac{\varphi}{2}(1-\theta)\tau_o^2 - P_L^2\frac{\varphi}{\psi}} \tag{104}$$

Taking account of the equation of continuity, we obtain:

$$\frac{\dot{\theta}}{1-\theta} = -\frac{\varphi}{\psi} P_{\mathrm{L}} \frac{|\dot{\beta}|}{\sqrt{\varphi(1-\theta)\tau_{\mathrm{o}}^2 - 4P_{\mathrm{L}}^2 \frac{\varphi}{\psi}}} \tag{105}$$

It follows from Eq. (105) that during plastic flow shear deformation produces an increase in the sintering rate in opposite to the linear-viscous case, where it does not affect the rate of densification (Eq. (20)).

6. Effect of porous structure topology on sintering kinetics

Here we analyze the influence of the two topological characteristics of the porous structure: pore size distribution and pore morphology (shape).

6.1. Effect of the pore (particle) size distribution

Considerable work has been carried out on this topic [50,52,63,64,229–256].

Petru [231] and Coble [232] performed some of the first work in this direction. Coble analyzed the influence of particle size distribution on the kinetics of sintering. For a system containing particles of two characteristic sizes, the microstresses were indicated which can either enhance or retard sintering.

Later Onoda elaborated a geometric model and used the Furnas relations to calculate the shrinkage due to the sintering of bimodally distributed powder systems. This model was developed by Messing and Onoda [235] to take account of packing heterogeneity. Here an attempt was made to describe theoretically the macrokinetics of sintering of polydispersed systems. However, this model does not take into consideration the influence of the coarse–fine particle contacts. Nevertheless, as noted by Messing and Onoda [235] and also pointed out in the experimental work of O'Hara and Cutler [230] and of Smith and Messing [240], the role of these contacts can be essential.

An article of Scherer [42] describes the influence of the pore size distribution on the kinetics of sintering.

The work of Raj and Bordia [50] is devoted to a theoretical description of the internal stresses initiated by heterogeneous sintering rates during thermal treatment of bimodal porous bodies. The spherical domain which can shrink faster or slower than the surrounding spherical matrix is considered. The processes of the densification and viscoelastic creep are represented by Kelvin–Voigt and Maxwell elements, respectively. A Laplace transformation method is used to obtain the time-dependent solutions. However, to obtain analytical solutions it is necessary to assume that the elastic modulus and the viscosity of the porous body are constant. But it is known that both these parameters depend on porosity.

Rhodes [234], Lange and Metcalf [236], Slamovich and Lange [253], and Dynys and Halloran [241] have shown experimentally that the density increases faster within the aggregates (domains with some characteristic scale of the particles) than for the interaggregate regions which contain large pores. Here, the rate of sintering is inversely proportional to the concentration of the aggregates (Dynys and Halloran [241]).

Evans and Hsueh [63] elaborated the viscoelastic model which describes the behavior of the large pores in the fine-grain medium. It was predicted that a dramatic increase of the densification rate can be expected when the size of the pores is close to the size of the grains. Consequently, as also supposed by Lange [242], grain growth can favor densification.

It should be noted that despite the great number of experimental and theoretical investigations on the question given, a unity of opinion about the influence of the pore (particle)-size distribution and the ratio of the pore (particle) scales on sintering kinetics has not been achieved.

Patterson and co-authors (Patterson and Benson [238], Patterson and Griffin [239] and Patterson et al. [243]) have shown experimentally that the pore (particle)-size distribution influences the integral shrinkage. Here an increase of the sintering rate is characteristic for the large particles if the width of the pore (particle) size distribution increases. Some nonmonotonous dependence of the densification on the distribution width, with a minimum in the intermediate region is characteristic for small particles. However, it was experimentally determined (Poster et al. [229], Yeh and Sacks [250]) that the distribution width does not influence the final sintered density. Thus, since the green density is higher for wide particle size distributions (because of the higher packing density), the integral shrinkage of the patterns with wide distributions must be smaller (this is at variance with the data of Patterson et al. [243]).

Liniger and Raj [244] and Liniger [247] have shown that the disordered structures (bimodal powder mixtures) can be sintered more homogeneously and intensively than the ordered (monomodal) structures. The powders with narrow but not monomodal particle size distributions are optimal for the sintering intensity (this does not coincide with the conclusions of Patterson et al. [243]). Such a difference between the results of the experimental investigations can be explained, for example, by the difference between the objects of research, or the methods of sample preparation. However, the lack of agreement is also characteristic for the conclusions of the theoretical investigations.

Zhao and Harmer [248,249] analyzed theoretically and experimentally the influence of the pore (particle) size distribution on the sintering kinetics. It was ascertained that narrowing the distributions leads to a decrease of grain growth, and thus to an increase of the sintering rate (but the grain growth can favor densification, according to the results of Lange [242], Evans and Hsueh [63]).

German and Bulger [255], by analogy with the methods of Messing and Onoda [235], use the mixture relationship for the prediction of the sintered density. This study indicates an improvement of the solid loading for a bimodal iron mixture, but a degradation of the sintered density when used in powder injection molding.

A number of ideologically close studies have been published by De Jonghe et al. [64], Hsueh et al. [62] and De Jonghe and Rahaman [74]. These works are devoted to the description of the stresses for bimodal compact sintering. The general procedure for the determination of the effective sintering stress as the equivalent applied stress which causes the same sintering rate without the influence of the surface tension is represented by De Jonghe and Rahaman [74]. The problem of the sintering of a bimodal porous system was also considered. However, the suggested model was used mainly for analysis of the stress-state parameters only.

Li and Funkenbusch [251] studied the behavior of the analogous dispersed system in conditions of hot isostatic pressing. The concept of the deformation maps of Frost and Ashby has been used for a bimodal porous system. The behavior of the two ‘averaged’ particles, with their respective ‘weight’ contributions to the general kinetics, was described.

Scherer [52] elaborated a model in the framework of continuum mechanics (this approach was also generalized for a polymodal porous system). Scherer used Selsing’s equation for the hydrostatic stress within the inclusion correlating it with the deformations in the matrix and inclusion. Here, the inclusion is represented by the porous material, containing either large or small pores, and the matrix is an effective porous material, consisting of a mixture of cells with large and small pores.

In the framework of the terminology suggested by Scherer [52] the model proposed corresponds to the so-called ‘anarchical’ porous structure of the material because of the chaotic arrangement of large and small pores or particles.

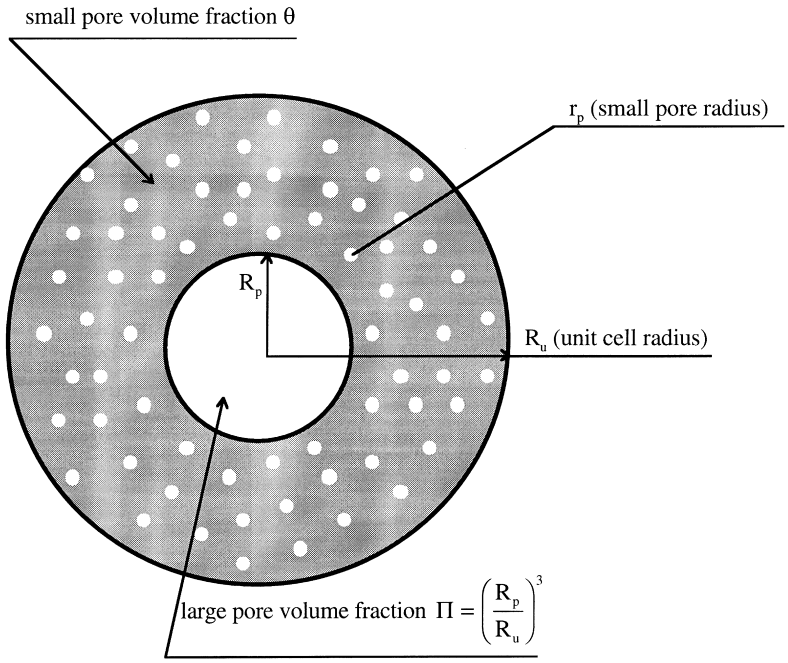

Fig. 9. Representative biporous element.

Olevsky and Rein [141] analyzed 'hierarchical' structure, characterized by an ordered arrangement of the small pores between the primary particles, and the large pores between the agglomerates (the case which is mostly met in practice). Here the representative element is considered in the form of a spherical layer containing small pores and surrounding a spherical large pore (Fig. 9).

The following kinetic equations for the evolution of 'small' and 'large' porosity (corresponding to the volume concentration of small and large pores) are obtained:

$$\frac{\mathrm{d}\theta}{\mathrm{d}\tau}=\frac{(1-\theta)^3[1+(\kappa-1)\Pi]}{2\psi(\Pi-1)} \qquad (106)$$

$$\frac{\mathrm{d}\Pi}{\mathrm{d}\tau}=-\frac{3(1-\theta)^2}{4\varphi}\kappa\Pi$$

where τ is the specific time of sintering determined by Eq. (74); Π is the porosity corresponding to the volume concentration of large pores; κ is the ratio of the small r_p and large R_p pore radii.

$$\kappa=\frac{r_\mathrm{p}}{R_\mathrm{p}} \qquad (107)$$

The kinetic equations describing the evolution of the small and large pore radii are:

$$\frac{\mathrm{d}R_\mathrm{p}}{d\tau}=\frac{R_\mathrm{p}(1-\theta)^2}{2(\Pi-1)}\left[\frac{1+(\kappa-1)\Pi}{3\psi}+\frac{\kappa}{2\varphi}\right] \qquad (108)$$

$$\frac{\mathrm{d}r_\mathrm{p}}{\mathrm{d}\tau}=-\frac{r_\mathrm{p}}{4(1-\theta)}$$

The results of the calculations in accordance with Eq. (108) are represented in Fig. 10. Here, the evolution of the relative density for a monomodal body with small pores, large pores, biporous body

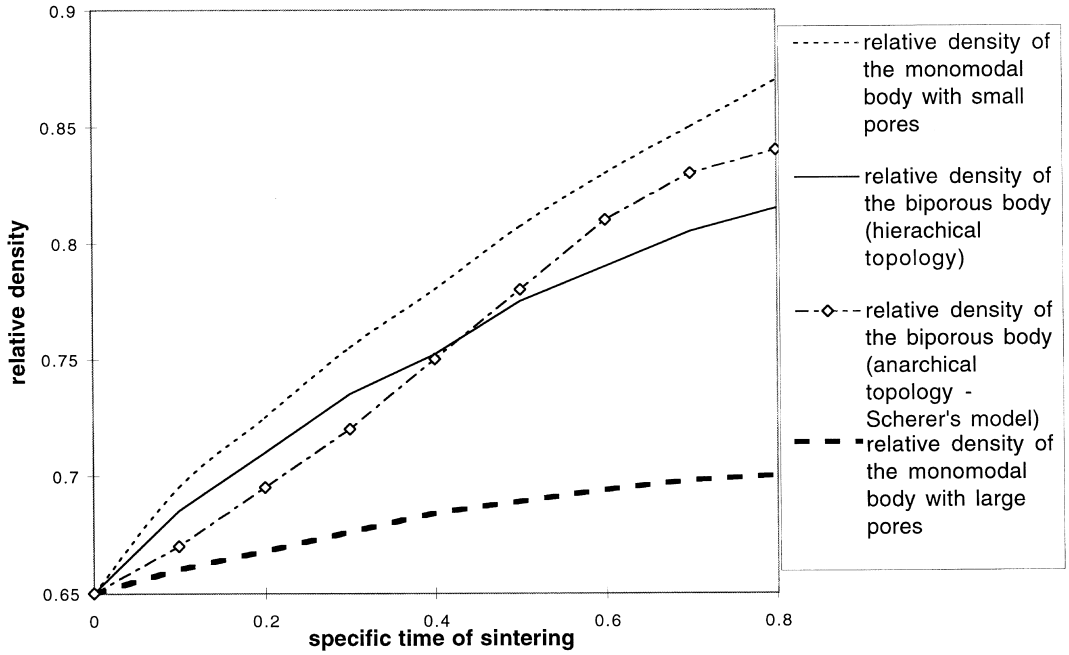

Fig. 10. Comparison of the calculation results for anarchical (Scherer's model [78]) and hierarchical (Eq. (108)) biporous topology.

(hierarchical topology—Eq. (108), anarchical topology—Scherer's model [78]) is represented. The concentrations of large and small pores are assumed to be initially equal. The initial ratio of large to small pore radii is 5:1. Small pore regions sinter faster, forming bands with higher resistance (viscosity). Apparently, this is a reason for the smaller final shrinkage of a bimodal body with the hierarchical pore structure topology (in comparison with the anarchical pore structure topology).

6.2. Effect of the pore morphology (shape) on the shrinkage anisotropy under sintering

In the sintering practice, anisotropy of shrinkage is a well-known phenomenon [23,59,71,121,166, 218,257–274]. For example, sintering a cylindrical sample, one can observe that the shrinkage in the axial direction differs from that in the radial direction.

An overview of the earlier experimental studies concerning shrinkage anisotropy under sintering has been published by Hausner [259]. In particular, the results of the experiments on sintering of carbonyl, and reduced and electrolytic iron powders are given in this paper. It is shown that, for these powders, the linear shrinkage ratio (ratio between radial and axial linear deformation) varies in the interval of 0.20…1.5 depending on the type and the particle size of powder. Also, the effect of the preliminary compaction method on shrinkage conditions under sintering was analyzed. It was demonstrated that, for uniaxially pressed powders, the linear shrinkage ratio was considerably greater than that of the isostatically pressed specimens.

The latter assertion leads to the conclusion of a possible dominant influence of oriented pore shape on the intensity of the shrinkage anisotropy. It is evident, that the uniaxially pressed samples should have a more elongated shape (with a decreased size in the direction of pressing) than those produced by isostatic pressing.

This idea is in good agreement with the results of the work of Roman and Hausner [258] on sintering of electrolytic copper powder samples. It is shown that, for the uniaxially pressed specimens,

the linear aspect ratio is always larger than unit (which means that the diameter shrank more than the height). Along with this, the linear shrinkage ratio increases with respect to the applied pressure. The same result was obtained by Arghir and Kuczynski [263]. The effect of applied stress on the intensity of shrinkage anisotropy was also analyzed by Stefanovic and Ristic [266] and was related to the creation of preferred orientations in a specimen after pressing.

Another theoretical hypothesis of Lenel et al. [257] includes gravity as a dominant factor for the shrinkage anisotropy. The authors postulated that gravity is responsible for the observed ratio of shrinkage in loose powder aggregates, while residual stresses could be responsible for the observed shrinkage effects in compacts with interconnected pores. However, Exner [262] has shown that preferred pore orientation exists even in cylindrical samples containing loosely filled copper spheres with a very narrow size distribution and that the effect of this pore orientation overrides the effect of gravity on the variation of radial shrinkage by a factor of more than three.

Ivensen [23], studying sintering of glass powders, postulated that the main reasons for the shrinkage anisotropy is the ''anisotropy of capillary forces caused by the change of the particle and pore shape in the direction perpendicular to the direction of uniaxial compaction.''

Cutler and Henrichsen [260] analyzed experimentally the effect of particle shape on the kinetics of sintering of glass. They have shown that nonequilibrium (elongated) particle shapes sinter more rapidly than equilibrium (spherical) particle shapes.

Giess et al. [267] studied experimentally isothermal sintering of jagged and spheroidized cordierite-type glass powders. Both jagged and spheroidized particle compacts showed about the same 0.7 anisotropy of the ratio of axial to diametrical shrinkage, but spheroidizing reduced the shrinkage rate (which confirms the results of Cutler and Henrichsen [260]). Thus, it is indicated that shrinkage anisotropy is not a simple particle shape effect (which is also supported by Exner and Giess [271]). Giess et al. [268] relate this effect to differences in the axial and radial distributions of particle sizes present in these compacts. This can be equivalent to the topology of an anisotropic–porous body with pores of elongated shape oriented in one direction.

This idea is also in good agreement with the results of the experimental work of Mitkov et al. [264] who analyzed the influence of the orientation of pore structure on shrinkage anisotropy. The authors concluded that preferred orientation of elongated pores exists in loose and compacted powder samples. After filling [a rigid die], an axial orientation exists, the extent of which is increased by isostatic pressing and reduced by uniaxial pressing. At higher pressures, uniaxial compression results in a radial orientation of elongated pores.

Rahaman et al. [71] and Rahaman and De Jonghe [166] observed and analyzed shrinkage anisotropy of crushed soda-lime glass powder. In Ref. [166], the axial–radial deformation ratio varied from 0.6 initially to 0.7 after 2 h of sintering. This is comparable to the shrinkage anisotropy observed by Giess et al. [268] for cordierite-type glass powder in the intermediate and final stages of sintering.

Ducamp and Raj [272] observed almost isotropic shrinkage for sintering of a borosilicate–glass powder. The axial–radial deformation ratio in their experiments varied from ~ 1 initially to 0.94 after 2 h of sintering.

Boccaccini and Ondracek [273], analyzing sintering of borosilicate–glass powder, obtained the axial–radial deformation ratio to be equal to 0.73 which is in good correlation with the results of Rahaman and De Jonghe [166].

Most of the models introduced for the description of shrinkage anisotropy under sintering consider the linear shrinkage ratio as a constant which, in general, contradicts the majority of the above-mentioned experimental data.

The anisotropy of shrinkage is a macroscopic event. In this concern, theoretically an appropriate description uses the apparatus of continuum mechanics. An anisotropic continuum model for defor-

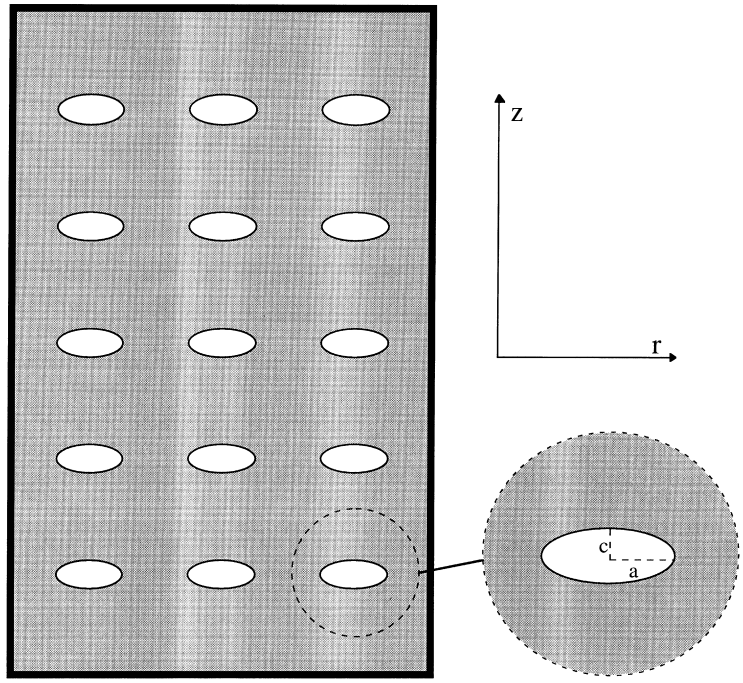

Fig. 11. Anisotropic–porous body.

mation of powder packings is elaborated by Jagota et al. [270]. This model is relevant for the early stages of densification of powder packing during sintering and compaction when powder material can be interpreted as an assembly of separated particles.

The problem of shrinkage anisotropy under sintering was considered by methods of continuum mechanics by Olevsky and Skorohod [121]. Here, we represent the model basis used by the authors and some of the results of the calculations.

Following the good agreement between the experimental interpretation of Mitkov et al. [264] and the results of Giess et al. [268] and Roman and Hausner [258], we describe a porous specimen after compaction as a body comprising oriented ellipsoidal voids. In view of the axisymmetry of the conditions of pressing in a rigid die, the pore shape is specified by ellipsoids of rotation (Fig. 11).

For this particular pore shape, the Laplace pressure is no longer a constant equal for all the directions. In such a case, the local Laplace pressure can be represented in a tensoric form:

$$P_{\mathrm{L}oij} = \frac{\alpha}{r_i}\delta_{ij} \tag{109}$$

where α is a surface tension and r_i is the pore surface curvature radius. For curvature radii in the ellipsoid's axial directions:

$$r_1 = \frac{a^2}{c}, \qquad r_2 = r_3 = \frac{c^2}{a} \tag{110}$$

where a and c are the ellipsoid's semi-axes.

Thus, the local Laplace pressure will be larger in the direction of the larger pore axis because of the smaller value of the radius of curvature in this direction.

Assuming linear-viscous properties of the matrix material, the Eshelby technique for the deformation of heterophase material with ellipsoidal inclusions can be used for the determination of the

effective Laplace pressure (sintering stress). Herewith voids are considered as ellipsoidal inclusions. Following Olevsky and Skorohod [121], the radial and axial components of the effective Laplace pressure have the form:

$$P_{\mathrm{Lr}}=\frac{\alpha\theta}{a^2/c}\,\frac{(1-S_{3333}-S_{3322})(c/a)^3+2S_{3311}}{(1-S_{3333}-S_{3322})(1-S_{1111})-2S_{1133}S_{3311}} \tag{111}$$

$$P_{\mathrm{Lz}}=\frac{\alpha\theta}{c^2/a}\,\frac{S_{1133}(c/a)^3+1-S_{1111}}{(1-S_{3333}-S_{3322})(1-S_{1111})-2S_{1133}S_{3311}}$$

where S_{iijj} are the components of Eshelby tensor.

A tensoric form of the effective Laplace pressure explains an anisotropic character of the shrinkage in such a body with a texture of porosity. However, one should take into consideration also the anisotropy of material response. In the framework of the model of transversal–isotropy, we obtain the expression for the radial and axial strain rates:

$$e_{\mathrm{r}}=\frac{\nu_{23}-1}{\eta_{22}}P_{\mathrm{Lr}}+\frac{\nu_{12}}{\eta_{11}}P_{\mathrm{Lz}} \tag{112}$$

$$e_z=\frac{\nu_{21}}{\eta_{22}}P_{\mathrm{Lr}}+\frac{1}{\eta_{11}}P_{\mathrm{Lz}}$$

where η_{11}, η_{22} and ν_{12}, ν_{21}, ν_{23} are the viscosity moduli and Poison's ratios in the corresponding directions, respectively. The values of viscosity module and Poison's ratios can be determined as effective properties of a composite material containing oriented inclusions. These properties depend on the current ellipsoid aspect ratio value (c/a) and porosity.

Besides, the proposed model [121] permits the description of the evolution of the morphology and pore size (values of pore semi-axes as functions of time).

The intensity of the shrinkage anisotropy is determined by the interplay between the two above-mentioned factors causing the anisotropy: (i) tensoric character of the effective Laplace pressure (Eq. (111)), and (ii) anisotropy of the porous material viscosity (Eq. (112)). Intuitively, it is understandable that while for elongated pores the component of the effective Laplace pressure in the direction of the bigger pore axis is larger, the viscosity will also be larger in the same direction, thereby reducing the overall anisotropy effect.

The results of the calculations in accordance with the given model agree well with the experimental data of Rahaman and De Jonghe [166] on sintering of a borosilicate glass (Fig. 12). Here, the initial porosity was accepted to be 0.39, and the initial pore aspect ratio $c/a=0.7$.

7. Inhomogeneous density (porosity) distribution and sintering kinetics

It is well known in powder metallurgy practice that the inhomogeneous spatial distribution of density can have a substantial effect on the kinetics of sintering. This inhomogeneity, and also non-uniformity in the physicochemical composition of a porous sample lead to an inhomogeneous shrinkage and warping during the sintering process, and in some cases to rupture of the porous material.

An inhomogeneous initial density distribution is usually created by pressing which precedes sintering.

This concerns mostly macroscopic variations of density. Local density fluctuations are associated usually with inclusions which differ from the surrounding matrix material by their porosity or chemical

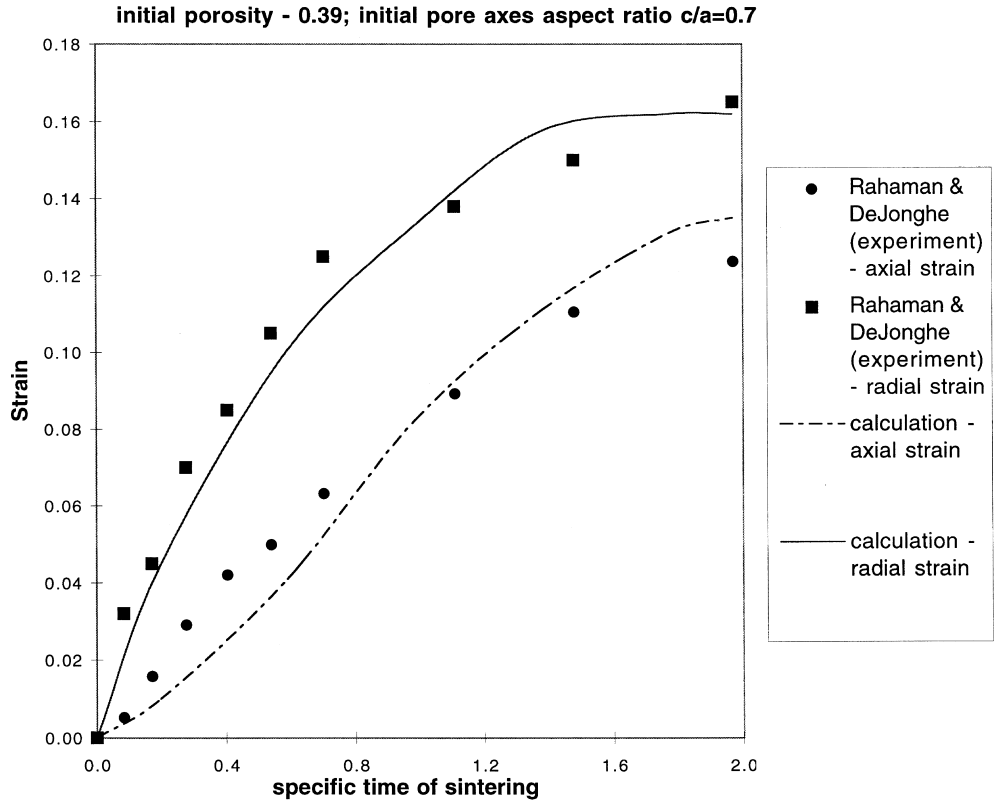

Fig. 12. Anisotropic kinetics of sintering obtained by calculations [121] and experiment of Rahaman and De Jonghe [166].

composition. Density nonuniformity causes variations in effective Laplace pressure and the effective rheological properties of the material (e.g., viscosity coefficients). It is known from sintering practice (see Lange and Metcalf [236], Rhodes [234], Weiser and De Jonghe [275], Tuan et al. [276], Tuan and Brook [277], Stearns et al. [278]) that these heterogeneities can cause differential shrinkage and damage during sintering.

One of the first modeling analyses in this area has been carried out by Scherer [43,70]. Later Scherer developed this direction in a number of publications [77,78,94], where the model was introduced based on the thermoelastic analogy of the constitutive equations for sintering of a linear-viscous porous body. Here the values of stresses initiated by shrinkage and the presence of inclusions were estimated. The problem of the determination of the transient stresses in the presence of inclusions under sintering has been considered also by Evans [47], Raj and Bordia [50], Hsueh [65,76], Hsueh et. al [62,66], De Jonghe et al. [64], Bordia and Raj [61,75], Rahaman and De Jonghe [72], De Jonghe and Rahaman [74]. Raj and Bordia [50] (see also Section 6.1) considered sintering of inclusions which can sinter faster or slower than a surrounding porous matrix. From their results it follows that, in the case of the faster sintered (more porous) inclusions, the higher possibility of the formation of circumferential cracks around inclusions exists (the same results were obtained by Evans [47]), whereas, for slower sintered (more dense) inclusions, the greater possibility of the formation of radial cracks is observed.

However, Scherer [70] and Bordia and Scherer [82] have shown that stresses estimated from the above-mentioned studies turned out to be too small to cause any substantial change of the matrix sintering rate. For example, during sintering with rigid inclusions a considerable retardation of the matrix densification should be expected. Scherer [77,78] noted that an additional influence of the

possible formation of the percolative network of inclusions impeding shrinkage is to be taken into account. A similar approach was developed by Sunderasan and Aksay [279], Lange [280], Lange et al. [281] and Sudre et al. [282–284].

Mataga and Bassani [285], following the idea suggested by Lange [286], described possible damage of the matrix due to the opening of pre-existing cracks.

All the above-mentioned models consider matrix properties to be uniform. However, it is evident that around an inclusion a nonuniform stress–strain state develops causing some inhomogeneity of the matrix density distribution. The problem of the evolution of density around inclusions is solved by Du and Cocks [104] (for the elliptical shape of the rigid inclusion). Skorohod et al. [93,112] and Olevsky and Bert [142] considered sintering with inclusions whose density differs from the density of the surrounding matrix and determined the distribution of it both in the inclusion and the matrix.

Below, it is demonstrated how the continuum theory of sintering can be employed for the solution of this problem.

7.1. One-dimensional problem of free isothermal sintering with initially nonuniform spatial distribution of density

In studying the influence of an inhomogeneous density distribution on the kinetics of sintering in a general form, it is necessary to simplify the geometry of the object under consideration. With this in mind, we shall consider a series of model one-dimensional problems concerning the sintering of a porous ball.

The problem is solved numerically by a modification of the finite-element method: the permeable element method (PEM) [142].

The volume of the porous ball is broken up into N parts, representing concentric spherical layers (Fig. 13).

Let V_{i-1i}, $i=1,\ldots,N-1$ be a material flow velocity from the $i-1$th element into the ith one. For the ith element, the radial velocity can be written as:

$$V_{ri}=\frac{r-R_{i-1}}{R_i-R_{i-1}}V_{ii+1}+\frac{r-R_i}{R_i-R_{i-1}}V_{i-1i}, \qquad i=1,\ldots,N \tag{113}$$

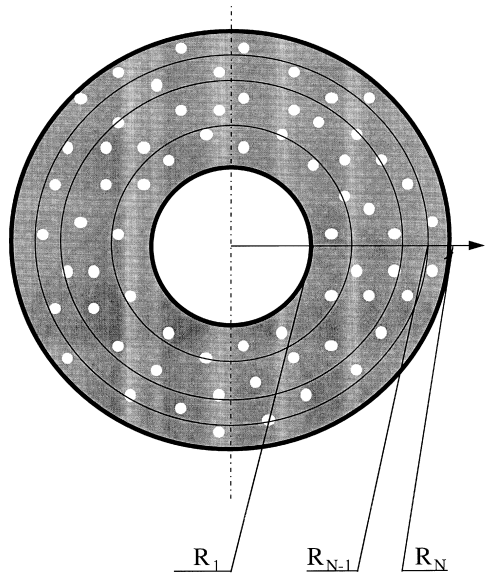

Fig. 13. Subdivision of a porous ball into permeable coaxial elements.

Here R_i is the external radius of the ith element ($R_o=0$); r is the current radial coordinate.

The strain rate of the ith element is:

$$\dot{\varepsilon}_{ri}=\frac{\partial V_{ri}}{\partial r}, \qquad \dot{\varepsilon}_{\phi i}=\frac{V_{ri}}{r}, \qquad i=1,\ldots,N \tag{114}$$

and the rates of change of its volume and shape:

$$e_i=\dot{\varepsilon}_{ri}+2\dot{\varepsilon}_{\phi i}, \qquad \gamma_i=\frac{2}{3}|\dot{\varepsilon}_{\phi i}-\dot{\varepsilon}_{ri}|, \qquad i=1\ldots,N \tag{115}$$

in order to calculate the unknown flow rates according to the PEM we use a variational principle. Assuming that the matrix material is linear-viscous, this principle is transformed to an extremum condition of the functional:

$$I=\int_{\vartheta}[\eta_o(\varphi\gamma^2+\psi e^2)+P_L e]\,d\vartheta\rightarrow \text{extr} \tag{116}$$

The latter condition has the following physical sense: the rate of energy dissipation during sintering defined by the functional I reaches its extremum for the true values of flow velocities V_{kk+1} which can be determined from the following equations:

$$\frac{\partial I}{\partial V_{kk+1}}=0, \qquad k=1,\ldots,N \tag{117}$$

To complete the system of linear Eq. (117) it is necessary to add the expression for the velocity in the center which is (due to a symmetry):

$$V_{01}=0 \tag{118}$$

and the condition of the free external surface:

$$\left[2R_N R_{N-1}\frac{(2\varphi_N+3\psi_N)}{R_{N-1}-R_N}\right]V_{N-1N} + \left[18\left(R_N-\frac{1}{2}R_{N-1}\right)^2+\frac{3}{2}R_{N-1}^2\left(\psi_N+\frac{4\varphi_N R_{N-1}^2}{R_N-R_{N-1}}\right)\right]V_{NN+1}=-3\frac{P_{Lo}}{\eta_o}(1-\theta_N)R_N \tag{119}$$

We find the density field by using the law of mass conservation, which in the given case is written in a discrete form:

$$\frac{dM_i}{dt}-\frac{\hat{\rho}_{i-1}+\hat{\rho}_i}{2}S_{i-1}(V_{i-1i}-\dot{R}_{i-1})+\frac{\hat{\rho}_{i+1}+\hat{\rho}_i}{2}S_i(V_{ii+1}-\dot{R}_i)=0 \tag{120}$$

where M_i and $\hat{\rho}_i$ are the mass and density of the ith element, respectively. S_i and $\dot{R}_i$ are the surface area and displacement velocity of the ith element's boundary.

Herewith:

$$S_i=4\pi R_i^2,\ M_i=\frac{4}{3}\pi(R_i^3-R_{i-1}^3)\hat{\rho}_i \tag{121}$$

Substituting Eq. (121) into Eq. (120) and taking into consideration that $\hat{\rho}_i=(1-\theta_i)\rho_m$ (ρ_m is the theoretical density of a fully-dense material), one obtains:

$$\dot{\theta}_i=-\frac{3}{2(R_i^3-R_{i-1}^3)}\{(1-\theta_{i-1})[R_{i-1}^2(V_{i-1i}-\dot{R}_{i-1})]+(1-\theta_i)[R_{i-1}^2V_{i-1i}-R_i^2V_{ii+1}$$
$$-R_i^2\dot{R}_i+R_{i-1}^2\dot{R}_{i-1}]+(1-\theta_{i+1})[R_i^2(\dot{R}_iV_{ii+1})]\} \qquad i=1,\ldots,N \tag{122}$$

Here we assume that $\theta_o=1$ and $\theta_{N+1}=1$.

The velocities of the permeable elements' boundaries are chosen in such a way that a transfusion between elements is absent for the uniform solution:

$$R_i=\frac{R}{N}i, \qquad \dot{}_i=\frac{\dot{R}}{N}R \qquad i=0,\ldots,N \tag{123}$$

The additional equation corresponding to the change of the external radius should supplement the set of the ordinary differential Eq. (122):

$$\dot{R}_N=\dot{R}=V_{NN+1} \tag{124}$$

The set of Eqs. (122) and (124) is solved with respect to the unknown functions θ_i, $i=1,\ldots,N$ and R_N by the Runge–Kutta method of the fourth order. For the integration, the specific time of sintering $\tau=(P_{Lo})/(\eta_o)t$, where t is a real time of the process, is an independent variable.

The analysis of the solutions obtained (see Fig. 14), for various initial radial distributions of porosity (linear (Fig. 14a), stepped (Fig. 14b,c), parabolic (Fig. 14d) and sinusoidal (Fig. 14e), indicates the following peculiarities of densification and flow under sintering of a porous ball.

- Flow velocities decrease monotonously to the center of the ball (excluding some deviations for the solutions of problems of sintering with inclusions; Fig. 14b,c). The decrease of the flow velocities becomes more intensive in regions of transition to larger porosities (a convex shape of curves of flow velocity distributions; Fig. 14b,c).
- For sintering with an inclusion of higher porosity, the distribution of flow velocities has a local maximum (by its absolute value) on the boundary of the inclusion. During sintering, the extremum character of flow velocity distribution becomes more pronounced (Fig. 14b). This, in turn, causes a local increase of density in the transition band between the inclusion and matrix.
- For all calculation examples (Fig. 14), porosity gradients decrease during sintering. The latter observation permits the following conclusion: A free surface energy, accumulated in a disperse medium, can be fully used as a moving factor of the densification under sintering only for some conditions. Such conditions can be a uniformity of porosity just as by pore sizes (which causes the uniformity of the local Laplace pressure in a porous volume), so by pore volume fraction (uniformity of porosity). These calculations indicate that nonuniformity of porosity cannot be the only reason of the localization of densification when linear-viscous properties of the material of the porous body matrix are assumed.

Thus, for an explanation of the effect of localization of densification under sintering, apparently, additional factors should be taken into consideration: nonuniformity of pore size distribution, nonlinearity of constitutive properties of porous body matrix, nonisothermicity of sintering.

7.2. Inhomogeneity of density distribution caused by influence of the external forces and preliminary pressing. Solution of certain technological problems

One of the most important applications of the continuum approach in the modeling of sintering is the solution of problems of density distribution in real porous samples. Due to high nonlinearity of the constitutive relationships, for most cases, it is impossible to obtain an analytical solution to such a

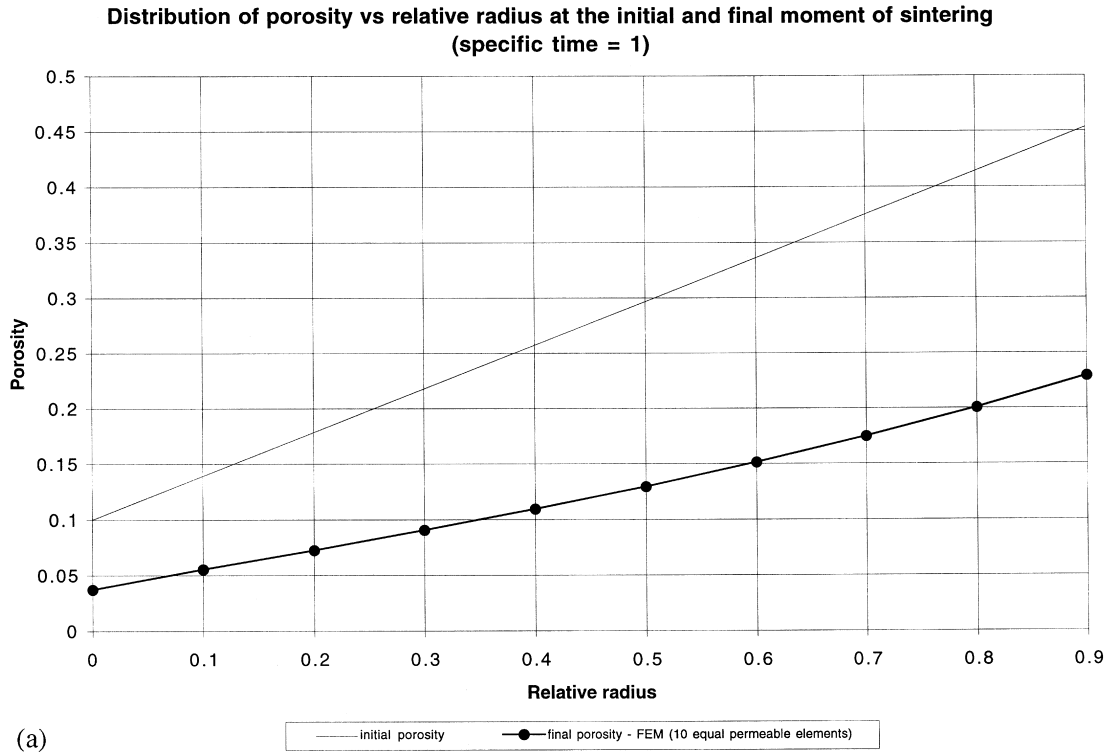

(a)

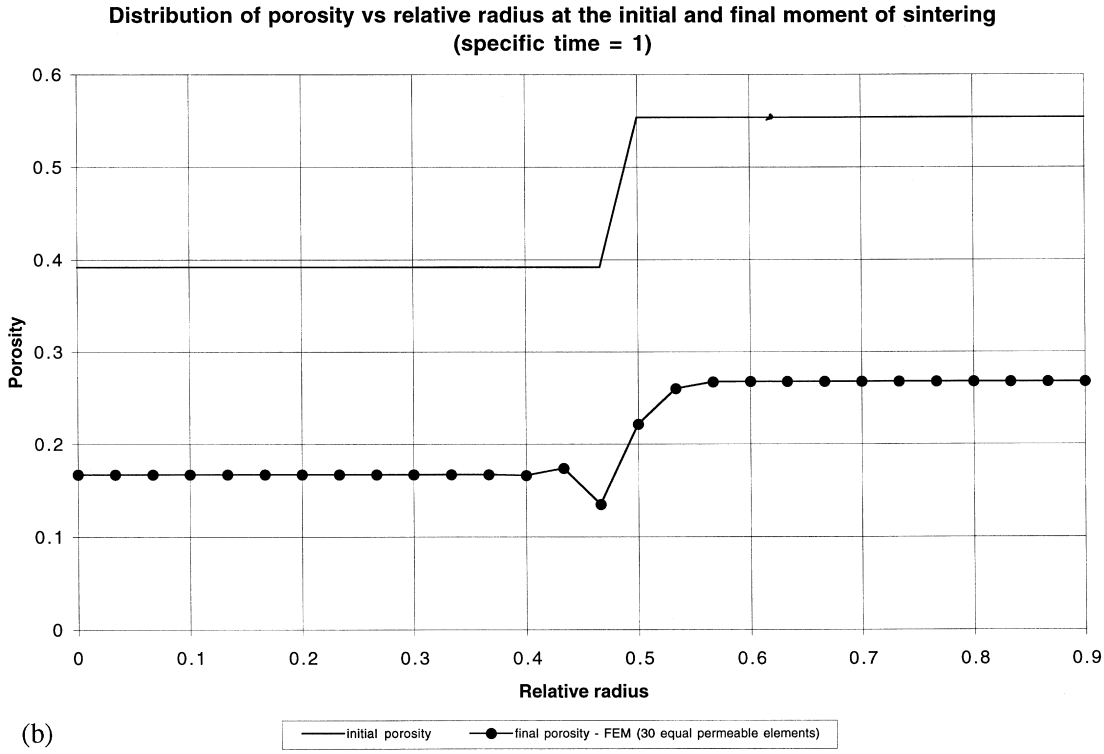

(b)

Fig. 14. *(continued)*

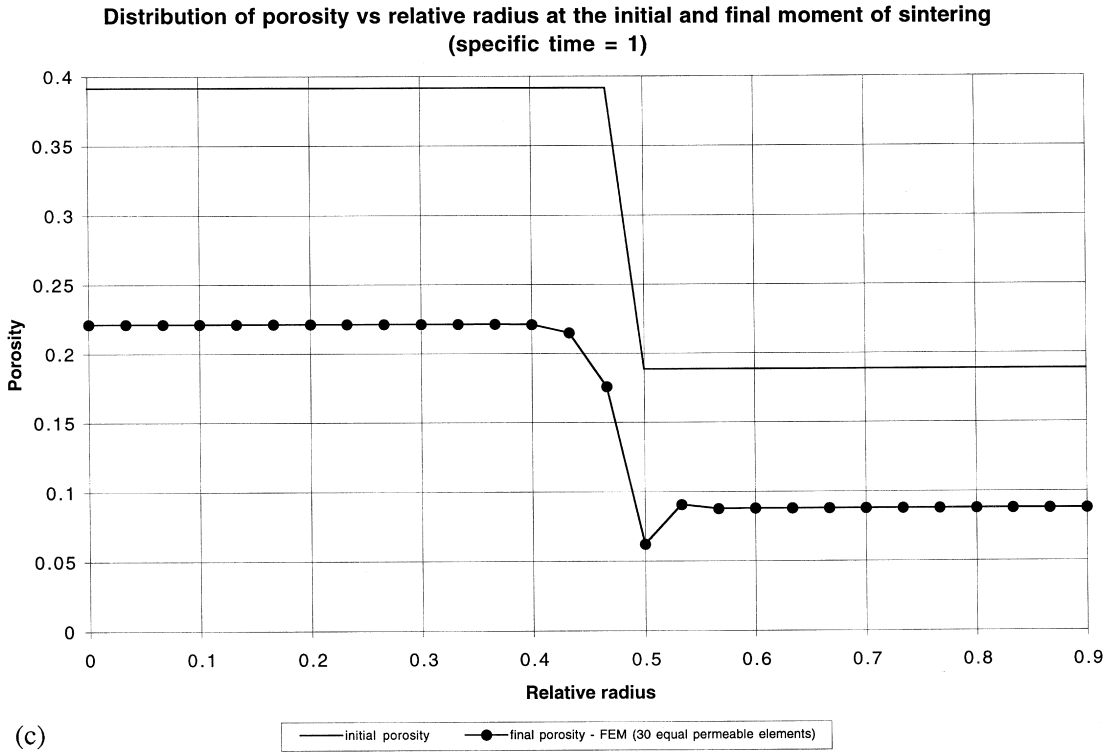

(c)

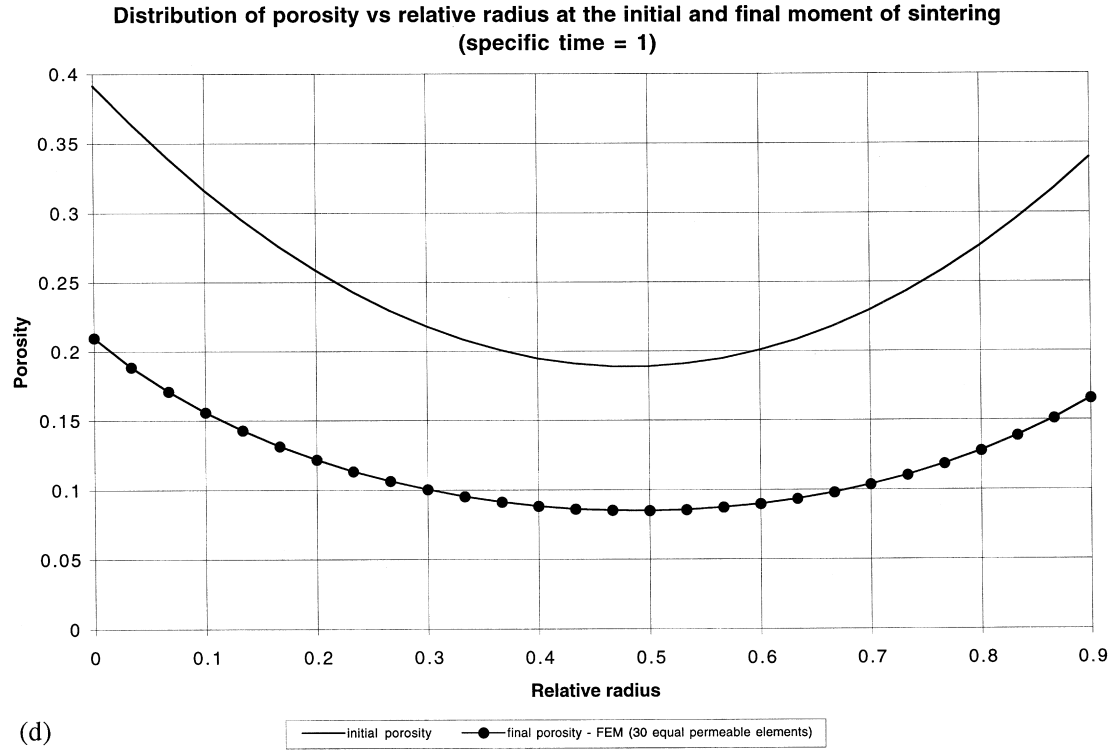

(d)

Fig. 14. *(continued)*

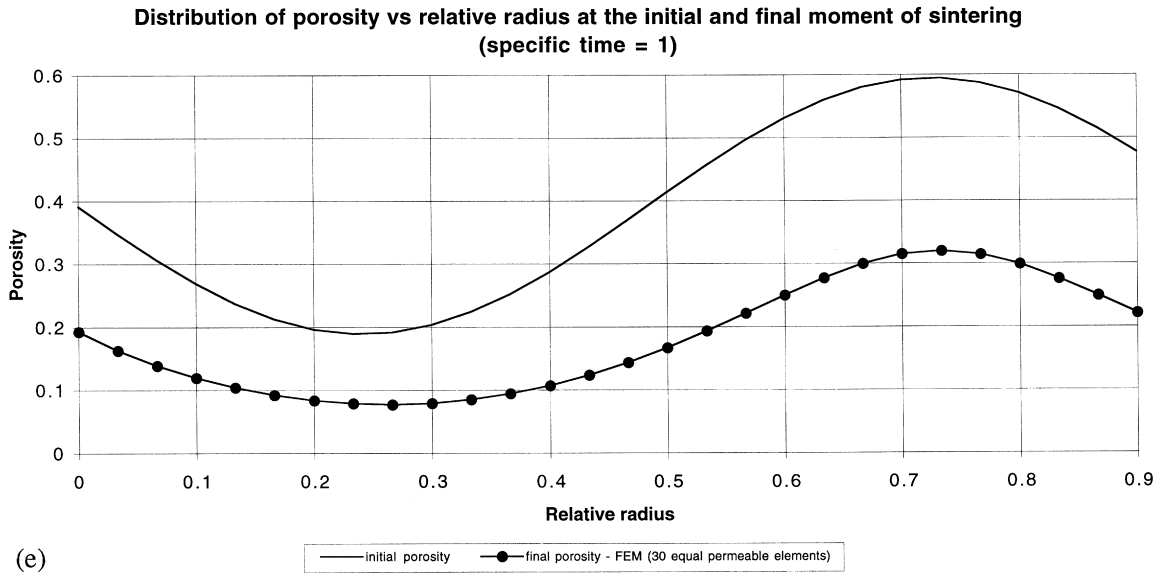

(e)

Fig. 14. Evolution of the radial porosity distribution of the initially heterogeneous porous ball. (a) Initial linear radial distribution of porosity. (b) Sintering with a porous inclusion. (c) Sintering with a dense inclusion. (d) Initial parabolic radial distribution of porosity. (e) Initial sinusoidal radial distribution of porosity.

problem. Therefore, a relevant numerical method should be used. For the solution of the problems concerning forming processes in compact materials, the finite element method (FEM) is widely used. Since the end of the 1970s the FEM was employed for the solution of the problems of working porous materials by pressure. Recently it has found a new area of application—modeling of pressureless sintering.

Skorohod et al. [85,93,112] and Olevsky [128] introduced the FEM approach for the solution of one-dimensional problems of sintering as well as problems of sintering of real porous bodies of cylindrical and stepped shape (see below). Riedel [87], Riedel and Sun [98] considered a two-dimensional problem of sintering of a cutting tool using a finite element code ADINA®. Mori [109] elaborated a finite-element code for simulating non-uniform shrinkage in sintering of ceramic powder compacts on the basis of the rigid-plastic finite element method. It should be noted that for sintering, for most cases, diffusion and viscous mechanisms of the material flow are dominant, and the rigid-plastic constitutive model is more relevant for the description of cold treatment by pressure.

Westerheide et al. [138] used the finite-element code ABAQUS® for simulation of the density distribution and shape change in a porous part with initial inhomogeneity of density distribution caused by preliminary uniaxial die pressing. In the sintering model grain boundary diffusion was considered to be the dominant mechanism for material transport responsible for shrinkage of the body.

Tsumori et al. [144] suggested an algorithm consisting of two-level modeling: a macro model to describe the geometric change of a bulk material and a micro model to predict local shrinkage. The constitutive properties of the porous body matrix are described in the framework of elasto-creep.

Bouvard and Gillia [145] considered sintering of a mixture of tungsten carbide and cobalt powders. The process was simulated using finite element code ABAQUS®. The mechanical behavior of the material was described by linear viscous constitutive equations whose parameters have been estimated from free sintering and sinter-forging experiments.

Here we consider several examples of the solution of technological problems of sintering on the basis of the continuum theory of sintering [110–112,140].

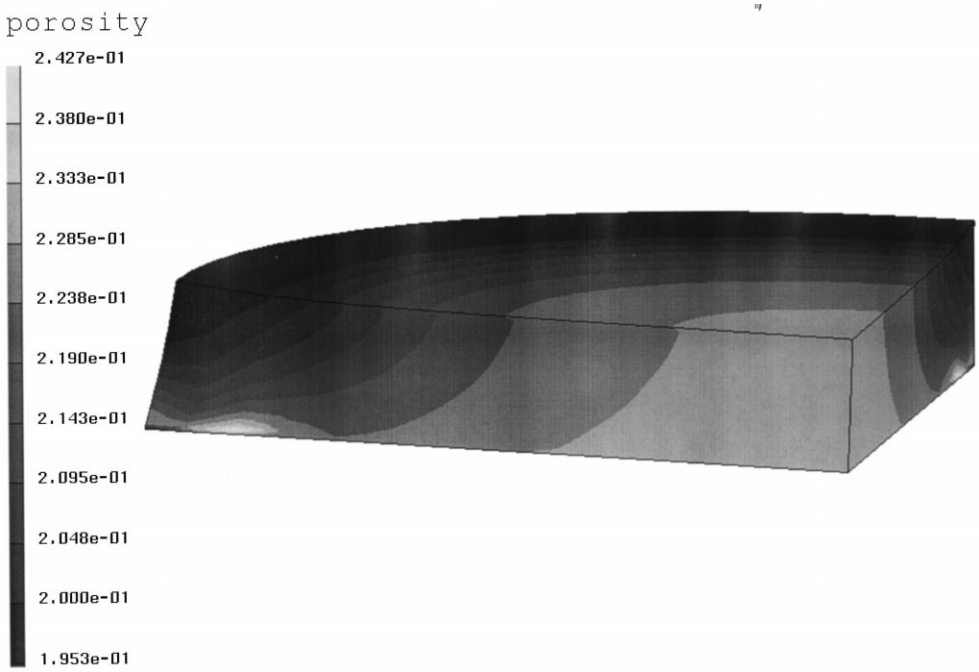

Fig. 15. Final configuration and density of sintered fiber on a rigid substrate.

7.2.1. Sintering of initially homogeneous cylindrical sample with fully-bonded end surface (model analogy of: the adhesion of the porous sample's end face and furnace surface; sintering of a film bonded on a rigid substrate)

Sintering of a film on a rigid substrate was studied by Scherer and Garino [55], Bordia and Raj [56], Hsueh [58], Cheng and Raj [211], Jagota and Hui [91,92], Bordia and Jagota [119], Zhao and Dharani [123] and German [27].

Here, we consider the constitutive properties of the matrix to be linear-viscous. The stress-strain state of the porous cylinder is axisymmetric. Because of symmetry one can consider only half of the specimen. We take as boundary conditions that on the lower face:

$$V_z = 0, \qquad V_r = 0 \tag{125}$$

The results of the calculations for the final field of porosity and for the macroscopic shape (the specific time of sintering = 1) are given in Fig. 15. The initial porosity is assumed to be uniformly distributed and equal to 0.4.

The highest density is reached at the peripheral top layers of the porous cylinder. An instability of material flow is indicated through the nonuniformity of the density distribution at the bottom of the sample. Apparently, this instability can be increased by an introduction of friction forces (at the specimen's bottom) in the model analysis.

7.2.2. Sinter-forging of an initially uniform porous cylindrical sample

The boundary conditions at the lower face are:

$$V_z = 0, \qquad V_r = 0 \tag{126}$$

and those on the upper face are:

$$V_r = -V_p, \qquad V_r = 0 \tag{127}$$

(V_p is the velocity of the upper punch, $V_p > 0$).

In distinction from Section 4, where the problem was considered assuming uniform distributions of stress and density, we will investigate the effect of the boundary conditions. An effect is pointed out in Section 4 consisting of a decrease in the radial flow rate, and in certain cases (in Section 4 this is described by Eq. (80)) even in a change in its direction. Here, the various factors which influence the course of sintering are considered more fully, since we solve a boundary-value problem. Therefore the number of possible qualitative outcomes of the solution is greater. However, as shown by the calculations (Fig. 16), there is a definite correlation between the results of the corresponding solutions of the homogeneous and boundary-value arrangements.

For a slow punch movement (with the velocity lower than that corresponding to Eq. (81)) during sinter forging, sintering 'wins' the competition with the axial external load, and the convex shape of the lateral surface is formed (Fig. 16a). The evolution of the geometry and the porosity distribution of a half-cross-section of a porous cylindrical specimen is represented in Fig. 16b. Here, starting from some intermediate time point, one can observe a uniformization of the density distribution in course of sinter forging. The highest density is reached at the middle peripheral layers of the porous cylinder.

A concave (barrel-like) shape is obtained (Fig. 16c) for sinter forging with a relatively fast punch movement (with the velocity higher than that corresponding to Eq. (81)). The highest density is reached in the center of the specimen (Fig. 16d).

For the values of the punch velocity predicted by Eq. (81), the corresponding solution of the boundary-value problem gives the final value of the specimen's radius equal to the initial radius.

7.2.3. Sintering with inclusions

In a one-dimensional form, this problem is considered in Section 7.1. The results of the solution of the corresponding boundary-value problem are represented in Fig. 17. One can see the 'densification waves' which are formed around inclusions.

7.2.4. Isothermal sintering of a porous cylinder with a nonuniform density distribution caused by previous compaction

Here, the results of the calculations for pressing copper powder in a rigid die (carried out by the permeable element method [287]) are used as the input parameters (field of porosity) for the calculation of the consequent free sintering. In Fig. 18, the evolution of porosity field and macroscopic shape is represented for a half-volume and a half-cross-section of the specimen. A nonuniformity of the porosity distribution after pressing is caused by friction between the powder and die walls.

7.2.5. Isothermal sintering of a stepped part with a nonuniform density distribution caused by previous compaction

By analogy with the previous section, 'pressing in a rigid die-free sintering'—processing sequence for a copper powder specimen is considered (Fig. 19). Here, the nonuniformity of the porosity distribution after pressing is caused mainly by different values of volume deformation in 'steps.'

8. Modeling of sintering with phase transformations

The modeling of sintering and hot isostatic pressing incorporating phase transformations has assumed a significance in the light of the developing technologies for the production of intermetallic

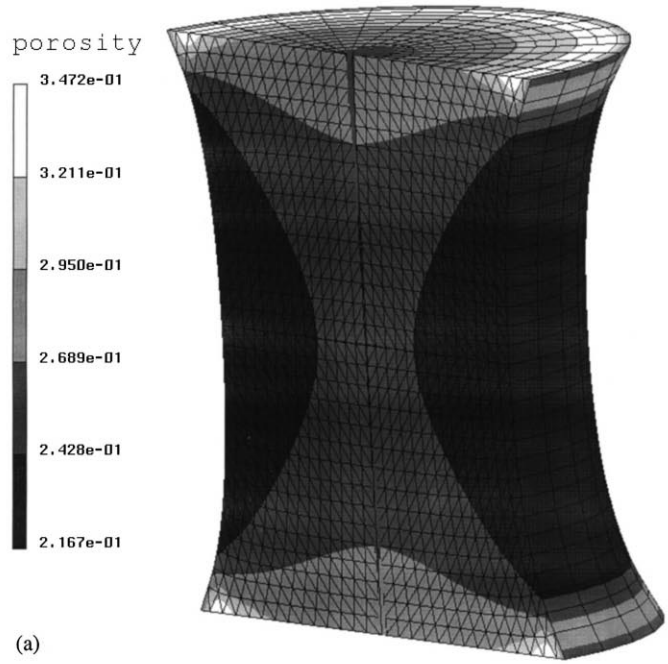

(a)

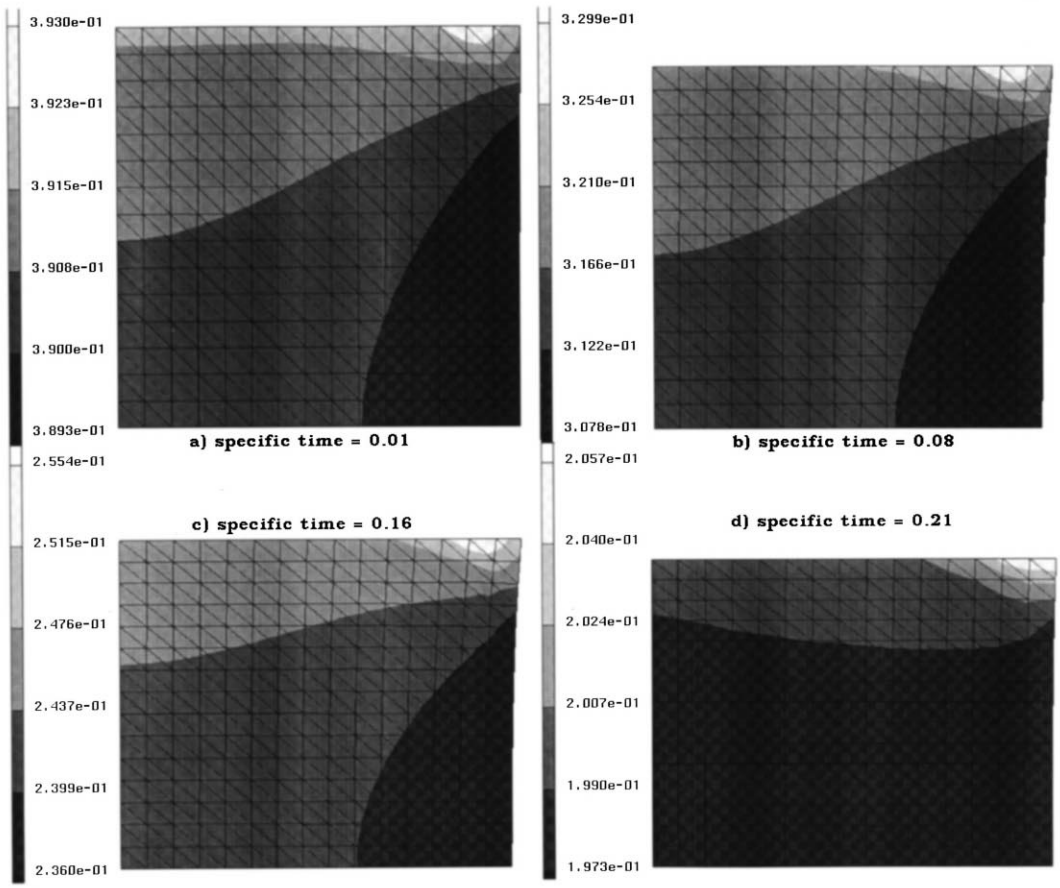

(b)

Fig. 16. *(continued)*

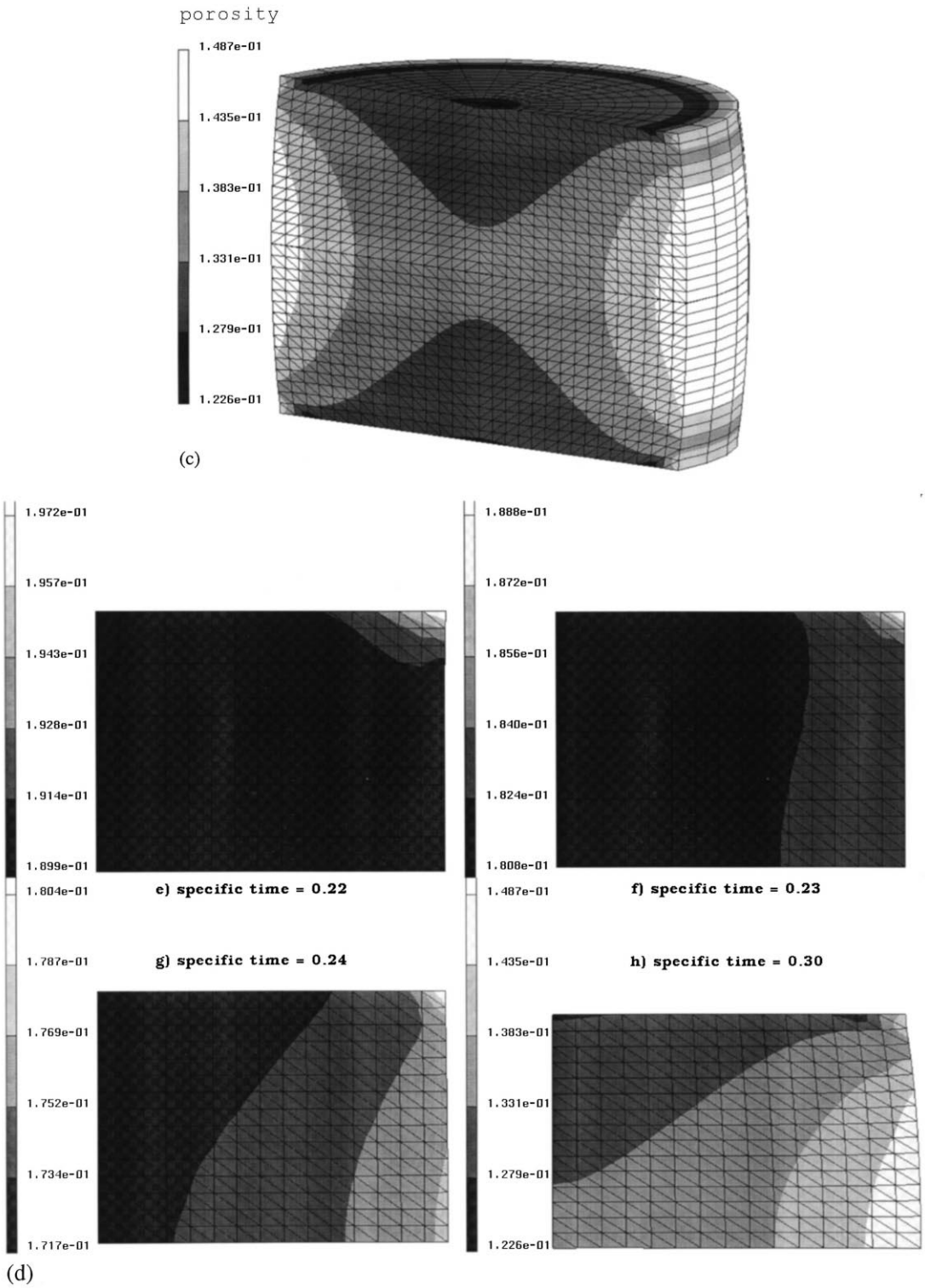

Fig. 16. Sinter-forging of a porous cylinder. (a) Slow punch movement. (b) Evolution of porosity distribution for a half-cross-section under slow punch movement. (c) Fast punch movement. (d) Evolution of porosity distribution for a half-cross-section under fast punch movement.

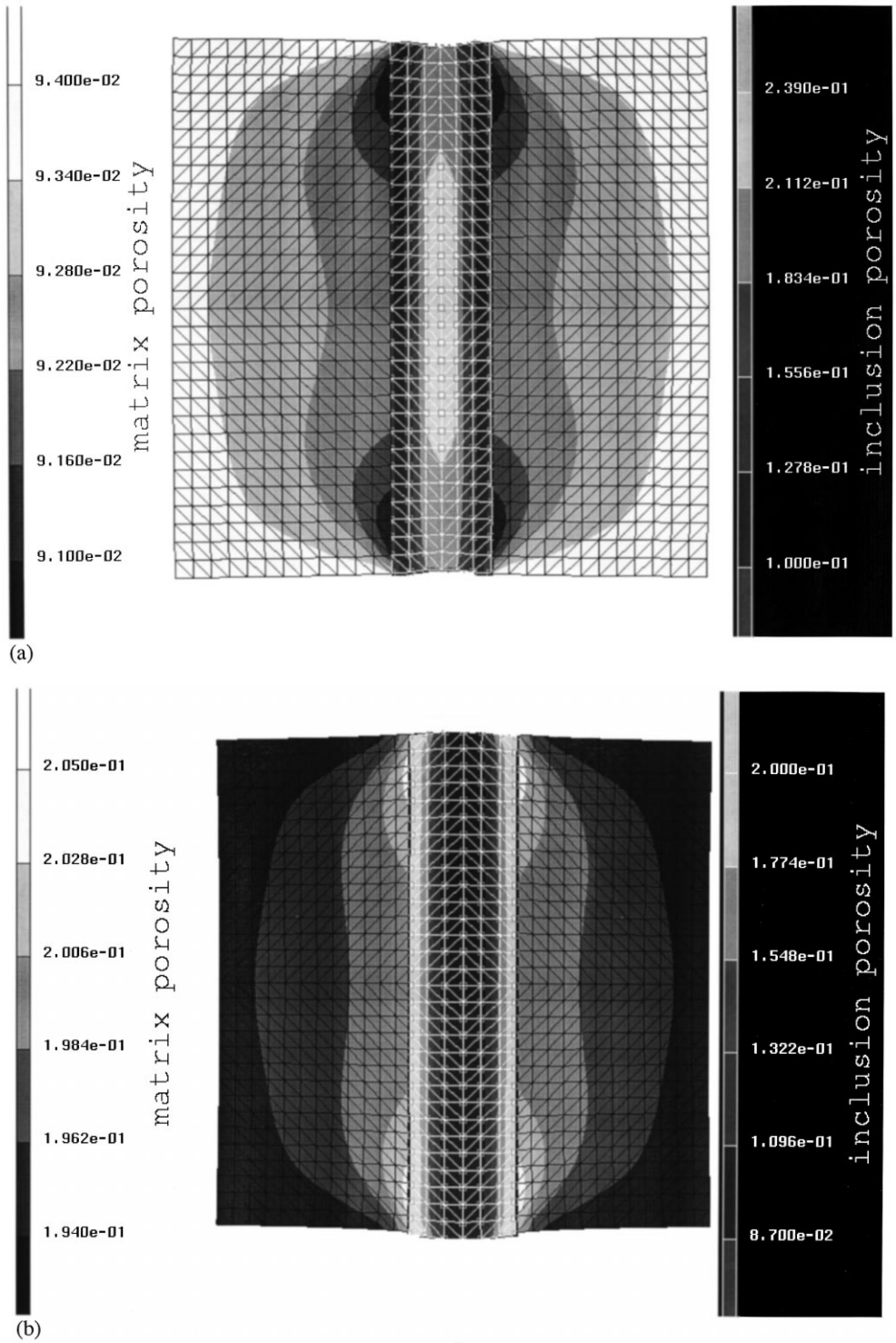

Fig. 17. Sintering with inclusions. (a) Porous inclusion (initial matrix porosity—0.2; initial inclusion porosity—0.4). (b) Dense inclusion (initial matrix porosity—0.4; initial inclusion porosity—0.2).

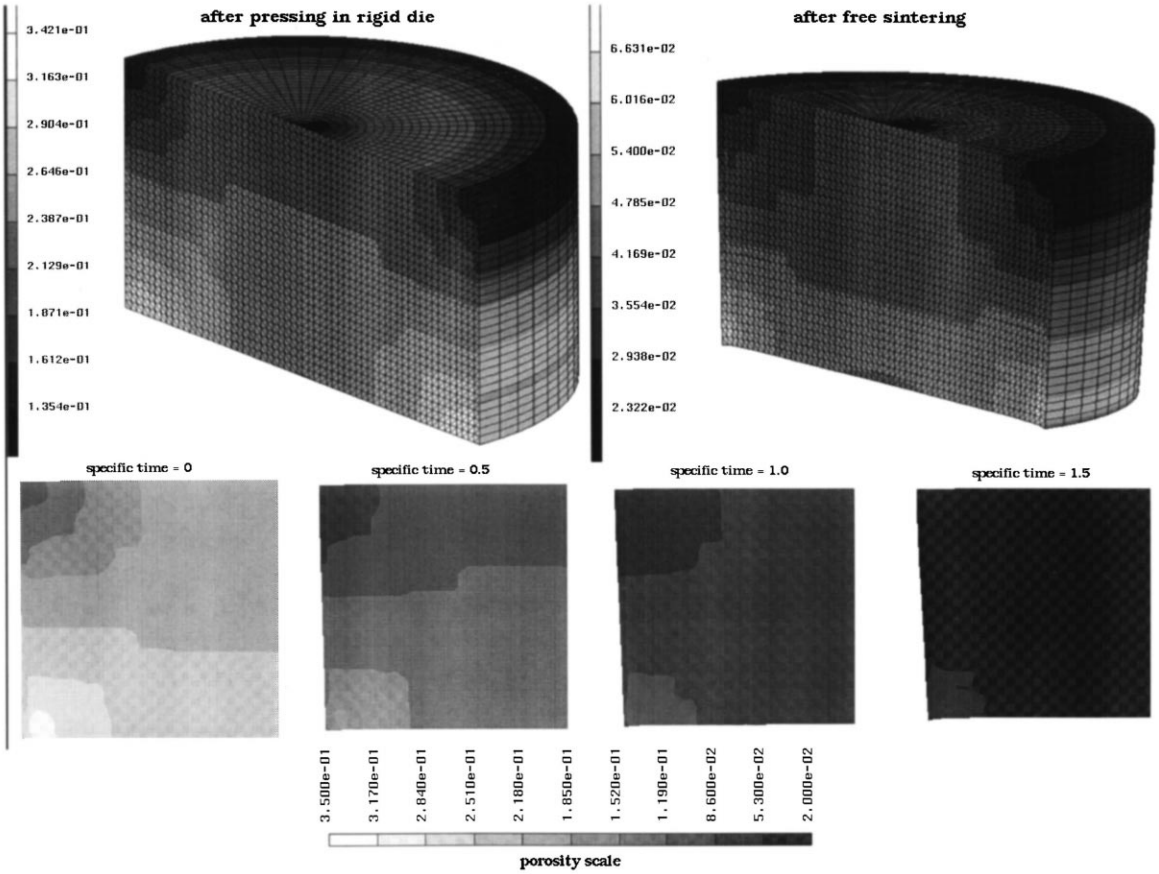

Fig. 18. Pressing in rigid die-free sintering processing sequence for a copper powder cylinder.

materials. Thermotreatment of these materials is frequently accompanied by intensive exothermic reactions causing the phenomenon of the so-called self-propagating high temperature synthesis.

Another very important application of modeling of sintering with phase transformations belongs to the area of sintering of crystallizing glasses, glass–ceramics and gels. Jagota and Raj [102] considered the crystallization and sintering of unseeded and seeded boehemite gels. The authors compared propagation velocities of densification and crystallization fronts. However, thermodynamically, crystallization and sintering were considered independently.

Olevsky et al. [129,137] have been developing a model approach based on the continuum model of sintering, where phase transformation and sintering are considered as thermodynamically coupled processes.

One of the evident manifestations of the influence of phase transformations on sintering is the change of the values of the rheological parameters of the material by virtue of their temperature dependence. The exo- and endothermic character of phase transformations and chemical reactions causes the change of material temperature and, correspondingly, the change of the values of the viscosity coefficients, the surface tension, diffusion and heat parameters, etc.

Along with this, a direct contribution of phase transformations into deformation process should be taken into consideration.

Based on the assumption that the main object of investigation of this contribution is the volume component of the deformation of the porous body skeleton, two additional items of the dissipative

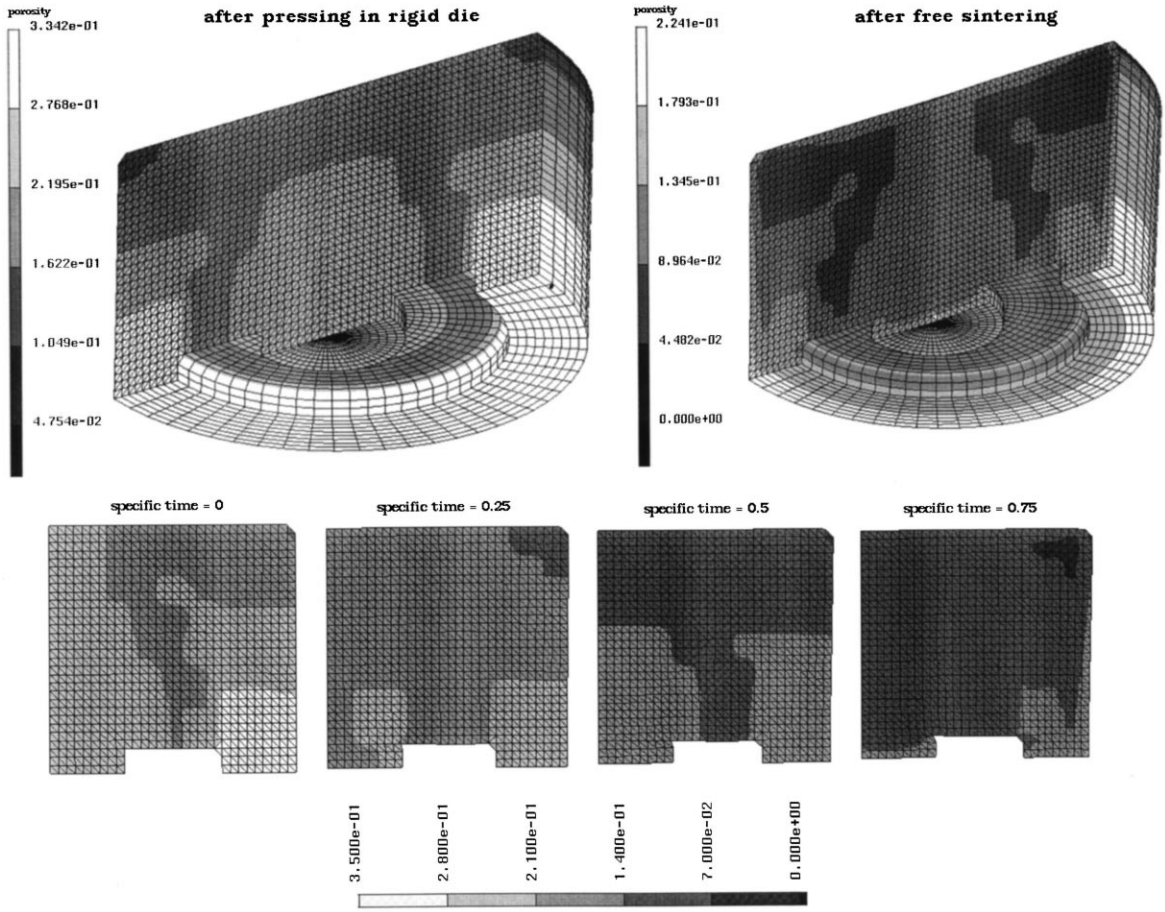

Fig. 19. Pressing in rigid die-free sintering processing sequence for a copper powder stepped-shape specimen.

balance, caused by the influence of phase transformations, can be determined. These are the change of the theoretical density of the material due to the evolution of the phase composition and the volume Kirkendall effect, conditioned by difference of intrinsic coefficients of diffusion.

8.1. The influence of the change of the theoretical density

In accordance with the local state principle [11], the contribution of the change of the theoretical density can be taken into consideration by introduction of an additional item into the dissipative balance Eq. (1):

$$D = D_0 + P_L e + P_{dc}\frac{\dot{\rho}_T}{\rho_T} \tag{128}$$

where D_0 is the dissipative potential determined by Eq. (30), ρ_T is the theoretical density of the matrix material (porous body skeleton), $\dot{\rho}_T$ is its derivative with respect to time, P_{dc} is a multiplier which represents an effective stress corresponding to the change of the theoretical density.

The kinetic equation for shrinkage has the following form:

$$e=\frac{\dot{\theta}}{1-\theta}-\frac{\dot{\rho}_{\mathrm{T}}}{\rho_{\mathrm{T}}} \tag{129}$$

where $\dot{\theta}$ is the porosity change rate.

The main problem is to determine the value of P_{dc} which can depend on porosity.

The following expression is derived by Olevsky et al. [137] for linear-viscous porous material:

$$P_{\mathrm{dc}}=\frac{4}{3}\eta_0\frac{\dot{\rho}_{\mathrm{T}}}{\rho_{\mathrm{T}}}\frac{\varphi}{1+\frac{2}{3}(\varphi/\psi)} \tag{130}$$

In view of Eq. (14), Eq. (130) can be written:

$$P_{\mathrm{dc}}=\frac{4}{3}\eta_0\frac{\dot{\rho}_{\mathrm{T}}}{\rho_{\mathrm{T}}}(1-\theta)^3 \tag{131}$$

8.2. The influence of a difference of the intrinsic heterodiffusion coefficients (Kirkendall effect)

Due to the inequality of the intrinsic heterodiffusion coefficients, the 'osmotic' swelling pressure P_{hd} appears in a powder product [19]. This pressure causes some volume deformation. An influence of this osmotic pressure is taken into consideration by an additional item in the equation of the dissipative balance:

$$D=D_0+P_{\mathrm{L}}e+P_{\mathrm{dc}}\frac{\dot{\rho}_{\mathrm{T}}}{\rho_{\mathrm{T}}}+P_{\mathrm{hd}}\frac{\dot{\rho}_{\mathrm{T}}}{\rho_{\mathrm{T}}} \tag{132}$$

The problem is to find the dependence of P_{hd} of the difference between the intrinsic diffusion coefficients and the degree of homogenization. Qualitatively, it is clear that P_{hd} should decrease as the homogenization proceeds. Besides, P_{hd} is a macroscopic value which should depend on porosity.

In accordance with Ref. [19], P_{hd} is caused by the inequality of diffusion fluxes in a powder particle volume, which are connected with the pressure of excess vacancies. P_{hd} can be evaluated upon the basis of the expression:

$$P_{\mathrm{hd}}=kTd^{-3}\frac{2\Delta c^{\max}}{D_{\mathrm{s}}\theta^{2/3}}|D_{\mathrm{A}}-D_{\mathrm{B}}|(1-\theta)^2 \tag{133}$$

where k is the Boltzman constant; T is the temperature, °K; d—a microstructure size parameter (e.g., grain size); c_{v}—the actual concentration of vacancies; c_0—its equilibrium value, D_{A} and D_{B} are the intrinsic diffusion coefficients for two diffusing substances A and B respectively; $\Delta c^{\max}$—the maximum concentration difference, D_{s} is the coefficient of self-diffusion.

The results of Sections 8.1 and 8.2 enable the representation of the rheological relationships for sintering, taking into consideration the volume effect of phase transformations:

$$\sigma_{ij}=\frac{\sigma(W)}{W}\left[\psi-\frac{1}{3}\varphi\right]e\delta_{ij}+\varphi e_{ij}+(P_{\mathrm{L}}-P_{\mathrm{dc}}-P_{\mathrm{hd}})\delta_{ij} \tag{134}$$

In the case of linear-viscous properties of the matrix phase, in view of the formulae (Eqs. (62), (131) and (133)), we have:

$$\sigma_{ij}=2\eta_0\left[\psi-\frac{1}{3}\varphi\right]e\delta_{ij}+\varphi e_{ij}\Big] + \frac{3\alpha}{r_0}(1-\theta)^2-\frac{4}{9}\eta_0\frac{\dot{\rho}_T}{\rho_T}(1-\theta)^3-kTd^{-3}\frac{2\Delta c^{max}}{D_s\theta^{2/3}}|D_A-D_B|(1-\theta)^2\ \delta_{ij} \tag{135}$$

Eq. (135), combined with Eq. (129), represents a basis for solving problems of sintering for certain powder systems incorporating phase transformations. An example of such a solution for sintering of Al–Ni reactive powder mixture is obtained by Olevsky et al. [137].

9. Further development

Schematically, possibilities of future development of the continuum theory of sintering are shown in Fig. 20.

It should be noted that, for most cases, modeling results represented in the review correspond to sintering as to a process of the volume and the macroscopic shape deformation.

Microscopically, however, sintering results in a change of both the pore volume and the inter-particle contact area. Considerable achievements in this direction belong to Svoboda and Riedel [106,132], Svoboda et al. [107,143], Reidel et al. [108,127], Reidel and Svoboda [115]. Investigations of this group of researchers are primarily based upon the consideration of diffusion mechanisms of sintering. The extrapolation of these results into range of nonlinear constitutive properties (power-law creep and plastic flow, in particular) can be of a great interest. Basically, this requires the incorporation of an additional dependence of the free surface energy F (per unit mass of porous medium) on specific surface area in definition (1). This direction includes also an analysis of grain growth (Ostwald ripening effect) and its influence on the stability of sintering.

The results of the modeling of the influence of a porous structure topology (size distribution and morphology) on sintering kinetics (see Section 6) are derived for the linear-viscous material properties. The extension of this approach for nonlinear-viscous properties, using the results of the micro-mechanical modeling at the unit-cell level (see, for example, publications of Budiansky et al. [147], Banks-Sills and Budiansky [148], and Fleck and Hutchinson [150]) can be useful for the analysis of sintering under pressure. Further generalization of pore morphology is of particular interest too.

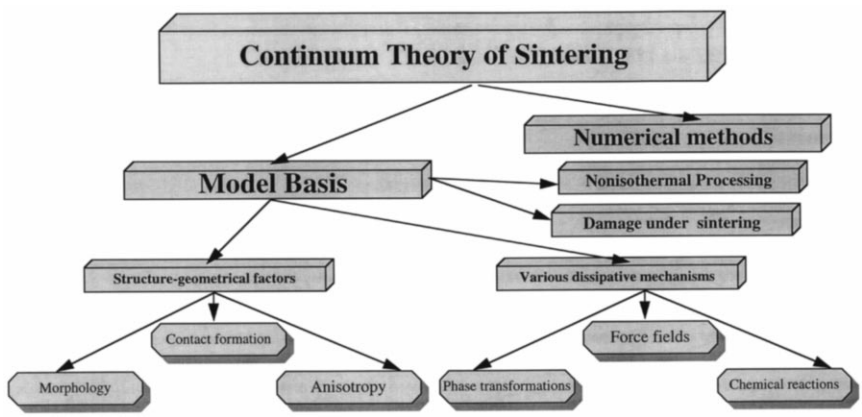

Fig. 20. Possibilities of future development of the continuum theory of sintering.

The generalization of the expression for the effective Laplace pressure including parameters of microstructure and, possibly, the strain rate sensitivity of the porous body skeleton, is also one of directions of further development.

The analysis of non-isothermal processing is poorly represented in continuum models of sintering. This area can include modeling and optimization of the heating regime (in particular, problems of rate-control sintering) as well as the prediction of the differential shrinkage due to a heterogeneity of the temperature spatial distribution (for instance, for fast-firing processing).

The modeling of sintering incorporating phase transformations (chemical reactions) has assumed a significance in the light of the developing technologies for the production of intermetallic and cermet materials.

Some first steps in this direction which have been made by Olevsky et al. [137,287] are represented in Section 8. Here the change of the theoretical density caused by diffusion and the Kirkendall effect influencing the shrinkage are taken into consideration. A development of this approach for a nonlinear constitutive behavior should include modifications of the dissipative balance equations (see Eqs. (3)–(9)). This direction is closely connected with modeling of liquid-phase sintering.

Presently, most of the model approaches and corresponding computer program codes (in particular, finite-element ones) are oriented to the calculation of configurational changes and evolution of the spatial density distribution during sintering. As has been stated above, this information is of great importance for sintering practice. At the same time, one can formulate the purpose of most of sintering processes in increase of the material *strength*. Therefore, modeling of the technological strength and possibility of damage under sintering is a very important direction. A very limited number of models developed in this area [66,285] include the heterogeneity of the structure (differential shrinkage of matrix and inclusions, etc.) causing tensile stresses which, in turn, provide fracturing of the porous material. However, models explaining the damage of mono-component materials and the related effects of the localization of densification [22,27] are presently not available. In this connection, the necessity of the stability analysis of the densification and the interparticle contacts development under sintering should be noted.

The prospects for the development of the continuum theory of sintering can also be related to novel heating techniques such as laser, induction, electric discharge and microwave sintering. The influence of additional force fields should be taken into consideration.

In conclusion, it may be said that, being a new fast developing interdisciplinary approach, the continuum theory of sintering offers considerable possibilities for progress in the area of mechanics and materials.

Acknowledgements

The author is very appreciative of Prof. R. German's idea of conducting this review work. The useful discussions with Profs. A. Molinari and R.K. Bordia are gratefully appreciated. The support of the NSF Institute for Mechanics and Materials, University of California, San Diego, is gratefully appreciated. This work is dedicated to Profs. V. Skorohod and M. Shtern who introduced the author to the exciting field of mechanics and materials, specifically the rheological theory of sintering and the theory of plasticity of porous bodies.

References

[1] J. Frenkel, Viscous flow of crystalline bodies under the action of surface tension, J. Phys. USSR 9 (5) (1945) 385–391.

[2] B.Ya. Pines, Mechanism of sintering, J. Tech. Phys. 16 (1946) 137.
[3] F.V. Lenel, Sintering in the presence of a liquid phase, Trans. AIME 175 (1948) 878–896.
[4] G.C. Kuczynski, Self-diffusion in sintering of metallic particles, Trans. AIME 185 (1949) 169–178.
[5] G.C. Kuczynski, Study of the sintering of glass, J. Appl. Phys 20 (1949) 1160–1163.
[6] K. Mackenzie, R. Shuttleworth, A phenomenological theory of sintering, Proc. Phys. Soc. 62 (12-B) (1949) 833–852.
[7] C. Herring, Effect of change of scale on sintering phenomena, J. Appl. Phys. 21 (1950) 301–303.
[8] W.D. Kingery, M. Berg, Study of the initial stages of sintering, solids by viscous flow, evaporation–condensation, and self-diffusion, J. Appl. Phys. 26 (1955) 1205–1212.
[9] V.V. Lifshitz, V.V. Slyozov, The kinetics of precipitation from supersaturated solid solutions, J. Phys. Chem. Solids 19 (1961) 35–46.
[10] R.L. Coble, Sintering crystalline solids: 1. Intermediate and final state diffusion models, J. Appl. Phys. 32 (1961) 787.
[11] F. Thummler, W. Thomma, The sintering process, Met. Rev. 12 (1967) 69–108.
[12] D.L. Johnson, New methods of obtaining volume, grain-boundary, and surface diffusion coefficients from sintering data, J. Appl. Phys. 40 (1969) 192–200.
[13] M.F. Ashby, A first report on sintering diagrams, Acta Metall. 22 (1974) 275–289.
[14] R.M. German, Z.A. Munir, Morphology relations during bulk-transport sintering, Met. Trans. A 6 (1975) 2229–2234.
[15] H.E. Exner, Principles of single phase sintering, Rev. Powd. Met. Phys. Ceram. 1 (1979) 7–251.
[16] F.B. Swinkels, M.F. Ashby, A second report on sintering diagrams, Acta Metall. 29 (1985) 259–281.
[17] W. Shatt, E. Fridrich, K.P. Wieters, Dislocation-activated sintering, Rev. Powd. Met. Phys. Ceram. 3 (1986) 1–111.
[18] H.U. Hausner, J.H. Dedrick, in: W. Kingston (Ed.), Physics of Powder Metallurgy, New York, 1951.
[19] V.V. Skorohod, Rheological basis of the theory of sintering, Naukova Dumka, Kiev, 1972.
[20] M.B. Waldron, L. Daniell, Sintering, Heyden, London, 1978.
[21] V.V. Skorohod, S.M. Solonin, Physical–metallurgical basis of sintering of powders, Metallurgiya, Moscow, 1984.
[22] Ya.E. Geguzin, Physics of sintering, 2nd edn., Moscow, Nauka, 1984.
[23] V.A. Ivensen, Phenomenology of sintering, Metallurgiya, Moscow, 1985.
[24] R.M. German, Liquid-phase Sintering, Plenum, New York, 1985.
[25] A.P. Savitskii, Liquid phase sintering of the systems with interacting components, Russian Academy of Sciences, 1991.
[26] M.N. Rahaman, Ceramic Processing and Sintering, Marcel Dekker, New York, 1995.
[27] R.M. German, Sintering Theory and Practice, Wiley, New York, 1996.
[28] H.A. Kuhn, C.L. Downey, Deformation characteristics and plasticity theory of sintered powder materials, Int. J. Powd. Metall. 7 (1) (1971) 15.
[29] M.M. Carroll, A.C. Holt, Static and dynamic pore-collapse relations for ductile porous materials, J. Appl. Phys. 72 (1972) 1326.
[30] R.G. Green, A plasticity theory for porous solids, Int. J. Mech. Sci. N4 (1972) 109–120.
[31] S. Shima, M. Oyane, Plasticity theory for porous metals, Int. J. Mech. Sci. N6 (1976) 285–291.
[32] A.L. Gurson, Continuum theory of ductile rupture by void nucleation and growth: Part I. Yield criteria and flow rules for porous ductile media, J. Eng. Mater. Technol. 99 (1977) 2.
[33] Y. Corapcioglu, T. Uz, Constitutive equations for plastic deformation of porous materials, J. Powd. Tech. 21 (1978) 269.
[34] M.B. Shtern, et. al., Phenomenological theories of pressing of powders, Naukova Dumka, Kiev, 1982.
[35] V. Tvergaard, On localization in ductile materials containing spherical voids, Int. J. Fracture 18 (1982) 237–252.
[36] S.M. Doraivelu, H.L. Gegel, J.S. Gunasekera, J.C. Malas, J.T. Morgan, A new yield function for compressible P/M materials, J. Mech. Sci. 26 (9/10) (1984) 527–535.
[37] K.T. Kim, M.M. Carroll, Compaction equations for strain hardening porous materials, Int. J. Plasticity 3 (1987) 63–73.
[38] B.A. Druyanov, Applied theory of plasticity of porous bodies, Mashinostroyeniye, Moscow, 1989.
[39] N.A. Fleck, L.T. Kuhn, R.M. McMeeking, Yielding of metal powder bonded by isolated contacts, J. Mech. Phys. Solids 40 (5) (1992) 1139.
[40] G.W. Scherer, Sintering of low-density glasses: I. Theory, J. Am. Ceram. Soc. 60 (5) (1977) 236.
[41] G.W. Scherer, Sintering of low-density glasses: II. Experimental study, J. Am. Ceram. Soc. 60 (5) (1977) 236.
[42] G.W. Scherer, Sintering of low-density glasses: I. Effect of a distribution of pore sizes, J. Am. Ceram. Soc. 60 (5) (1977) 236.
[43] G.W. Scherer, Sintering of inhomogeneous glasses: Application to optical waveguides, J. Non-Cryst. Solids 34 (1979) 239.
[44] T.B. Bhat, V.S. Arunachalam, Inhomogeneous flow and the effective pressure concept in pressure sintering, J. Mater. Sci. 15 (1980) 1614–1618.

[45] T.B. Bhat, V.S. Arunachalam, N. Ramakrishnan, An equation for pressure sintering, Scripta Metall., (1981) 339–342.
[46] R. Raj, Separation of cavitation-strain and creep strain during deformation, J. Am. Ceram. Soc. 65 (3) (1982) C–46.
[47] A.G. Evans, Consideration of inhomogeneity effects in sintering, J. Am. Ceram. Soc. 65 (10) (1982) 497.
[48] N. Ramakrishnan, V.S. Arunachalam, T.B. Bhat, An analysis of pressure sintering by computer-simulation, Acta Metall. 32 (1984) 357–370.
[49] B. Kellett, F.F. Lange, Stresses induced by differential sintering in powder compacts, J. Am. Ceram. Soc. 67 (1984) 369–371.
[50] R. Raj, R.K. Bordia, Sintering behavior of bimodal powder compacts, Acta Metall. 32 (7) (1984) 1003.
[51] L.C. Dejonghe, M.L. Rahaman, Pore shrinkage and sintering stress, J. Am. Ceram. Soc. 67 (1984) C214–C215.
[52] G.W. Scherer, Viscous sintering of a bimodal pore-size distribution, J. Am. Ceram. Soc. 67 (11) (1984) 709.
[53] B.A. Druyanov, K.B. Vartanov, A thermomechanical theory of deformation of porous and powder media incorporating 'spontaneous' densification, Sov. Powd. Metall. 263 (11) (1984) 29.
[54] G.W. Scherer, E.P. Roth, C.J. Brinker, Sol–Gel–Glass: 3. Viscous sintering, J. Non-Cryst. Solids 72 (1985) 369–389.
[55] G.W. Scherer, T. Garino, Viscous sintering on a rigid substrate, J. Am. Ceram. Soc. 68 (4) (1985) 216.
[56] R.K. Bordia, R. Raj, Sintering behavior of ceramic films constrained by a rigid substrate, J. Am. Ceram. Soc. 68 (4) (1985) 287.
[57] C.H. Hsueh, Effects of heterogeneity shape on sintering induced stresses, Scripta Metall. 19 (1985) 977–982.
[58] C.H. Hsueh, Sintering of a ceramic film on a rigid substrate, Scripta Metall. 19 (1985) 1213–1217.
[59] M.N. Rahaman, R.J. Brook, L.C. DeJonghe, Effect of shear-stress on sintering, J. Am. Ceram. Soc. 69 (1986) 53–58.
[60] M.N. Rahaman, L.C. DeJonghe, C.H. Hsueh, Creep during sintering of porous compacts, J. Am. Ceram. Soc. 69 (1986) 58–60.
[61] R.K. Bordia, R. Raj, Analysis of sintering of a composite with a glass or ceramic matrix, J. Am. Ceram. Soc. 69 (3) (1986) C55–C57.
[62] C.H. Hsueh, A.G. Evans, R.M. McMeeking, Influence of multiple heterogeneities on sintering rates, J. Am. Ceram. Soc. 69 (4) (1986) C64–C66.
[63] A.G. Evans, C.H. Hsueh, Behavior of large pores during sintering and hot isostatic pressing, J. Am. Ceram. Soc. 69 (6) (1986) 444.
[64] L.C. De Jonghe, M.N. Rahaman, C.H. Hsueh, Transient stresses in bimodal compacts during sintering, Acta Metall. 34 (1986) 927.
[65] C.H. Hsueh, Sintering behavior of powder compacts with multiheterogeneities, J. Mat. Sci. 21 (1986) 2067.
[66] C.H. Hsueh, A.G. Evans, R.M. Cannon, R.J. Brook, Visco-elastic stresses and sintering damage in heterogeneous powder compacts, Acta Metall. 34 (1986) 927.
[67] K.R. Venkatachari, R. Raj, Shear deformation and densification of powder compacts, J. Am. Ceram. Soc. 69 (6) (1986) 499.
[68] G.W. Scherer, Viscous sintering under a uniaxial load, J. Am. Ceram. Soc. 69 (9) (1986) C206.
[69] R. Raj, Analysis of the sintering pressure, J. Am. Ceram. Soc. 70 (1987) C210–C211.
[70] G.W. Scherer, Sintering with rigid inclusions, J. Am. Ceram. Soc. 70 (10) (1987) 719.
[71] M.N. Rahaman, L.C. De Jonghe, G.W. Scherer, R.J. Brook, Creep and densification during sintering of glass powder compacts, J. Am. Ceram. Soc. 70 (10) (1987) 766.
[72] M.N. Rahaman, L.C. De Jonghe, Effect of rigid inclusions on the sintering of glass-powder compacts, J. Am. Ceram. Soc. 70 (12) (1987) C348.
[73] E. Olevsky, V. Skorohod, Some questions of sintering kinetics under external forces influence, Technol. Construction Plasticity Porous Mater. NAS Ukraine 97 (1988) (in Russian).
[74] L.C. De Jonghe, M.N. Rahaman, Sintering stress of homogeneous and heterogeneous powder compacts, Acta Metall. 36 (1) (1988) 223.
[75] R.K. Bordia, R. Raj, Sintering of TiO_2–Al_2O_3 composites: A model experimental investigation, J. Am. Ceram. Soc. 71 (4) (1988) 302.
[76] C.H. Hsueh, Comment on 'Sintering with rigid inclusions', J. Am. Ceram. Soc. 71 (6) (1988) C314.
[77] G.W. Scherer, Reply, J. Am. Ceram. Soc. 71 (6) (1988) C315.
[78] G.W. Scherer, Viscous sintering with a pore-size distribution and rigid inclusions, J. Am. Ceram. Soc. 71 (10) (1988) C447.
[79] A. Jagota, P.R. Dawson, J.T. Jenkins, An anisotropic continuum model for the sintering and compaction of powder packings, Mech. Mater. 7 (1988) 255.
[80] R.K. Bordia, G.W. Scherer, Overview No. 70. On constrained sintering: I. Constitutive model for a sintering body, Acta Metall. 36 (9) (1988) 2393.

[81] R.K. Bordia, G.W. Scherer, Overview No. 70. On constrained sintering: II. Comparison of constitutive models, Acta Metall. 36 (9) (1988) 2399.
[82] R.K. Bordia, G.W. Scherer, Overview No. 70. On constrained sintering: III. Rigid inclusions, Acta Metall. 36 (9) (1988) 2411.
[83] A. Jagota, P.R. Dawson, Micromechanical modeling of powder compacts: I. Unit problems for sintering and traction induced deformation, Acta Metall. 36 (9) (1988) 2551.
[84] A. Jagota, P.R. Dawson, Micromechanical modeling of powder compacts: II. Truss formulation of discrete packings, Acta Metall. 36 (9) (1988) 2551.
[85] V.V. Skorohod, E.A. Olevsky, M.B. Shtern, Questions of the mathematical modeling of sintering under the external force influence, Proc. of IX Int Conf. on Powder Metallurgy, Dresden, Vol. 2, 1989, pp. 43–57.
[86] M.F. Ashby, Background reading, HIP 6.0, University of Cambridge, Cambridge, U.K., 1990.
[87] H. Riedel, A constitutive model for the finite-element simulation of sintering—distortions and stresses, in: G.L. Messing (Ed.), Ceramic Powder Science III, Am. Ceram. Soc., Westerville, OH, 1990, p. 619.
[88] H.K. Kuiken, Viscous sintering—the surface-tension-driven flow of a liquid form under the influence of curvature gradients at its surface, J. Fluid Mech. 214 (1990) 503–515.
[89] A. Jagota, K. Mikeska, R.K. Bordia, An isotropic constitutive model for sintering particle packings, J. Am. Ceram. Soc. 73 (8) (1990) 2266.
[90] C.R. Reid, R.G. Oakberg, A continuum theory for the mechanical response of materials to the thermodynamic stress of sintering, Mech. Mater. 10 (1990) 203–213.
[91] A. Jagota, C.Y. Hui, Mechanics of sintering thin films: I. Formulation and analytical results, Mech. Mater. 1 (1990) 221.
[92] A. Jagota, C.Y. Hui, Mechanics of sintering thin films: II. Cracking due to self-stress, Mech. Mater. 9 (1990) 107.
[93] V. Skorohod, E. Olevsky, M. Shtern, Continuum theory of sintering of porous bodies: model and application, J. Sci. Sintering 23 (2) (1991) 79–91.
[94] G.W. Scherer, Viscous sintering of particle-filled composites, Am. Ceram. Soc. Bull. 70 (1991) 1059–1063.
[95] G.W. Scherer, Cell models for viscous sintering, J. Am. Ceram. Soc. 74 (1991) 1523–1531.
[96] G.A.L. Vandevorst, R.M.M. Mattheij, H.K. Kuiken, A boundary element solution for 2-dimensional viscous sintering, J. Comput. Phys. 100 (1992) 50–63.
[97] H. Su, D.L. Johnson, Master sintering curve: a practical approach to sintering, J. Am. Ceram. Soc. 79 (1996) 3211–3217.
[98] H. Riedel, D.-Z. Sun, Simulation of die pressing and sintering of powder metals, hard metals and ceramics, NUMIFORM'92, Sophia-Antipolis, Rotterdam, 1992.
[99] G.A.L. Vandevorst, R.M.M. Mattheij, Numerical analysis of a 2-d viscous sintering problem with nonsmooth boundaries, Computing 49 (1992) 239–263.
[100] R.M. McMeeking, Constitutive laws for sintering and pressing of powders, Mech. Granular Mater. Powd. Sys. ASME 37 (1992) 51.
[101] R.M. McMeeking, L.T. Kuhn, Diffusional creep law for powder compacts, Acta Mater. 40 (5) (1992) 961.
[102] S. Jagota, R. Raj, Model for the crystallization and sintering of unseeded and seeded boehmite gels, J. Mater. Sci. 27 (1992) 2251–2257.
[103] Z.-Z. Du, A.C.F. Cocks, Constitutive models for the sintering of ceramic components: I. Material models, Acta Metall. 40 (8) (1992) 1969.
[104] Z.-Z. Du, A.C.F. Cocks, Constitutive models for the sintering of ceramic components: II. Sintering of inhomogeneous bodies, Acta Metall. 40 (8) (1992) 1981.
[105] J. Besson, M. Abouaf, Rheology of porous alumina and simulation of hot isostatic pressing, J. Am. Ceram. Soc. 75 (8) (1992) 2165.
[106] J. Svoboda, H. Riedel, Pore-boundary interactions and evolution equations for the porosity and the grain size during sintering, Acta Metall. 40 (11) (1992) 2829.
[107] J. Svoboda, H. Riedel, H. Zipse, Equilibrium pore surfaces, sintering stresses and constitutive equations for the intermediate and late stages of sintering: Part I. Computation of equilibrium surfaces, Acta Met. Mater. 42 (1994) 435.
[108] H. Riedel, H. Zipse, J. Svoboda, Equilibrium pore surfaces, sintering stresses and constitutive equations for the intermediate and late stages of sintering: Part II. Diffusional densification and creep, Acta Met. Mater. 42 (1994) 445.
[109] K. Mori, Finite element simulation of nonuniform shrinkage in sintering of ceramic powder compact, in: Chenot, Wood and Zienkevich (Eds.), NUMINFORM, 1992, p. 69.
[110] V. Skorohod, E. Olevsky, M. Shtern, Continuum theory of sintering: I. Phenomenological model. Analysis of the external forces influence on the sintering kinetics, Powd. Metall. Metal. Ceram. 361 (1) (1993) 22.
[111] V. Skorohod, E. Olevsky, M. Shtern, Continuum theory of sintering: II. Effect of the rheological properties of the solid phase on the sintering kinetics, Powd. Metall. Metal. Ceram. 362 (2) (1993) 16.

[112] V. Skorohod, E. Olevsky, M. Shtern, Continuum theory of sintering: III. Effect of the nonhomogeneous distribution of the compact parameters and their fixation conditions on the sintering kinetics, Sov. Powd. Metall. 363 (3) (1993) 208.
[113] D. Bouvard, Modelling the densification of powder composites by powder law creep, Acta Metall. 41 (5) (1993) 1413.
[114] E. Olevsky, V.V. Skorohod, Continuum simulation of anisotropic shrinkage during sintering, in: H. Bildstein, R. Eck (Eds.), XIII Intern. Plansee-Seminar Proc., v.1 High Temperature Materials, 1993, p. 175.
[115] H. Riedel, J. Svoboda, A theoretical study of grain growth in porous solids during sintering, Acta Metall. 41 (6) (1993) 1929.
[116] S.J.L. Kang, Analysis of the sintering pressure—comment, J. Am. Ceram. Soc. 76 (1993) 1902.
[117] R. Raj, Analysis of the sintering pressure—reply, J. Am. Ceram. Soc. 76 (1993) 1903.
[118] A.C.F. Cocks, Z.-Z. Du, Pressureless sintering and HIPing of inhomogeneous ceramic compacts, Acta Metall. 41 (7) (1993) 2113.
[119] R.K. Bordia, A. Jagota, Crack growth and damage in constrained sintering films, J. Am. Ceram. Soc. 76 (10) (1993) 2475.
[120] A. Jagota, G.W. Scherer, Viscosities and sintering rates of a two-dimensional granular composite, J. Am. Ceram. Soc. 76 (12) (1993) 3123.
[121] E. Olevsky, V. Skorohod, Deformation aspects of anisotropic–porous bodies sintering, J. de Physique IV C7 (3) (1993) 739.
[122] G.A.L. Vandevorst, Integral method for a 2-dimensional stokes-flow with shrinking holes applied to viscous sintering, J. Fluid Mech. 257 (1993) 667–689.
[123] Y. Zhao, L.R. Dharani, Theoretical model for the analysis of a ceramic thin-film sintering on a non-sintering substrate, Thin Solid Films 245 (1994) 109–114.
[124] C.R. Reid, Numerical simulation of free shrinkage using a continuum theory for sintering, Powd. Technol. 81 (1994) 287–291.
[125] A.C.F. Cocks, Overview No.117. The structure of constitutive laws for the sintering of fine grained materials, Acta Metall. 42 (7) (1994) 2191.
[126] A. Jagota, Simulation of the viscous sintering of coated particles, J. Am. Ceram. Soc. 77 (1994) 2237–2239.
[127] H. Riedel, V. Kozak, J. Svoboda, Densification and creep in the final stage of sintering, Acta Metall. 42 (9) (1994) 3093.
[128] E. Olevsky, On continuum simulation of consolidation in porous media, Proc. of Powder Metallurgy World Congress, Paris, Vol. 2, 1994, p. 697.
[129] E. Olevsky, M. Bohsmann, S. Domsa, F. Aldinger, G. Petzow, Diffusion in nickel–aluminium system and mathematical modeling of reaction sintering, Proc. of Powder Metallurgy World Congress, Paris, Vol. 2, 1994, p. 1481.
[130] Y.S. Kwon, G. Son, J. Suh, K.T. Kim, Densification and grain growth of porous alumina compacts, J. Am. Ceram. Soc. 77 (12) (1994) 3137.
[131] J. Svoboda, H. Riedel, New solutions describing the formation of interparticle necks in solid-state sintering, Acta Metall. 43 (1) (1995) 1.
[132] J. Svoboda, H. Riedel, Quasi-equilibrium sintering for coupled grain-boundary and surface diffusion, Acta Metall. 43 (2) (1995) 499.
[133] A.C.F. Cocks, N.D. Aparicio, Diffusional creep and sintering—the application of bounding theorems, Acta Metall. 43 (2) (1995) 731.
[134] A. Jagota, G.W. Scherer, Viscosities and sintering rates of composite packings of spheres, J. Am. Ceram. Soc. 78 (1995) 521–528.
[135] J. Pan, A.C.F. Cocks, A numerical technique for the analysis of coupled surface and grain-boundary diffusion, Acta Metall. 43 (4) (1995) 1395.
[136] W. Hong, L.R. Dharani, Pressureless sintering of a ceramic-matrix with multiple rigid inclusions—finite-element model, J. Am. Ceram. Soc. 78 (1995) 1593–1600.
[137] E. Olevsky, V. Skorohod, G. Petzow, Densification by sintering incorporating phase transformations, Scripta Mater. 37 (1997) 635–643.
[138] R. Westerheide, K.A. Drusedau, T. Hollstein, T. Schwickert, H. Zipse, Advances in characterization of machined green-compacts, Proc. Int. Conf. Shaping of Advanced Ceramics, Mol, Belgium, 1995, 305–308.
[139] G.A.L. Vandevorst, Integral formulation to simulate the viscous sintering of a 2-dimensional lattice of periodic unit cells, J. Eng. Math. 30 (1996) 97–118.
[140] E. Olevsky, H.J. Dudek, W.A. Kaysser, HIPing conditions for processing of metal matrix composites using continuum theory for sintering: I. Theoretical analysis, Acta Mater. 44 (N2) (1996) 707–713.
[141] E. Olevsky, R. Rein, Kinetics of sintering for powder systems with bimodal pores distribution, Int. J. High Temp.–High Pressures 27/28 (1995) 81–90.
[142] E. Olevsky, C. Bert, Evolution of porosity distribution for one-dimensional problem of viscous sintering, Comm. Num. Meth. Eng. 13 (1997) 355–372.

[143] J. Svoboda, H. Riedel, R. Gaebel, A model for liquid phase sintering, Acta Mater. 44 (8) (1996) 3215.
[144] F. Tsumori, T. Aizawa, J. Kihara, Macro–micro modeling for viscous sintering and HIPing, Adv. in Powder Metallurgy and Particulate Materials, in press.
[145] D. Bouvard, O. Gillia, Finite element simulation of the sintering of cemented carbide compacts, Adv. in Powder Metallurgy and Particulate Materials, in press.
[146] D.S. Wilkinson, M.F. Ashby, Pressure sintering by power law creep, Acta Metall. 23 (1975) 1277–1285.
[147] B. Budiansky, J.W. Hutchinson, S. Slutsky, Void growth and collapse in viscous solids, in: H.G. Hopkins, M.J. Sewell, (Eds.), Mechanics of Solids, Pergamon, 1982, p. 13.
[148] L. Banks-Sills, B. Budiansky, On void collapse in viscous solids, Mech. Mater., (1982) 209–218.
[149] J.M. Duva, J.W. Hutchinson, Constitutive potentials for dilutely voided nonlinear materials, Mech. Mater. 3 (1984) 41.
[150] N.A. Fleck, J.W. Hutchinson, Void growth in shear, Proc. R. Soc. London, Ser. A 407 (1986) 435.
[151] J.M. Duva, A constitutive description of nonlinear materials containing voids, Mech. Mater. 5 (1986) 137–144.
[152] M. Abouaf, J.L. Chenot, Modelisation numerique de la deformation à chaud de poudres metalliques, J. Mech. Theor. et Appl. 5 (1986) 121.
[153] V.V. Skorohod, M.B. Shtern, I.F. Martynova, Theory of nonlinearly viscous and plastic behavior of porous materials, Sov. Powd. Metall. 8 (1987) 23–30.
[154] A.C.F. Cocks, F.A. Leckie, Creep constitutive equations for damaged materials, Adv. Appl. Mech. 25 (1987) 239–294.
[155] P. Ponte, J.R. Willis, On the overall properties of nonlinearly viscous composites, Proc. R. Soc. London, Ser. A 416 (1988) 217.
[156] J. Tirosh, A. Miller, Damage evolution and rupture in creeping of porous materials, Int. J. Solids Struct. 24 (6) (1988) 567–580.
[157] A.C.F. Cocks, Inelastic deformation of porous materials, J. Mech. Phys. Solids 37 (1989) 693.
[158] J. Tirosh, Bulk forming by densification of dilatant time-dependent materials, Mech. Mater. 9 (1990) 121–128.
[159] P. Ponte Castaneda, The effective mechanical properties of nonlinear isotropic composities, J. Mech. Phys. Solids 39 (1991) 45.
[160] J.M. Duva, P.D. Crow, The densification of powders by power-law creep during hot isostatic pressing, Acta Metall. 40 (1) (1992) 31–35.
[161] L.T. Kuhn, R.M. McMeeking, Power law creep of powder bonded by isolated contacts, Int. J. Mech. Sci. 34 (1992) 563.
[162] P. Sofronis, R.M. McMeeking, Creep of power-law material containing spherical voids, Trans. Am. Soc. Met. 59 (1992) 88–95.
[163] B.J. Lee, M.E. Mear, Effective properties of power-law solids containing elliptical inhomogeneities: Part II. Voids, Mech. Mater. 13 (1992) 337–356.
[164] B.J. Lee, M.E. Mear, Constitutive relations for power-law solids containing aligned spheroidal voids, J. Mech. Phys. Solids 40 (1992) 1805.
[165] Y.-M. Liu, H.N.G. Wadley, J.M. Duva, Densification of porous materials by power-law creep, Acta Metall. 7 (1994) 2247–2260.
[166] M.N. Rahaman, L.C. De Jonghe, Sintering of spherical glass powder under a uniaxial stress, J. Am. Ceram. Soc. 73 (3) (1990) 707.
[167] F.A. Nichols, W.W. Mullins, Surface-(interface) and volume-diffusion contributions to morphological changes driven by capillarity, Trans. TMS-AIME 233 (10) (1965) 1840–1848.
[168] F.A. Nichols, Coalescence of two spheres by surface diffusion, J. Appl. Phys. 37 (1966) 2805–2808.
[169] F.A. Nichols, Theory of sintering of wires by surface diffusion, Acta Met. 16 (1968) 103–113.
[170] H.E. Exner, G. Petzow, Shrinkage and rearrangement during sintering of glass spheres, in: G.C. Kuczynski (Ed.), Sintering and Catalysis, Plenum, New York, 1975.
[171] R.M. German, Z.A. Munir, The geometry of sintering wires, J. Mater. Sci., (1975) 1719–1724.
[172] R.M. German, Z.A. Munir, Identification of the initial stage sintering mechanism using aligned wires, J. Mater. Sci., (1976) 71–77.
[173] G.J. Cosgrove, J.A. Strozier, L.L. Seigle, An approximate analytical model for the late-stage sintering of an array of rods by viscous flow, J. Appl. Phys. 47 (4) (1976) 1258–1264.
[174] R.M. German, J.F. Lathrop, Simulation of spherical powder sintering by surface diffusion, J. Mater. Sci., (1978) 921–929.
[175] F.A. Nichols, Numerical methods for analyzing sintering by surface-diffusion, Scripta Metall. 14 (1980) 951–954.
[176] R.M. German, Problems with computer-simulation of sintering kinetics, Scripta Metall. 14 (1980) 955–957.
[177] F.A. Nichols, Comments on problems with computer-simulation of sintering kinetics, Scripta Metall. 14 (1980) 1267–1268.
[178] N. Rosenzweig, M. Narkis, Coalescence phenomenology of spherical polymer particles by sintering, Polymer 21 (1980) 988–989.

[179] V.G. Kononenko, V.S. Gostomelsky, Coalescence and sintering of pores in plane group, Ukrainskii Fizicheskii Zhurnal 25 (1980) 1648–1653.
[180] J.W. Ross, W.A. Miller, G.C. Weatherly, Dynamic computer-simulation of viscous-flow sintering kinetics, J. Appl. Phys. 52 (1981) 3884–3888.
[181] N. Rosenzweig, M. Narkis, Dimensional variations of 2 spherical polymeric particles during sintering, Polymer Eng. Sci. 21 (1981) 582–585.
[182] J.W. Ross, W.A. Miller, G.C. Weatherly, Computer simulation of sintering in powder compacts, Acta Metall. 30 (1982) 203–212.
[183] Y. Hiram, A. Nir, Surface tension driven flow—a mathematical simulation of polymer sintering or vesicular coalescence, Ann. NY Acad. Sci. 404 (1983) 420–423.
[184] N. Rosenzweig, M. Narkis, Newtonian sintering simulator of 2 spherical-particles, Polymer Eng. Sci. 23 (1983) 32–35.
[185] R.W. Hopper, Coalescence of two equal cylinders: exact results for creeping viscous plane flow driven by capillarity, J. Am. Ceram. Soc. 67 (1984) C262–C264.
[186] T.L. George, K.L. Peddicord, T.C. Kennedy, An elastic stress–strain relation for sphere arrays undergoing initial-stage sintering, J. Appl. Mech.-Trans. ASME 52 (1985) 98–104.
[187] A.W. Searcy, Driving force for sintering of particles with anisotropic surface energies, J. Am. Ceram. Soc. 68 (1985) C267–C268.
[188] H.E. Exner, Neck shape and limiting gbd sd ratios in solid-state sintering, Acta Metall. 35 (1987) 587–591.
[189] K.S. Hwang, R.M. German, F.V. Lenel, Capillary forces between spheres during agglomeration and liquid-phase sintering, Metall. Trans. A 18 (1987) 11–17.
[190] V.I. Kostikov, L.P. Kozyreva, Theory of sintering of 2-phase systems including hollow microspheres, Doklady Akademii Nauk SSSR 303 (1988) 1370–1374.
[191] A. Jagota, P.R. Dawson, Simulation of the viscous sintering of 2 particles, J. Am. Ceram. Soc. 73 (1990) 173–177.
[192] R.W. Hopper, Plane Stokes flow driven by capillarity on a free surface, J. Fluid Mech. 213 (1990) 349–375.
[193] S. Richardson, Two-dimensional slow viscous flows with time-dependent free boundaries driven by surface tension, Eur. J. Appl. Math. 3 (1991) 193–207.
[194] R.W. Hopper, Plane Stokes flow driven by capillarity on a free surface: Part 2. Further developments, J. Fluid Mech. 230 (1991) 355–364.
[195] R.W. Hopper, Stokes flow of a cylinder and half-space driven by capillarity, J. Fluid Mech. 243 (1992) 171–181.
[196] T.M. Shaw, Model for the effect of powder packing on the driving force for liquid-phase sintering, J. Am. Ceram. Soc. 76 (1993) 664–670.
[197] R.W. Hopper, Coalescence of two viscous cylinders by capillarity: Part I. Theory, J. Am. Ceram. Soc. 76 (11) (1993) 2947–2952.
[198] R.W. Hopper, Coalescence of two viscous cylinders by capillarity: Part II. Shape evolution, J. Am. Ceram. Soc. 76 (11) (1993) 2953–2960.
[199] J.I. Martinez-Herrera, J.J. Derby, Analysis of capillary-driven viscous flows during the sintering of ceramic powders, AICHE J. 40 (1994) 1794–1803.
[200] W. Zhang, J.H. Schneibel, C.H. Hsueh, Sintering of regular 2-dimensional arrays of particles by surface and grain-boundary diffusion, Phil. Mag. A 70 (1994) 1107–1118.
[201] M.K. Akhtar, G.G. Lipscomb, S.E. Pratsinis, Monte-Carlo simulation of particle coagulation and sintering, Aerosol Sci. Technol. 21 (1994) 83–93.
[202] W. Zhang, J.H. Schneibel, The sintering of 2 particles by surface and grain-boundary diffusion—a 2-dimensional numerical study, Acta. Mater. 43 (1995) 4377–4386.
[203] J.I. Martinez-Herrera, J.J. Derby, Viscous sintering of spherical-particles via finite-element analysis, J. Am. Ceram. Soc. 78 (1995) 645–649.
[204] H.L. Zhu, R.S. Averback, Sintering processes of 2 nanoparticles—a study by molecular-dynamics, Phil. Mag. Lett. 73 (1996) 27–33.
[205] F.V. Lenel, H.H. Hausner, E. Hayashi, G.S. Ansell, The driving force for shrinkage in copper powder compacts during the early stages of sintering, Powder Metall. 8 (1961) 186–198.
[206] R.A. Gregg, F.N. Rhines, Surface tension and the sintering force in copper, Metall. Trans. 4 (5) (1973) 1365–1374.
[207] W. Beere, The second stage sintering kinetics of powder compacts, Acta Metall. 23 (1) (1975) 139–145.
[208] E.H. Aigeltinger, Relating microstructure and sintering force, Int. J. Powd. Met. Powd. Technol. 11 (1975) 195–203.
[209] L.U.J.T. Ogbuji, Finite element analysis of sintering stress, Sci. Sinter. 18 (1986) 21–31.
[210] S.T. Lin, R.M. German, Compressive stress for large-pore removal in sintering, J. Am. Ceram. Soc. 71 (1988) C432–C433.
[211] T.N. Cheng, R. Raj, Measurement of the sintering pressure in ceramic films, J. Am. Ceram. Soc. 71 (1988) 276–280.
[212] L. Dejonghe, C.M.Y. Chu, M.K.F. Lin, Pore-size distribution, grain-growth, and the sintering stress, J. Mater. Sci. 24 (1989) 4403–4408.

[213] D. Bouvard, R.M. McMeeking, The deformation of interparticle necks by diffusion controlled creep, J. Am. Ceram. Soc. 79 (1996) 666–672.
[214] I.M. Fedorchenko, R.A. Andrievski, Rep. Ukr. Acad. Sci. 3 (1959) 95 (in Russian).
[215] A. Venkateswaran, D.P.H. Hasselman, On the effect of porosity on the kinetics of densification during pressure sintering, J. Mater. Sci. Lett. 1 (1982) 400–402.
[216] M.N. Rahaman, L.C. De Jonghe, Sintering of CdO under low applied stress, J. Am. Ceram. Soc. 67 (10) (1984) C205–C207.
[217] L.C. De Jonghe, M.N. Rahaman, A loading dilatometer, Rev. Sci. Instrum. 55 (12) (1984) 2007.
[218] M.N. Rahaman, L.C. De Jonghe, Creep-sintering of zinc oxide, J. Mater. Sci. 22 (1987) 4326–4330.
[219] M. Lin, L.C. Dejonghe, M.N. Rahaman, Creep-sintering and microstructure development of heterogeneous MgO compacts, J. Am. Ceram. Soc. 70 (1987) 360–366.
[220] Y. Geguzin, V. Matsokin, D. Pluzhnikova, H. Dayad, Creep of porous billets under uniaxial tensile stresses in heating regime: II. Correlation between shrinkage and uniaxial creep, Sov. Powd. Met. 2 (1987) 39.
[221] P.C. Panda, R.R. Lagraff, Shear deformation and compaction of nickel–aluminide powders at elevated temperatures, Acta Mater. 36 (8) (1988) 1929.
[222] R. Andrievski, An influence of uniaxial stresses on shrinkage under sintering, Sov. Powd. Met. 11 (1988) 11.
[223] M.-Y. Chu, L.C. De Jonghe, M.N. Rahaman, Effect of temperature on the densification/creep viscosity during sintering, Acta Metall. 37 (5) (1989) 1415–1420.
[224] V.C. Ducamp, R. Raj, Shear and densification of glass powder compacts, J. Am. Ceram. Soc. 72 (5) (1989) 798.
[225] M.N. Rahaman, L.C. Dejonghe, Sintering of particulate composites under a uniaxial-stress, J. Am. Ceram. Soc. 73 (1990) 602–606.
[226] M.N. Rahaman, L.C. De Jonghe, M.-Y. Chu, Effect of green density on densification and creep during sintering, J. Am. Ceram. Soc. 74 (3) (1991) 514–519.
[227] D. Beruto, M. Capurro, R. Novakovic, R. Botter, Effect of weak uniaxial loads on creep strain-rate in high-porosity MgO compacts during early sintering stages, J. Mater. Sci. 30 (1995) 4994–5001.
[228] H.M. Tong, D. Goland, D. Chance, Theory of pressure sintering of glass–ceramic multichip carriers, IEEE Trans. Components Packaging Manuf. Technol. Part B 19 (1996) 203–214.
[229] A.R. Poster, C.T. Waldo, H.H. Hausner, The effect of particle size distribution on the sintering of molybdenum, Prog. Powd. Metall. 16 (1960) 56.
[230] M.J. O'Hara, I.B. Cutler, Sintering kinetics of binary mixtures of alumina powders, Proc. Br. Ceram. Soc. 12 (1969) 145.
[231] Z. Petru, Sinterung von polydispersen Glaspulvern, Silic. Ind. 36 (1971) 247.
[232] R.L. Coble, Effects of particle-size distribution in initial stage of sintering, J. Am. Ceram. Soc. 56 (9) (1973) 461.
[233] R.M. German, Prediction of sintered density for bimodal powder mixtures, Met. Trans. 23A (1992) 1455.
[234] W.H. Rhodes, Agglomerate and particle size effects on sintering yittria-stabilized zirconia, J. Am. Ceram. Soc. 64 (1) (1981) 19.
[235] G.L. Messing, G.Y. Onoda, Sintering of inhomogeneous binary powder mixtures, J. Am. Ceram. Soc. 64 (8) (1981) 468.
[236] F.F. Lange, M. Metcalf, Processing related fracture origins: II. Agglomerate motion and cracklike internal surfaces caused by differential sintering, J. Am. Ceram. Soc. 66 (1983) 398.
[237] F.F. Lange, M. Metcalf, Processing related fracture origins: III. Differential sintering of ZrO_2 agglomerates in Al_2O_3/ZrO_2 composite, J. Am. Ceram. Soc. 66 (1983) 407.
[238] B.R. Patterson, L.A. Benson, The effect of powder size distribution on sintering, Prog. Powd. Metall. 39 (1983) 215.
[239] B.R. Patterson, J.A. Griffin, Effect of particle size distribution on sintering of tungsten, Mod. Dev. Powd. Metall. 15 (1984) 279.
[240] J.P. Smith, G.L. Messing, Sintering of bimodally distributed alumina powders, J. Am. Ceram. Soc. 67 (4) (1984) 238.
[241] F.W. Dynys, J.W. Halloran, Influence of aggregates on sintering, J. Am. Ceram. Soc. 67 (9) (1984) 596.
[242] F.F. Lange, Sinterability of agglomerated powders, J. Am. Ceram. Soc. 67 (2) (1984) 83.
[243] B.R. Patterson, V.D. Parkhe, J.A. Griffin, Effect of particle size distribution on sintering, in: G.C. Kuczynski, D.P. Uskokovich, H. Palmour, M.M. Ristic (Eds.), Sintering '85, Plenum, New York, 1987, p. 93.
[244] E. Liniger, R. Raj., Packing and sintering of two-dimensional structures made from bimodal particle size distributions, J. Am. Ceram. Soc. 71 (11) (1987) 843.
[245] T. Harrett, Particle-size distribution effects on sintering rates—comment, J. Appl. Phys. 61 (1987) 5202–5203.
[246] T.A. Ring, J.D. Birchall, J.S. Chappel, Particle-size distribution effects on sintering rates—comment, J. Appl. Phys. 61 (1987) 5203–5203.
[247] E.G. Liniger, Spatial variations in the sintering rate of ordered and disordered particle structures, J. Am. Ceram. Soc. 71 (9) (1988) C408.
[248] J. Zhao, M.P. Harmer, Effect of pore distribution on microstructure development: I. Matrix pores, J. Am. Ceram. Soc. 71 (2) (1988) 113.

[249] J. Zhao, M.P. Harmer, Effect of pore distribution on microstructure development: II. First and second generations pores, J. Am. Ceram. Soc. 71 (7) (1988) 530.
[250] T.S. Yeh, M.D. Sacks, Effect of particle size distribution on the sintering of alumina, J. Am. Ceram. Soc. 71 (2) (1988) C484.
[251] E.K.H. Li, P.D. Funkenbusch, Modelling of the densification rates of monosized and bimodal-sized particle systems during hot isostatic pressing, Acta Metall. 37 (6) (1989) 1645.
[252] A.V. Galakhov, V.Y. Shevchenko, N.M. Zhavoronkov, Pore-size distribution and formal analysis of sintering kinetics, Doklady Akademii Nauk SSSR 316 (1991) 1444–1446.
[253] E.B. Slamovich, F.F. Lange, Densification of large pores: I. Experiments, J. Am. Ceram. Soc. 75 (9) (1992) 2498.
[254] R.M. German, Sintering densification for powder mixtures of varying distribution widths, Acta Metall. Mater. 40 (1992) 2085–2089.
[255] R.M. German, M. Bulger, A model for densification by sintering of bimodal particle size distributions, Int. J. Powd. Metall. 28 (3) (1992) 301.
[256] J.M. Ting, R.Y. Lin, Effect of particle-size distribution on sintering: 1. Modeling, J. Mater. Sci. 29 (1994) 1867–1872.
[257] F.V. Lenel, H.H. Hausner, E. Hayashi, G.S. Ansell, Some observations on the shrinkage behavior of copper compacts and of loose powder aggregates, Powder Metall. 8 (1961) 25–36.
[258] O.V. Roman, H.H. Hausner, Investigation in the linear shrinkage of metal powder compacts during sintering, J. Jpn. Soc. Powd. Metall. 9 (1962) 228–236.
[259] H.H. Hausner, The linear shrinkage behavior of metal powder compacts during sintering, Progr. Powd. Metall. 19 (1963) 67–85.
[260] I.B. Cutler, R.E. Henrichsen, Effects of particle shape on the kinetics of sintering of glass, J. Am. Ceram. Soc. 51 (10) (1968) 604–605.
[261] I.H. Moon, W.J. Huppmann, Change of shrinkage anisotropy during sintering, Powd. Metall. Int. 6 (1974) 143.
[262] H.E. Exner, New models for theoretical description of sintering processes, Monograph, Stuttgart, 1976.
[263] G. Arghir, G.C. Kuczynski, Short note: anisotropic shrinkage of copper contacts, Powder Metall. Int. 10 (1978) 73.
[264] M. Mitkov, H.E. Exner, G. Petzow, Orientation of pore structure in loose and pressed carbonyl iron and its influence on shrinkage anisotropy, Sintering—New developments, (1979) 90–98.
[265] H.E. Exner, Solid-state sintering: critical assessment of theoretical concepts and experimental methods, Powder Metall. 23 (1980) 203.
[266] D.C. Stefanovic, M.M. Ristic, The effects of pressing process on sintering process and final compact properties, Sintering-Theory Practice 14 (1981) 431–437.
[267] E.A. Giess, J.P. Fletcher, L.W. Herron, Isothermal sintering of cordierite-type glass powders, J. Am. Ceram. Soc. 67 (8) (1984) 549.
[268] E.A. Giess, C.F. Guerci, G.F. Walker, S.H. Wen, Isothermal sintering of speroidized cordierite-type glass powders, J. Am. Ceram. Soc. 68 (1985) C328–C329.
[269] H. Kuroki, M. Hiraishi, Mechanism of anisotropic dimensional changes during sintering of metal powder compact, in: D.P. Uskokovich, H. Palmour, R.M. Sproggs (Eds.), Science of Sintering, Plenum, New York, 1988, pp. 91–98.
[270] A. Jagota, P.R. Dawson, J.T. Jenkins, An anisotropic continuum model for the sintering and compaction of powder packings, Mech. Mater. 7 (1988) 255.
[271] H.E. Exner, E.A. Giess, A stereology-based equation for isotropic shrinkage during sintering by viscous flow, in: Proc. Round Table on Sintering, Herzeg-Novi, 1989.
[272] V.C. Ducamp, R. Raj, Shear and densification of glass powder compacts, J. Am. Ceram. Soc. 72 (5) (1989) 798.
[273] A.R. Boccaccini, G. Ondracek, Viscous sintering of non-spherical borosilicate glass powder, Int. J. Glass Sci. Technol. 65 (1992) 73–78.
[274] A.R. Boccaccini, D.M.R. Taplin, P.A. Trusty, C.B. Ponton, Creep and densification during anisotropic sintering of glass powders, J. Mater. Sci. 30 (1995) 5652–5656.
[275] M.W. Weiser, L.C. Dejonghe, Rearrangement during sintering in two-dimensional arrays, J. Am. Ceram. Soc. 69 (1986) 822–826.
[276] W.H. Tuan, E. Gilbart, R.J. Brook, Sintering of heterogeneous ceramic compacts: 1. Al_2O_3– Al_2O_3, J. Mater. Sci. 24 (1989) 1062–1068.
[277] W.H. Tuan, R.J. Brook, Sintering of heterogeneous ceramic compacts: 2. ZrO_2–Al_2O_3, J. Mater. Sci. 24 (1989) 1953–1958.
[278] L.C. Stearns, M. Harmer, H.M. Chan, Effect of inclusions on the sintering behavior of $YBa_2Cu_3O_{6+x}$, J. Am. Ceram. Soc. 73 (9) (1990) 2740–2742.
[279] S. Sundaresan, I.A. Aksay, Sintering with rigid inclusions—pair interactions, J. Am. Ceram. Soc. 73 (1990) 54–60.
[280] F. Lange, Constrained network model for predicting densification behavior of composite powders, J. Mater. Res. 2 (1) (1987) 59–65.
[281] F.F. Lange, L. Atteraas, F. Zok, Deformation consolidation of metal powders containing steel inclusions, Acta Metall. 39 (2) (1991) 209–219.

[282] O. Sudre, F. Lange, Effect of inclusions on densification: I. Microstructural development in an Al_2O_3 matrix containing a high volume fraction of ZrO_2 inclusions, J. Am. Ceram. Soc. 75 (3) (1992) 519–524.
[283] O. Sudre, G. Bao, B. Fan, F.F. Lange, A.G. Evans, Effect of inclusions on densification: II. Numerical model, J. Am. Ceram. Soc. 75 (3) (1992) 525–531.
[284] O. Sudre, F.F. Lange, Effect of inclusions on densification: III. The desintering phenomenon, J. Am. Ceram. Soc. 75 (12) (1992) 3241–3251.
[285] P.A. Mataga, J.L. Bassani, Damage effects in sintering of particulate composites, in: S.V. Hanagud, M.P. Kamat C.E. Ueng, (Eds.), Developments in Theoretical and Applied Mechanics, Vol. 15, Georgia Institute of Technology, Atlanta, GA, 1990, p. 646.
[286] F.F. Lange, Densification of powder rings constrained by dense cylindrical cores, Acta Metall. 37 (2) (1989) 697–704.
[287] E. Olevsky, G. Timmermans, M. Shtern, L. Froyen, L. Delaey, The permeable element method for modeling of deformation processes in porous and powder materials: Theoretical basis and checking by experiments, Powd. Technol. 93 (1997) 127–141.